5. *RESULTS*

5.1 Bioinformatics analysis of *MoALR2*, *MoMNR2* and *MoMRS2*

We identified CorA Magnesium transporters from the *M. oryzae* genome (http://www.broadinstitute.org/annotation/genome/magnaporthe_grisea/MultiHome.html) by a BLAST_P search using the full length *S. cerevisiae* Alr1 protein sequence (859 amino acids) and Mrs2 protein sequence (470 amino acids). Using *S. cerevisiae* Alr1 protein sequence we obtained two putative orthologues in the *M. oryzae* genome: Mgg_08843 (47% identity) and Mgg_09884 (49% identity), which are named as MoAlr2 and MoMnr2, respectively. Both these proteins have two transmembrane domains towards the carboxy terminus, which are followed by conserved residues of (W/F) GMN, and hence belong to the CorA superfamily of Mg^{2+} transporters. Strongly preferred model (ExPASy, TMpred) for MoAlr2 predicts that the protein has two transmembrane helices (565-582; in-out) and (596-615; out-in), with the N-terminus facing the cytosol; the protein has been predicted to be localised to the plasma membrane (WoLFPSORT). MoMnr2 is predicted to have two transmembrane helices (756-773; in-out) and (788-806; out-in), with the N- terminus facing the cytosol. In *S. cerevisiae*, the ScMnr2 protein has been shown to be localised to vacuolar membrane. The MoAlr2 and MoMnr2 CorA domains have ~48% identity with the Alr1 CorA domain of *S. cerevisiae*.

Using the *S. cerevisiae* Mrs2 protein sequence we identified two putative orthologues in the *M. oryzae* genome: Mgg_02763 (39% identity) and Mgg_06582 (33% identity), which are both named as MoMrs2 in the database. Both are predicted to be localised to the mitochondria (WoLFPSORT). Both these proteins have two transmembrane domains towards the carboxy terminus, which are followed by conserved residues of YGMN, and hence belong to the CorA superfamily of Mg^{2+} transporters. Strongly preferred model (ExPASy, TMpred) for Mgg_02763 predicts that the protein has two transmembrane helices (439-457;

in-out) and (472-492; out-in), with the N-terminus facing the mitochondria matrix; Mgg_06582 is predicted to have two transmembrane helices (357-380; in-out) and (383-409; out-in), with the N- terminus facing the mitochondria matrix.

Multiple sequence alignment of CorA superfamily transporters across different species including yeast and several filamentous pathogenic and non-pathogenic fungi was done using full length protein sequence and the phylogenetic relationship of these CorA proteins is presented (Figure 7A). The CorA transporters included in the analysis form three clades. The **MNR clade** has **W** (tryptophan) just before the conserved sequence motif of GMN, the **ALR clade** has **F** (phenylalanine) prior to the GMN sequence, while the **MRS clade** has **Y** (Tyrosine) prior to the GMN sequence (Figure 7B). MoAlr2 is a 622 amino acid protein with a CorA domain spanning amino acids 310-617, MoMnr2 is a 814 amino acid protein with a CorA domain spanning amino acids 491-809, MoMrs2 (Mgg_02763) is a 557 amino acid protein with a CorA domain spanning amino acids 269-496, while MoMrs2 (Mgg_06582) is a 431 amino acid protein with a CorA domain spanning amino acids 82-411 (Pfam) (shown in green) (Figure 7C).

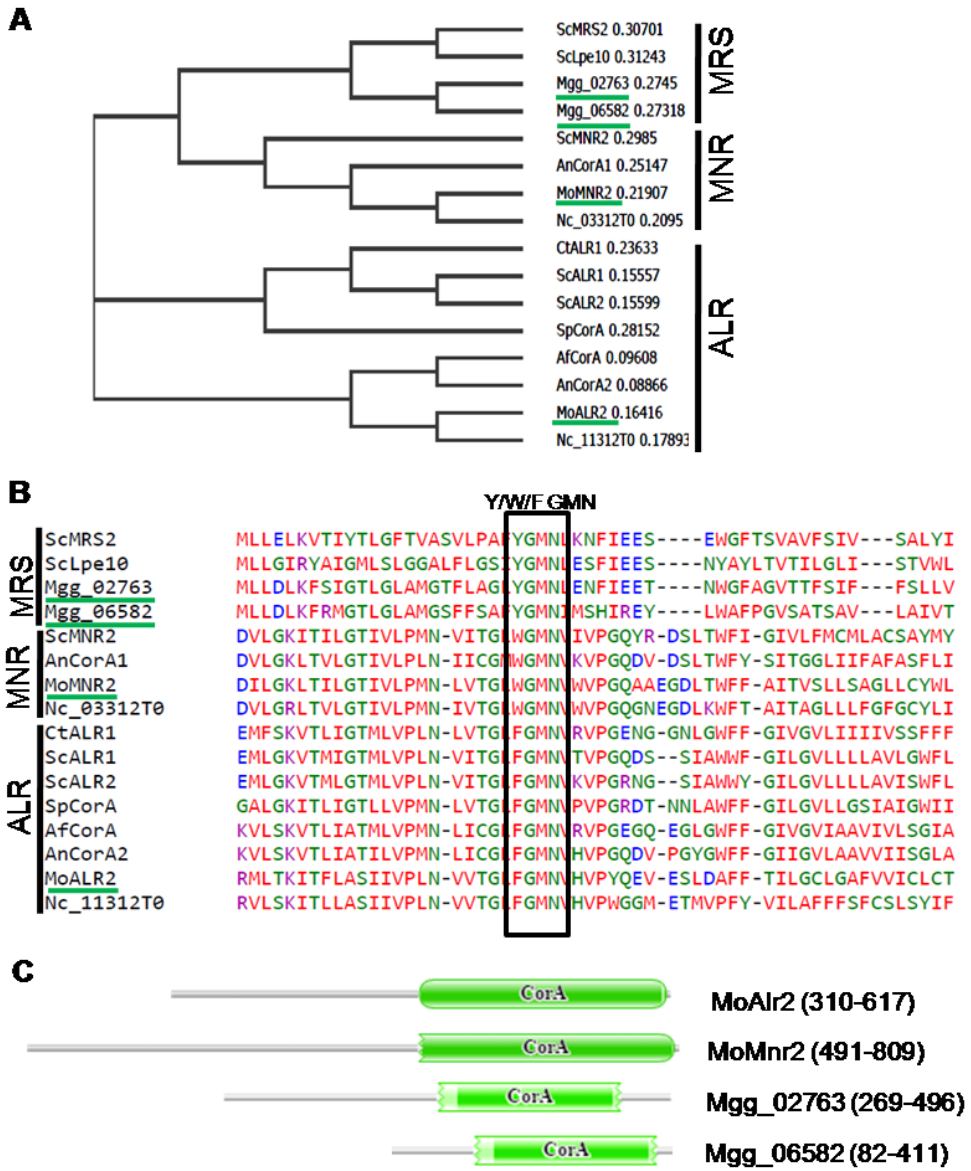

Figure 7: Bioinformatics analysis of *MoALR2, MoMNR2* and *MoMRS2*. (A) The tree was constructed using the Neighbor-Joining method based on alignment of full length sequences of CorA proteins of *M. oryzae* (XP_003713862, XP_003709977, Mgg_02763, Mgg_06582), *S. cerevisiae* (EDV10489, EDV09793, YKL064W, YOR334W, YPL060W), *A. fumigatus* (XP_754049), *A. nidulans* (CBF70700, CBF77902), *C. tropicalis* (XP_002548119), *S. pombe* (NP_595545) and *N. crassa* (NCU11312, NCU03312). The evolutionary distances were computed using the Poisson correction method and are in the units of the number of amino acid substitutions per site. All positions containing gaps and missing data were eliminated. Evolutionary analyses were conducted in MEGA5. (B) The amino acid sequence alignment of CorA proteins *M. oryzae* (XP_003713862, XP_003709977, Mgg_02763, Mgg_06582), *S. cerevisiae* (EDV10489, EDV09793, YKL064W, YOR334W, YPL060W), *A. fumigatus* (XP_754049), *A. nidulans* (CBF70700, CBF77902), *C. tropicalis* (XP_002548119), *S. pombe* (NP_595545) and *N. crassa* (NCU11312, NCU03312) was performed using Clustal Omega. CorA consensus sequence motifs (Y/F/W GMN) for above proteins are highlighted. (C) The conserved domain prediction was done using Pfam tool. CorA domain present in the CorA transporters, MoAlr2, MoMnr2, MoMrs2 (Mgg_02763) and MoMrs2 (Mgg_06582) are shown in green.

5.2 Cloning of *MoALR2* and *MoMNR2* in pYES2 vector to give pYES2-*MoALR2*, pYES2-*MoMNR2* and pYES2-*MoMNR2*$_{489\text{-}812}$

The full length gene of *MoALR2* (1.9 kb) was amplified from genomic DNA and cloned at a *Pvu*II site in the Yeast Episomal Vector pYES2 (Invitrogen, California, USA) to generate pYES2-*MoALR2*.

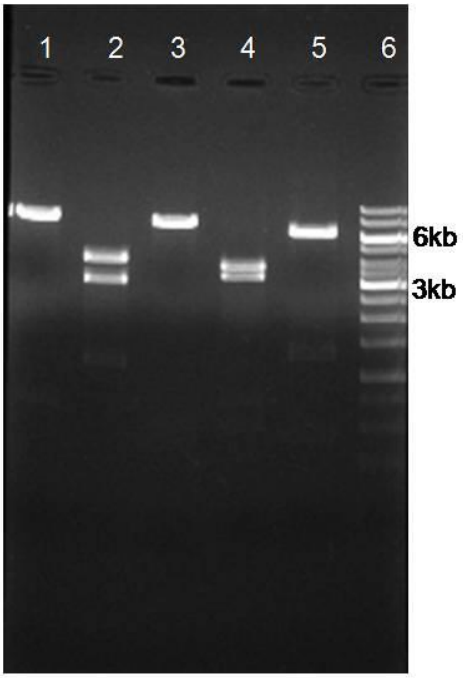

Figure 8: Cloning of *MoALR2* in pYES2 at *Pvu*II site to give pYES2-*MoALR2*. pYES2-*MoALR2* cloning was confirmed by restriction digestion and run on 0.8% agarose gel. Lane 1, 2, 3, 4 and 5 pYES2-*MoALR2* digested with *BamH*1, *EcoR*V, *Hind*III, *Pst*I, *Xho*I respectively. Lane 6 is 1 kb DNA ladder.

pYES2-*MoALR2* cloning was confirmed by restriction digestion with *BamH*1 (7.141 kb + 665 bp), *EcoR*V (3.795 kb + 2.864 kb + 1.147 kb), *Hind*III (6.818 kb + 525 bp + 416 bp + 47 bp), *Pst*I (3.524 kb + 3.077 kb + 717 bp + 488 bp) and *Xho*I (5.892 kb + 1.262 kb + 423 bp + 229 bp) (Figure 8).

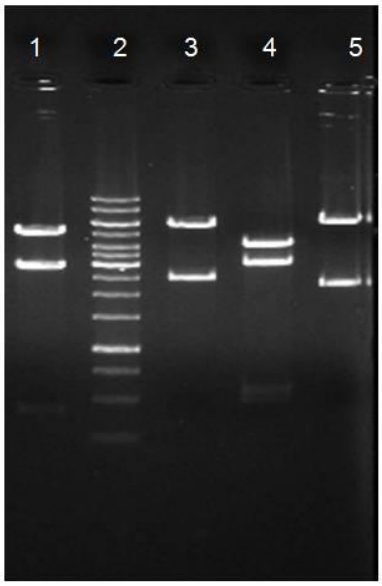

Figure 9: Cloning of *MoMNR2* in pYES2 at *PvuII* site to give pYES2-*MoMNR2*. pYES2-*MoMNR2* cloning was confirmed by restriction digestion and run on 0.8% agarose gel. Lane 1, 3, 4 and 5 pYES2-*MoMNR2* digested with *EcoR*V, *Hind*III and *BamH*1, *Pst*I, *Xho*I respectively. Lane 2 is 1 kb DNA ladder.

The full length gene of *MoMNR2* (2.5 kb) was amplified from genomic DNA and cloned at a *Pvu*II site in the Yeast Episomal Vector pYES2 (Invitrogen, California, USA) to generate pYES2-*MoMNR2*. pYES2-*MoMNR2* cloning was confirmed by restriction digestion with *EcoR*V (5.036 kb + 2.864 kb + 410 bp), *Hind*III and *BamH*1 (5.838 kb + 2.472 kb), *Pst*I (4.145 kb + 3.077 kb + 552 bp + 488 bp + 48bp), and *Xho*I (6.085 kb + 2.225 kb) (Figure 9).

A truncated portion of *MoMNR2* (1.0 kb) was amplified from genomic DNA and cloned at a *Pvu*II site in the Yeast Episomal Vector pYES2 (Invitrogen, California, USA) to generate pYES2- $MoMNR2_{489\text{-}812}$.

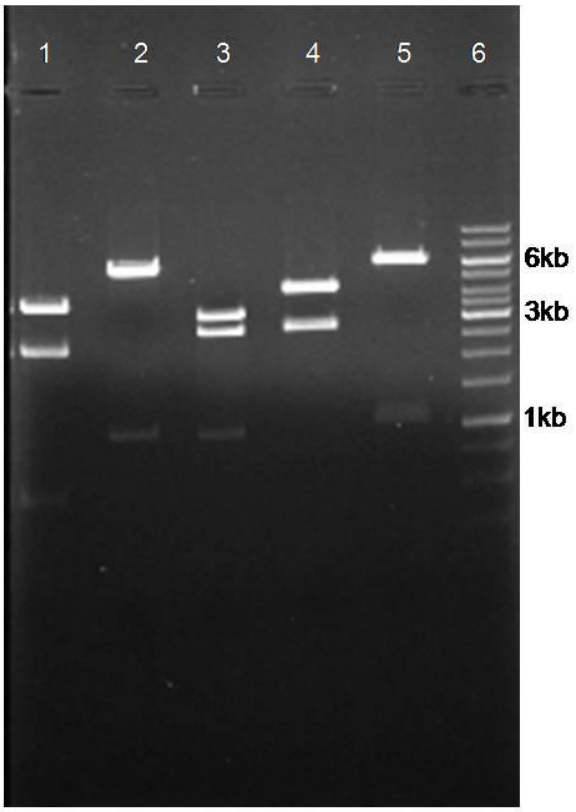

Figure 10: Cloning of *MoMNR2*$_{489-812}$ in pYES2 at *Pvu*II site to give pYES2-*MoMNR2*$_{489-812}$. pYES2-*MoMNR2*$_{489-812}$ cloning was confirmed by restriction digestion and run on 0.8% agarose gel. Lane 1, 2, 3, 4 and 5 pYES2-*MoALR2* digested with *Pst*I, *Kpn*I, *Nde*I and *Kpn*I, *Nde*I, *Xho*I and *BamH*1 respectively. Lane 6 is 1 kb DNA ladder.

pYES2-*MoMNR2*$_{489-812}$ cloning was confirmed by restriction digestion with *Pst*I (3.621 kb + 2.267 kb + 488 bp + 459 bp), *Kpn*I (5.813 kb + 1.022 kb), *Nde*I and *Kpn*I (3.145 kb + 2.668 kb + 983 bp), *Nde*I (4.128 kb + 2.707 kb), and *Xho*I and *BamH*1 (5.792 kb +1.043 kb) (Figure 10).

5.3 Complementation of *S. cerevisiae* Δ*alr1*Δ*alr2* mutant (CM66)

To confirm the nature of CorA Mg^{2+} transporters functionally, complementation with the *M. oryzae* genes was carried out in yeast. The yeast strain CM66 (Δ*alr1*Δ*alr2* mutant), was transformed with the plasmid pYES2, pYES2-*MoALR2*, pYES2-*MoMNR2* and pYES2-*MoMNR2*$_{489-812}$ and transformed colonies were selected on SD medium lacking uracil and having lysine, leucine, 2% Galactose and 500mM $MgSO_4$. The *S. cerevisiae* Δ*alr1*Δ*alr2* mutant CM66 is a haploid disruptant for both *ALR1* and *ALR2* genes. Unlike the wild type

(CM52), the double mutant is unable to grow at 4mM Mg^{2+}, indicating a defect in Mg^{2+} uptake. To test the ability of *MoALR2* and *MoMNR2* to complement the Mg^{2+} uptake defect in CM66, transformants over-expressing either *MoALR2* or *MoMNR2* were first grown in SD media containing 500mM Mg^{2+} and then different dilutions were spotted on SD media containing 4mM Mg^{2+}. The transformants were able to grow even at 4mM Mg^{2+} like the wild type, while the mutant could not (Figure 11A), suggesting that both *MoALR2* and *MoMMR2* could rescue the Mg^{2+} uptake defect and hence have a role in Mg^{2+} transport.

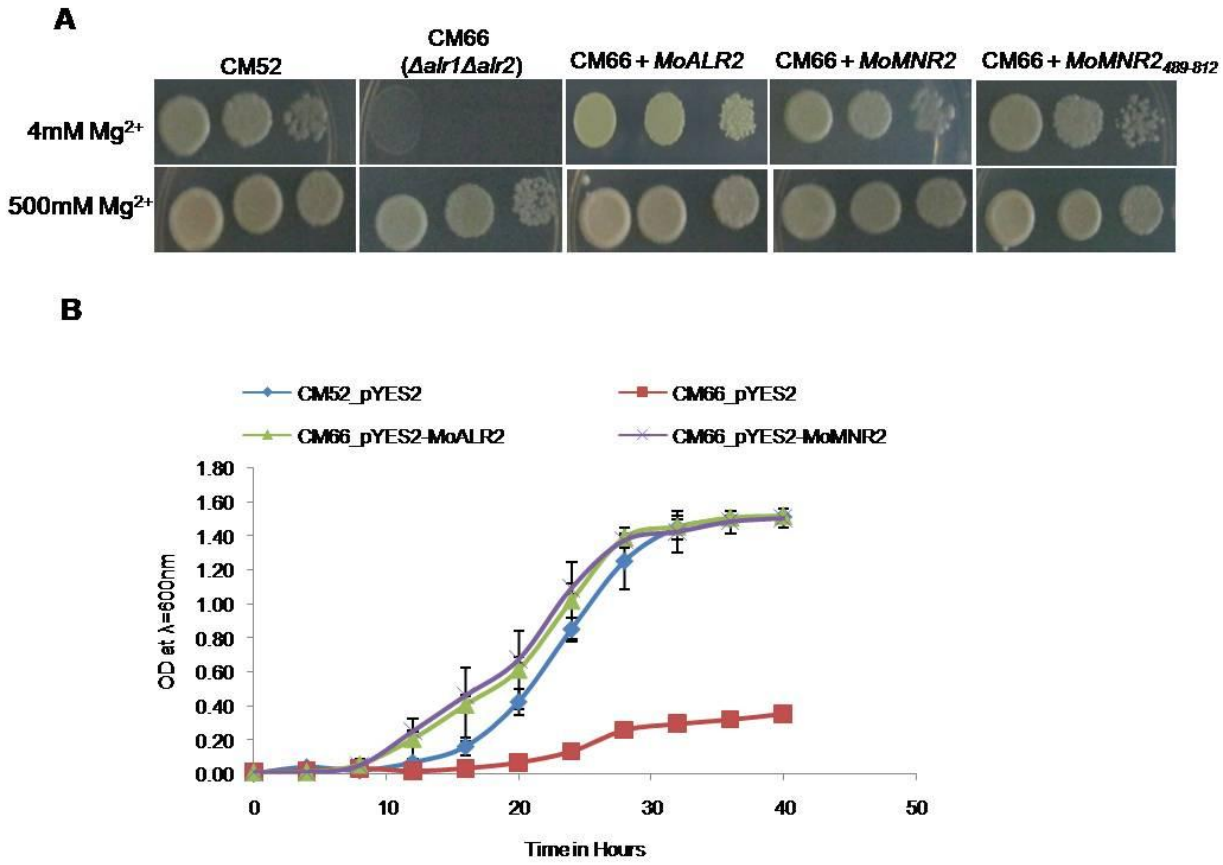

Figure 11: Complementation of *S. cerevisiae* Δ*alr1*Δ*alr2* mutant (CM66). (A) *S. cerevisiae* Δ*alr1*Δ*alr2* mutant (CM66) was transformed with pYES2-*MoALR2*, pYES2-*MoMNR2* and pYES2-*MoMNR2*$_{489-812}$. The transformants were grown overnight on SD+Gal+leu+lys-ura+500mM Mg^{2+} and different dilutions were spotted on SD+Gal–ura+leu+lys containing 4mM Mg^{2+} and 500mM Mg^{2+} and then grown at 28^{0}C for 4 days. (B) Growth curve of CM52_pYES2, CM66_pYES2, CM66_pYES2-*MoALR2* and CM66_pYES2-*MoMNR2* in SD medium with galactose in presence of 4mM Mg^{2+}. The experiments were repeated in triplicate.

Further, a truncated *MoMNR2* having the CorA domain was also able to complement the function in the yeast mutant, suggesting that amino acids of the CorA domain at the Carboxyl terminus (489-812 aa) are sufficient for Mg^{2+} transport. Earlier mutagenesis experiments in

ScAlr1 showed similar effects, where the 239 amino acids at the N-terminal and 53 amino acids at the C-terminal are not essential for Mg^{2+} uptake (Lee and Gardner, 2006).

To validate the growth defect restoration by *M. oryzae* CorA transporters of *S. cerevisiae* Δ*alr1*Δ*alr2* mutant CM66, growth curves of CM52_pYES2, CM66_pYES2, CM66_pYES2-*MoALR2* and CM66_pYES2-*MoMNR2* were done in SD medium supplemented with 4mM Mg^{2+} only and growth of the transformed cells was monitored at intervals of 4 hours up to 40 hours. The growth of CM66_pYES2-*MoALR2* and CM66_pYES2-*MoMNR2* was comparable to that of wild type CM52 transformed with pYES2 only, suggesting restoration of growth even at lower levels of extracellular Mg^{2+} (Figure 11B).

5.4 Generation of knockout cassette for *MoMNR2*, transformation, screening and confirmation of *Δmnr2* knockout transformants

A PCR based technique was used to generate a knockout cassette of *MoMNR2* (Yu JH *et al.*, 2004) wherein the three fragments- 5' Flank, Zeo^r and 3' Flank were taken in 1:3:1 molar ratio and a touch-down PCR (60^0C to 50^0C) was performed for fusion of the three fragments with 1 min elongation time. The final ~3 kb knockout cassette of *MoMNR2* was obtained by using Nested primers which increased the specificity of the product (Figure 12C).

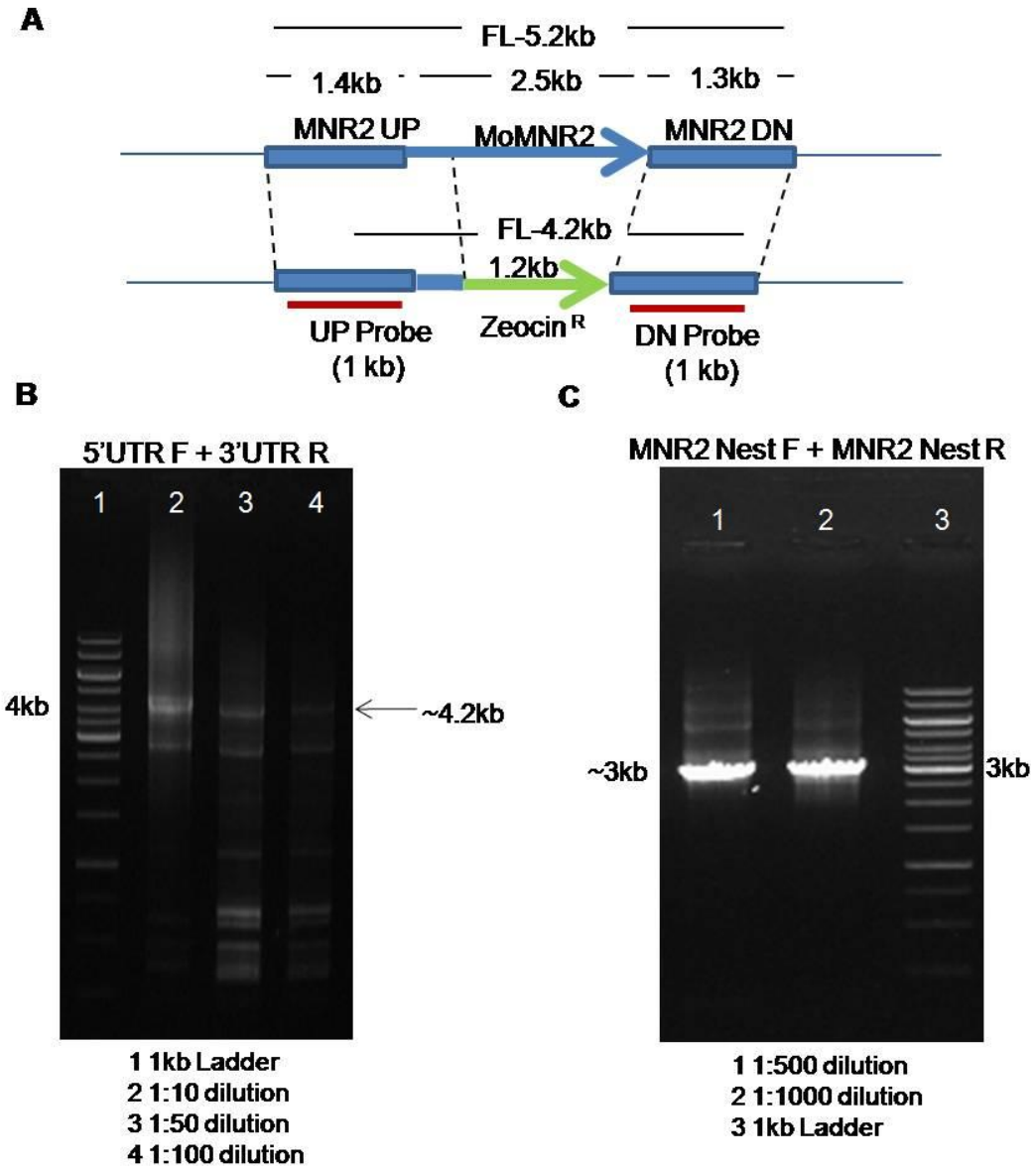

Figure 12: Double joint PCR based generation of knockout cassette for *MoMNR2*. (A) Schematic representation of *MoMNR2* locus and *MoMNR2* knockout cassette. (B) PCR amplification of full knockout cassette of *MoMNR2* (~4.2 kb) was kept with 5' Flank For and 3' Flank Rev using 1:10, 1:50 and 1:100 diluted product obtained after fusion PCR shown in Lane 1, 2 and 3 respectively. Lane 4 is 1 kb DNA ladder. (C) PCR amplification of knockout cassette of *MoMNR2* (~3 kb) with *MoMNR2* Nest For and *MoMNR2* Nest Rev was kept with 1:500 and 1:1000 diluted product obtained from above PCR shown in Lane 1 and 2 respectively. Lane 3 is 1 kb DNA ladder.

The knockout cassette of *MoMNR2* thus obtained was gel purified and used for protoplast transformation of WT *M. oryzae*. A total of 25 transformants were obtained which grew on Zeocin selection. The transformants were screened with PCR using MNR2 (UP) F and MNR2 (DN) R primer pair. The expected size of amplified fragments was 4.6 kb in WT and 4.1 kb in *MoMNR2* knockout transformants.

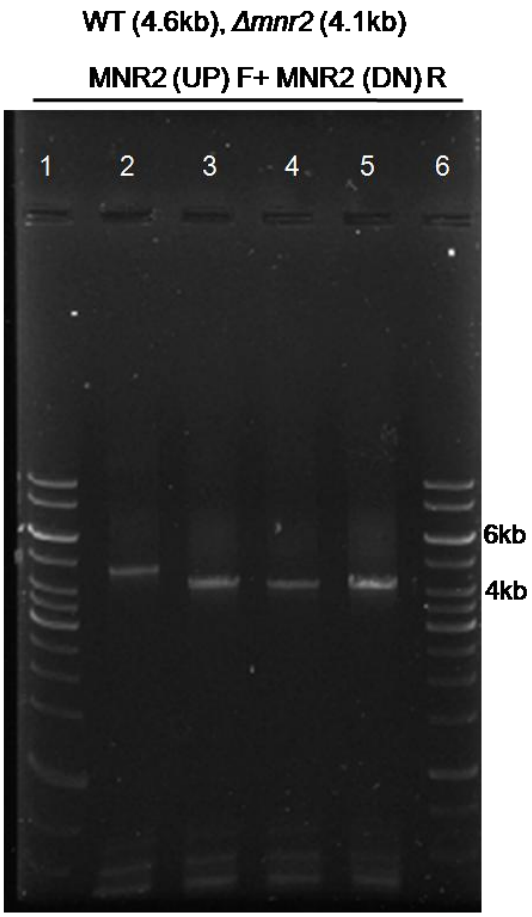

Figure 13: Screening of *Δmnr2* knockout transformants with PCR. Targeted replacement of ***MoMNR2*** with knockout cassette was confirmed with PCR using ***MNR2*** (UP) F and ***MNR2*** (DN) R. Lane 2 PCR with WT genomic DNA, Lane 3, 4, 5 PCR with ***Δmnr2*** knockout transformants. Lane 1 and 6 is 1 kb DNA ladder. The expected size of the product in WT was 4.6 kb and in ***Δmnr2*** knockout 4.1 kb.

3 out of 25 transformants showed the expected size of 4.1 kb with MNR2 (UP) F and MNR2 (DN) R primer pair (Figure 13). Targeted integration of the *MoMNR2* knockout cassette in these three transformants was confirmed by Southern blots, where genomic DNA of WT and three *Δmnr2* knockouts (T1, T2 and T3) was digested with five different enzymes and the blots were probed with two different probes.

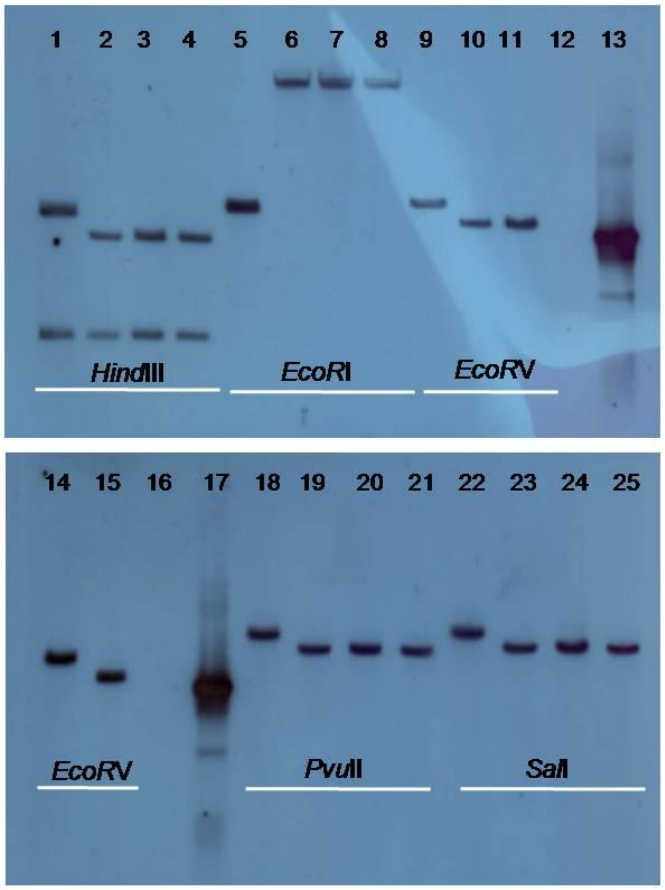

Figure 14: Southern blot analysis of *Δmnr2* and WT with 1 kb of *MNR2* (UP) probe. Wild type (WT) and three independent transformants (T1, T2, T3) for *Δmnr2* were digested with five different restriction enzymes and the blot was probed with *MNR2* (UP) probe to confirm targeted replacement of *MoMNR2*. Lane 1, 9, 14, 18 and 22 WT, Lane 2, 6, 10, 19 and 23 *Δmnr2* T1, Lane 3, 7, 11, 20 and 24 *Δmnr2* T2, Lane 4, 8, 15, 21 and 25 *Δmnr2* T3, Lane 12 and 16 1 kb ladder, Lane 13 and 17 Positive control (3 kb).

With the *MNR2* UP probe, the expected sizes were *Hind*III (WT -1.2 kb and 3.2 kb; Δ*mnr2* -1.2 kb and 2.7 kb), *Eco*RI (WT -3.4 kb; Δ*mnr2* ->11 kb), *Eco*RV (WT -3.7 kb; Δ*mnr2* -3.2 kb), *Pvu*II (WT- 4.5 kb; Δ*mnr2* -4.0 kb) and *Sal*I (WT -4.7 kb; Δ*mnr2* -4.1 kb) (Figure 14).

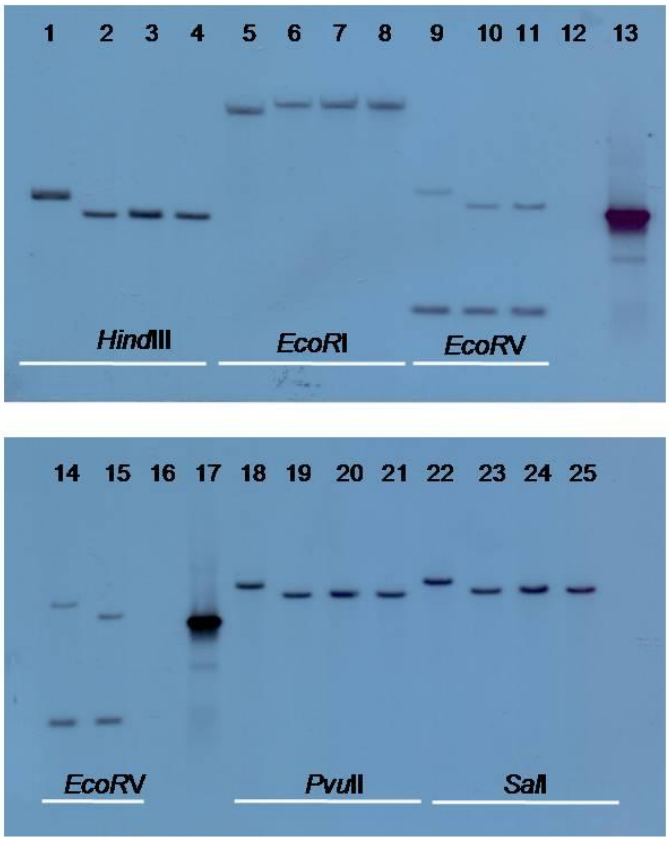

Figure 15: Southern blot analysis of *Δmnr2* and WT with 1 kb of *MNR2* (DN) probe. Wild type (WT) and three independent transformants (T1, T2, T3) for *Δmnr2* were digested with five different restriction enzymes and the blot was re-probed with *MNR2* (DN) probe to confirm targeted replacement of *MoMNR2*. Lane 1, 9, 14, 18 and 22 WT, Lane 2, 6, 10, 19 and 23 *Δmnr2* T1, Lane 3, 7, 11, 20 and 24 *Δmnr2* T2, Lane 4, 8, 15, 21 and 25 *Δmnr2* T3, Lane 12 and 16 1 kb ladder, Lane 13 and 17 Positive control (3 kb).

With the *MNR2* DN probe, the expected sizes were *Hind*III (WT -3.2 kb; Δ*mnr2* -2.7 kb), *EcoR*I (WT ->8.0 kb; Δ*mnr2* ->11 kb), *EcoR*V (WT -3.7 kb and 1.0 kb; Δ*mnr2* -3.2 kb and 1.0 kb), *Pvu*II (WT- 4.5 kb; Δ*mnr2* -4.0 kb) and *Sal*I (WT -4.7 kb; Δ*mnr2* -4.1 kb) (Figure 15). Southern blot analysis confirmed targeted gene deletion of *MoMNR2* in *M. oryzae*.

5.5 Generation of knockout cassette for *MoMRS2* (Mgg_02763 and Mgg_06582), transformation and screening of knockout transformants

Double joint PCR was used to generate a knockout cassette of *MoMRS2* (Mgg_02763 and Mgg_06582) as for *MoMNR2*.

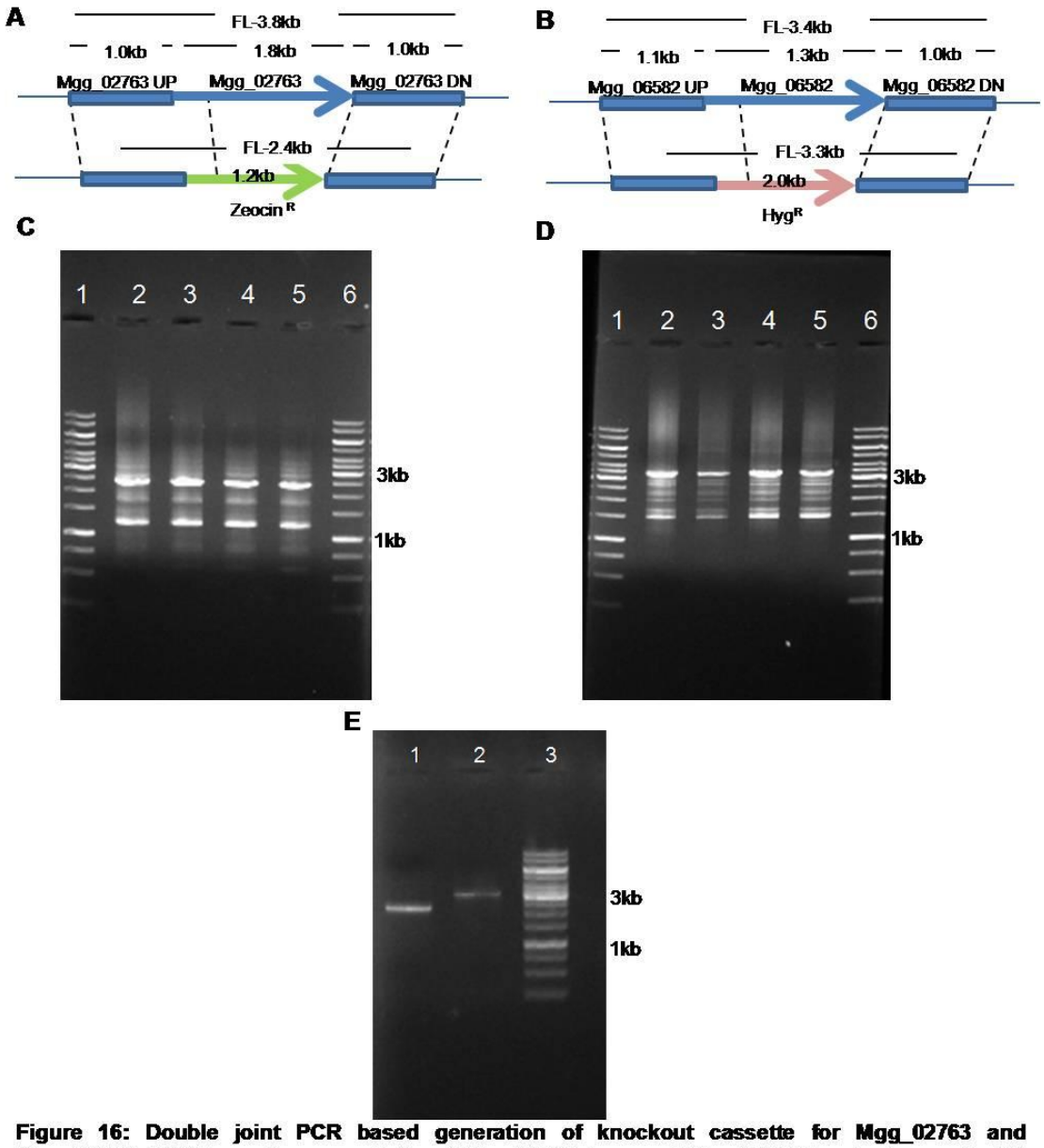

Figure 16: Double joint PCR based generation of knockout cassette for Mgg_02763 and Mgg_06582. (A) Schematic representation of Mgg_02763 locus and Mgg_02763 knockout cassette. (B) Schematic representation of Mgg_06582 locus and Mgg_06582 knockout cassette. (C) PCR amplification of knockout cassette of Mgg_02763 (~2.4 kb) with Mgg_02763 Nest For and Mgg_02763 Nest Rev was kept with 1:50, 1:100, 1:500 and 1:1000 diluted product obtained from full length PCR using 5' UP For and 3' DN Rev. Lane 1 and 6 is 1 kb DNA ladder. (D) PCR amplification of knockout cassette of Mgg_06582 (~3.3 kb) with Mgg_06582 Nest For and Mgg_06582 Nest Rev was kept with 1:50, 1:100, 1:500 and 1:1000 diluted product obtained from full length PCR using 5' UP For and 3' DN Rev. Lane 1 and 6 is 1 kb DNA ladder. (E) Gel elution of knockout cassette of Mgg_02763 (Lane 1) and Mgg_06582 (Lane 2). Lane 3 is 1 kb DNA ladder.

The final ~2.4 kb knockout cassette of Mgg_02763 (having Zeo^r) and the ~3.3 kb knockout cassette of Mgg_06582 (having Hyg^r) was obtained by using nested primers (Figure 16C, 16D). The knockout cassettes for both the genes were gel purified (Figure 16E) and used for protoplast transformation of WT *M. oryzae*.

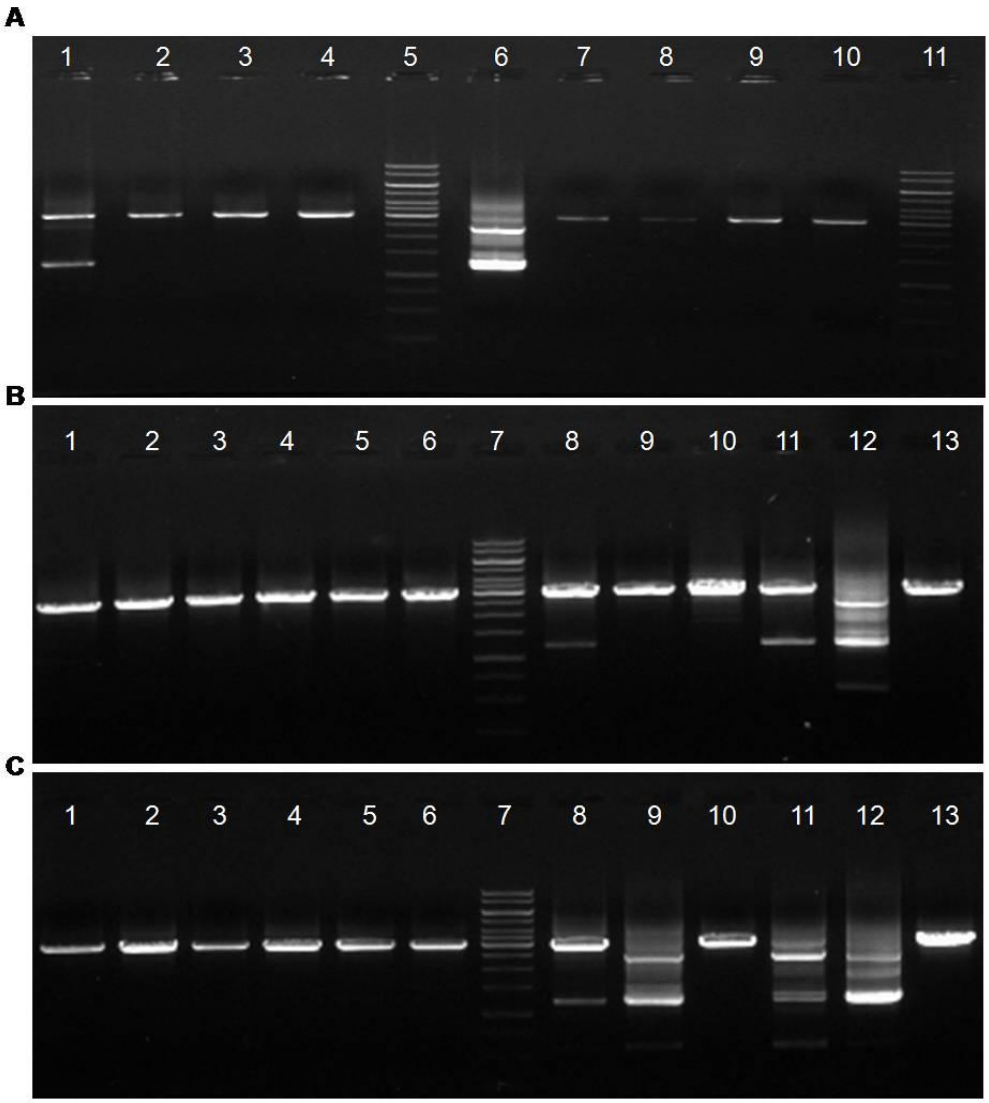

Figure 17: PCR screening of the putative disruption transformants for Mgg_02763. PCR screening of the transformants with Mgg_02763 Nest For and Mgg_02763 Nest Rev. Expected size in true disruptants is ~2.4 kb. (A) Lane 1-4 and Lane 6-9 are different putative transformants, Lane 10 is WT and Lane 5 and 11 is 1 kb DNA ladder. (B) Lane 1-6 and Lane 8-12 are different putative transformants, Lane13 is WT and Lane 7 is 1 kb DNA ladder. (C) Lane 1-6 and Lane 8-12 are different putative transformants, Lane13 is WT and Lane 7 is 1 kb DNA ladder.

55 transformants were obtained growing on Zeocin selection for Mgg_02763. The transformants were screened with PCR using Mgg_02763 Nest F and Mgg_02763 Nest R primer pair. The expected sizes of the amplification products were 3 kb in WT and 2.4 kb in Mgg_02763 knockout transformants. Screening of all the 55 transformants did not yield any true knockouts (Figure 17).

34 transformants were obtained on Hygromycin selection for Mgg_06582.

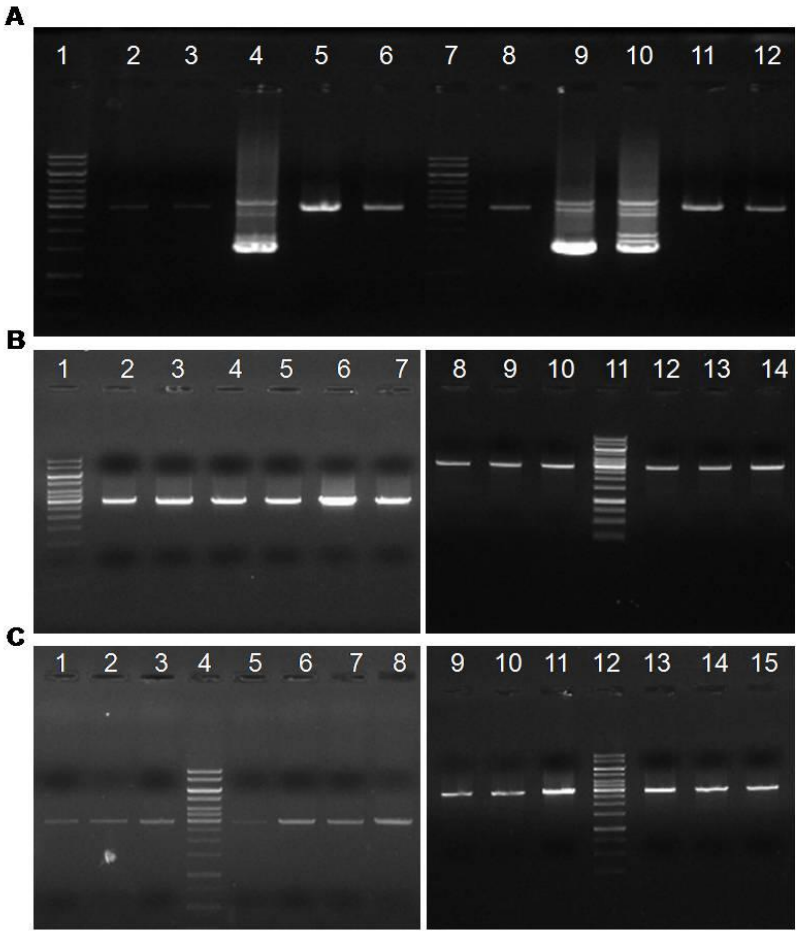

Figure 18: PCR screening of the putative disruption transformants for Mgg_06582. PCR screening of the transformants with Mgg_06582 Nest For and Mgg_06582 Nest Rev. Expected size in true disruptants is ~3.3 kb. (A) Lane 1-6 and Lane 8-11 are different putative transformants, Lane 12 is WT and Lane 7 is 1 kb DNA ladder. (B) Lane 2-7, Lane 8-10 and Lane 12-14 are different putative transformants and Lane 1, 11 is 1 kb DNA ladder. (C) Lane 1-3, Lane 5-8, Lane 9-11 and Lane 13-15 are different putative transformants and Lane 4, 12 is 1 kb DNA ladder.

They were screened with PCR using Mgg_06582 Nest F and Mgg_06582 Nest R primer pair. The expected sizes of amplification products were 3 kb in WT and 3.3 kb in Mgg_06582 knockout transformants. Screening of all the 34 transformants did not yield any true knockout (Figure 18).

5.6 Cloning of disruption cassette of *MoALR2*, *siALR2* in pSD2 site to give pSD2-*siALR2* and $MoALR2_{1400bp}$ in pSilent-1 to give pSilent-$MoALR2_{1400bp}$

The *MoALR2* disruption cassette (*MoALR2*-HPT~6 kb) was moved from pBluescript KS (+) and cloned into a binary vector pGKO2 at *Kpn*I and *Spe*I site to give pGKO2-*MoALR2*-HPT. pGKO2-*MoALR2*-HPT cloning was confirmed by restriction digestion with *BamH*1 (10.989

kb + 3.644 kb + 639 bp), *Spe*I *and Kpn*I (9.258 kb + 6.014 kb), *Pvu*II (7.037 kb + 5.150 kb + 3.085 kb) and *Hind*III (9.343 kb + 4.988 kb + 525 bp + 416 bp) (Figure 19A).

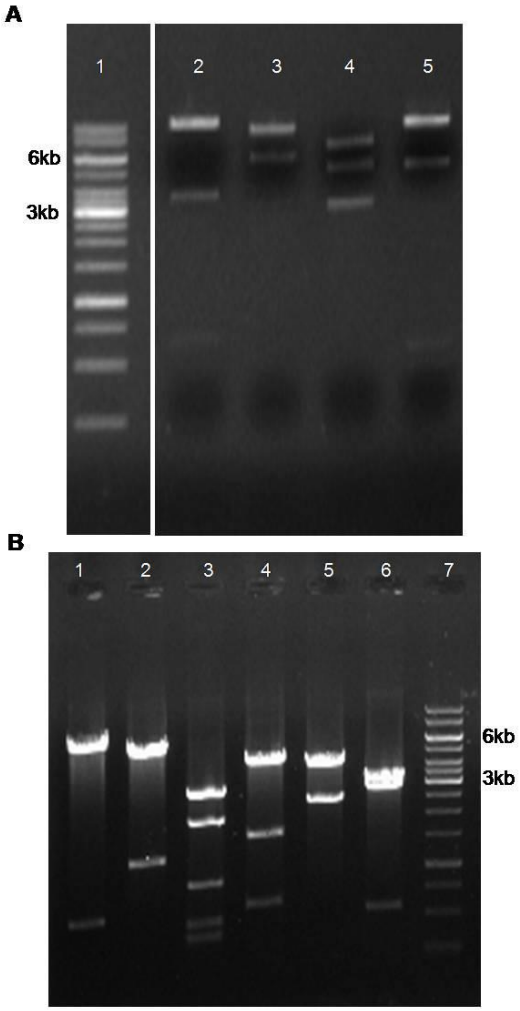

Figure 19: Cloning of Disruption cassette of *MoALR2*. (A) Cloning of *MoALR2* in pGKO2 vector to give pGKO2-*MoALR2*-HPT. pGKO2-*MoALR2*-HPT cloning was confirmed by restriction digestion and run on 0.8% agarose gel. Lane 2, Lane 3, Lane 4 and Lane 5 pGKO2-*MoALR2*-HPT digested with *BamH*1, *Spe*I *and Kpn*I, *Pvu*II and *Hind*III respectively. Lane 1 is 1 kb DNA ladder. (B) Cloning of *MoALR2* in pBSKS+ vector to give pBSKS-*MoALR2*-HPT. pBSKS-*MoALR2*-HPT cloning was confirmed by restriction digestion and run on 0.8% agarose gel. Lane 1, 2, 3, 4, 5 and 6 pBSKS-*MoALR2*-HPT digested with *BamH*1, *Cla*I, *Hind*III, *Pst*I, *Pvu*II and *Sac*I respectively. Lane 7 is 1 kb DNA ladder.

A smaller disruption cassette of *MoALR2* (~4 kb) was also cloned in the vector pBluescript KS (+) to give pBSKS-*MoALR2*-HPT, which was confirmed by restriction digestion with *BamH*1 (6.178 kb + 639 bp), *Cla*I (4.495 kb + 1.275 kb + 1.048 kb), *Hind*III (2.8 kb + 2.1 kb + 906 bp + 525 bp + 416 bp), *Pst*I (4.55 kb + 1.6 kb + 643 bp), *Pvu*II (4.304 kb + 2.513 kb) and *Sac*I (3.316 kb + 2.958 kb + 543 bp) (Figure 19B).

For knockdown of *MoALR2* a ~110 bp fragment of *MoALR2* (*siALR2*), which spans a stretch corresponding to the 5' UTR, was amplified and cloned in the pSilent-Dual 2 vector at *Sma*I site to give pSD2-*siALR2*.

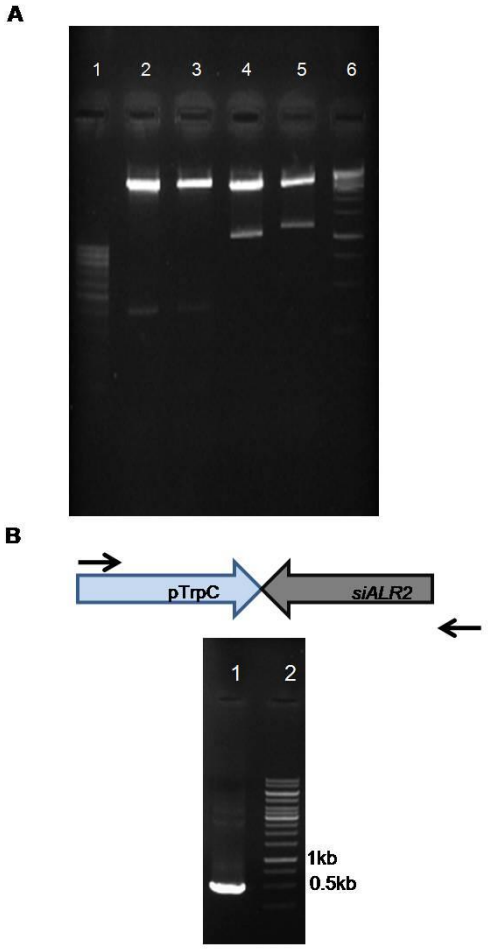

Figure 20: Cloning of *siALR2* in pSD2 at *Sma*I site to give pSD2-*siALR2*. (A) pSD2-*siALR2* cloning at *Sma*I site in pSD2 was confirmed by restriction digestion and run on 2.0% agarose gel. Lane 2 and 4 pSD2 digested with *EcoR*I and *Sac*I, *Bam*HI respectively. Lane 3 and 5 pSD2-*siALR2* digested with *EcoR*I and *Sac*I, *Bam*HI respectively. Lane 1 is 100 bp DNA ladder. (B) pSD2-*siALR2* cloning confirmation using PCR and run on 0.8% agarose gel. Lane 1 PCR amplification of pSD2-*siALR2* with pTrpC For and siALR2 For. Lane 2 is 1 kb DNA ladder.

The clone was confirmed by restriction digestion with *EcoR*I and *Sac*I (5.4 kb + 400 bp), and *Bam*HI (4.5 kb + 1.2 kb) (Figure 20A). The antisense orientation of *siALR2* was confirmed by PCR with pTrpC For and siALR2 For, which gave amplification of the expected size of 500 bp (Figure 20B).

For simultaneous silencing of *MoALR2* and *MoMNR2*, a fragment of 1.4 kb (encoding a portion of the CorA domain) of *MoALR2* was cloned in antisense orientation in pSilent-1 at *Kpn*I and *Bgl*II site to give pSilent-*MoALR2*$_{1400bp}$.

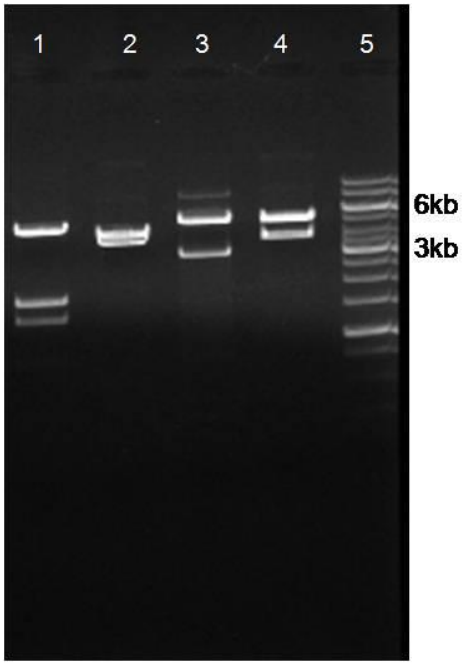

Figure 21: Cloning of *MoALR2*$_{1400bp}$ in pSilent at *Kpn*I and *Bgl*II site to give pSilent-*MoALR2*$_{1400bp}$- pSilent-*MoALR2*$_{1400bp}$ cloning at *Kpn*I and *Bgl*II site in pSilent was confirmed by restriction digestion and run on 0.8% agarose gel. Lane 1, 2, 3 and 4 pSilent-*MoALR2*$_{1400bp}$ digested with *EcoR*I, *Sac*I, *Kpn*I and *Bam*HI, *Xba*I respectively. Lane 5 is 1 kb DNA ladder.

The clone was confirmed by restriction digestion with *EcoR*I (4.619 kb + 1.644 kb + 1.320 kb + 775 bp), *Sac*I (4.125 kb + 3.690 kb + 543 bp), *Kpn*I and *Bam*HI (4.791 kb + 2.839 kb + 718 bp + 10 bp), and *Xba*I (4.785 kb + 3.573 kb) (Figure 21).

5.7 Transformation of *M. oryzae* B157 using *MoALR2* Disruption cassette (pGKO2-*MoALR2*-HPT)

The *A. tumefaciens* strain LBA4404/pSB1 was first transformed with pGKO2-*MoALR2*-HPT via triparental mating (Helper plasmid pRK2013). The transformed *Agrobacterium* was then used to carry out *A. tumefaciens* mediated transformation of *M. oryzae* and transformants were selected on Hygromycin (200µg ml^{-1}) containing 10mM Mg^{2+}. Supplementation of different Mg^{2} concentrations during selection was done to overcome the selective disadvantage facing slow growing mutants. 202 transformants were obtained on the selection plate (Figure 22A). We took the advantage of the dual selection property of the vector

pGKO2, where the herpes simplex virus thymidine kinase (*HSVtk*) gene product converts 5-fluoro-2'-deoxyuridine (F2DU) to a toxic compound in ectopic transformants (ectopic transformants express *HSVtk*, while gene replacement mutants lack *HSVtk*). This helps in recognition of targeted mutants, counter selecting against ectopic transformants by growing the transformants on medium supplemented with 5-fluoro-2'-deoxyuridine. After plating all the 202 transformants on media supplemented with Hygromycin (200µg ml^{-1}), 100mM Mg^{2+} and 5µM F2DU, we obtained only 20 transformants growing on media with F2DU (Figure 22B). These 20 transformants were checked for targeted integration of the disruption cassette. However, all transformants showed the native gene amplification pattern, indicating that they were not true disruptants. We also screened the remaining transformants, but none of them were true disruptants (Figure 22C, 22D).

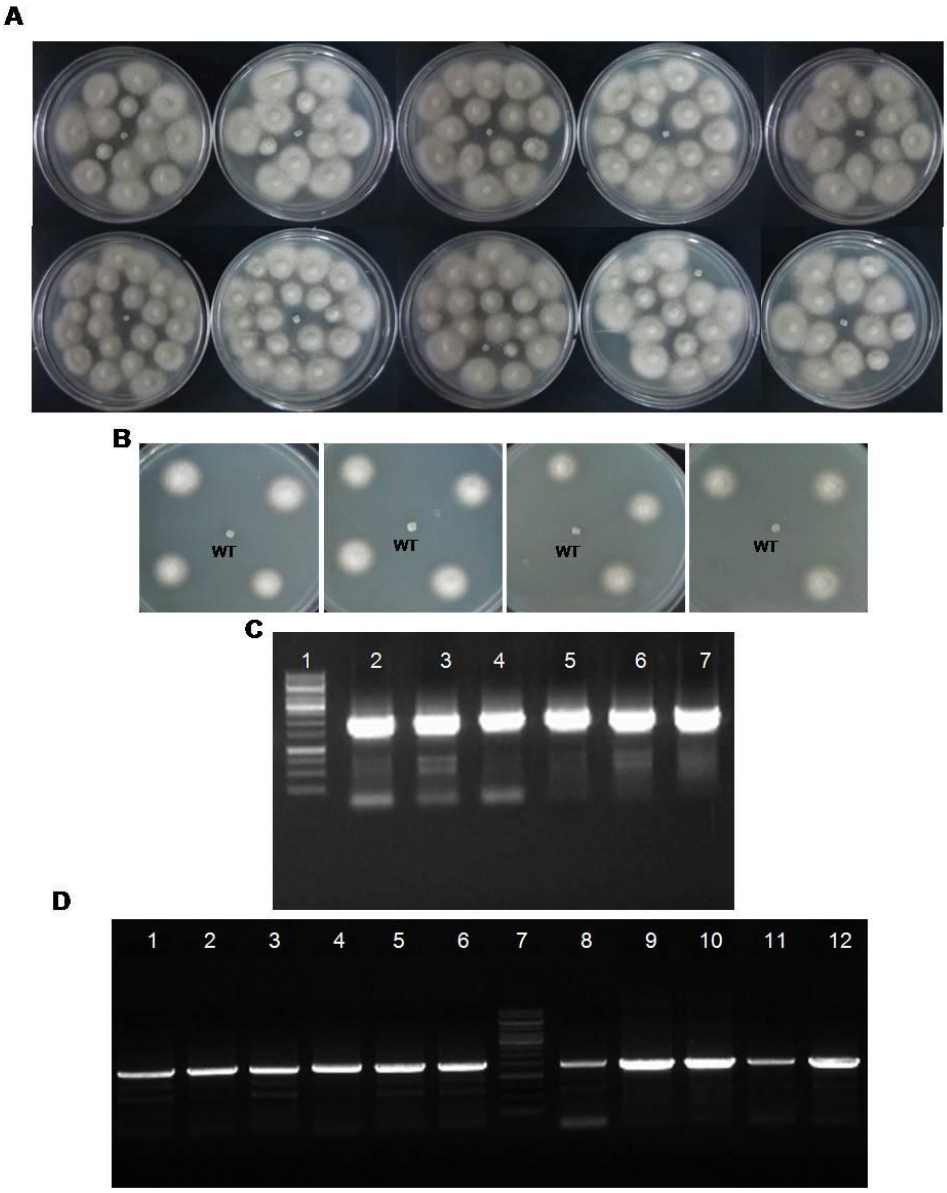

Figure 22: Transformants (obtained after ATMT) growing on selection plate. (A) Representative pictures of transformants obtained after ATMT growing on YEGA containing Hygromycin (200µg ml^{-1}) with 10mM Mg^{2+}. (B) Representative pictures of transformants growing on YEGA containing Hygromycin (200µg ml^{-1}) with 10mM Mg^{2+} and 5µM F2DU. WT represents Wild type. **PCR screening of the putative disruption transformants for *MoALR2* using pGKO2-*MoALR2*-HPT.** (C) PCR screening of the transformants with *MoALR*2 For and *MoALR*2 Rev. Expected size in true disruptants is ~6 kb. Lane 1 is 1 kb DNA ladder and Lane 2-7 are different putative transformants. (D) PCR screening of the transformants with *MoALR*2 For and Real *MoALR*2 Rev. Expected size in true disruptants is ~5 kb. Lane 1-6 and 8-12 are different putative transformants and Lane 7 is 1 kb DNA ladder.

5.8 Protoplast transformation of *M. oryzae* B157 using split marker

Protoplast transformation of *M. oryzae* B157 was also carried out by the split marker technique, using two different overlap regions. Equal molar ratio of products with an overlap of 1088 bp and 401 bp was used to carry out transformation and the transformants were selected on Hygromycin (200µg ml^{-1}) containing 10mM/100mM Mg^{2+}.

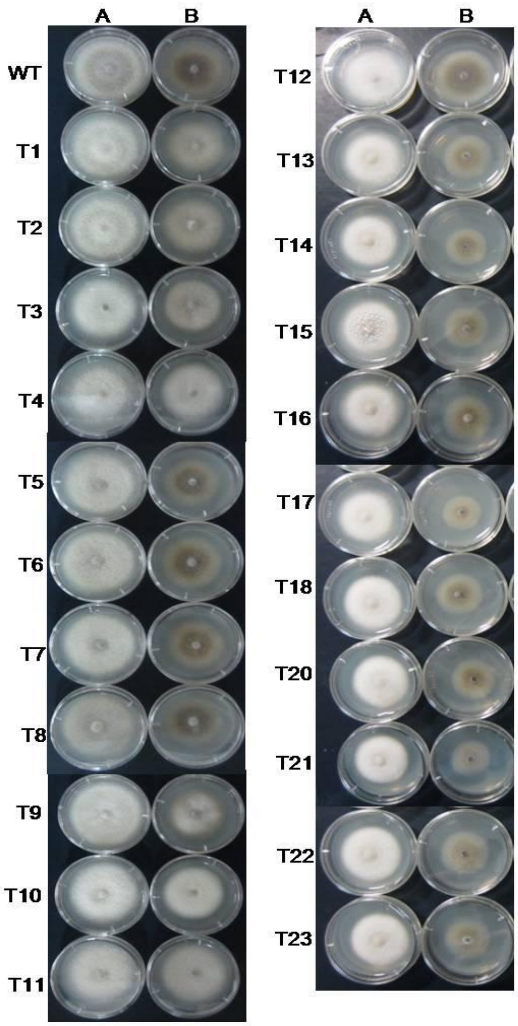

Figure 23: Growth of putative disruption transformants for *MoALR2* on Co(III)Hex. The transformants obtained on media containing Hygromycin (200µg ml^{-1}) and 10mM/100mM Mg^{2+} were also put on media containing 350µM Co(III)Hexaammine. The sensitivity in terms of growth was compared with growth on YEGA (A) and YEGA + 350µM Co(III)Hex.(B).

99 transformants (55 with 1088 bp overlap and 44 with 401 bp overlap) were obtained. The transformants growing on the selection plates were also put on media containing 350µM Co(III)Hexaammine. Cation hexaammines like Co(III)Hexaammine are selective inhibitors of CorA Mg^{2+} transporters that prevent Mg^{2+} uptake, while they are not themselves

transported into the cell. Unlike WT, growth of CorA knockout/knockdown strains is not sensitive to cation hexaammines, demonstrating that the inhibition is mediated by an interaction between CorA and the hexaammines). Of the 99 transformants, 43 transformants showed better growth on Co(III)Hex. than WT (Figure 23).

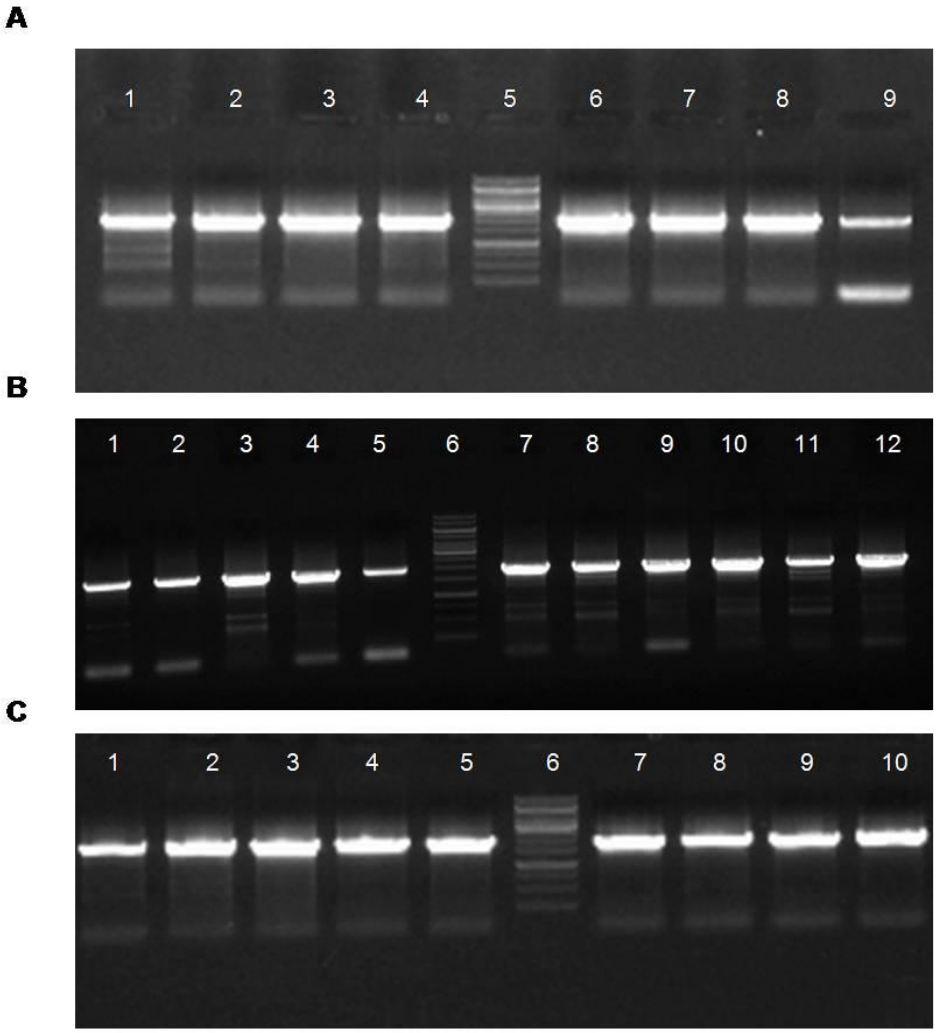

Figure 24: PCR screening of the putative disruption transformants using split marker for *MoALR2*. PCR screening of the transformants with *MoALR2* For and *MoALR2* Rev. Expected size in true disruptants is ~6 kb. (A) Lane 1-4 and Lane 6-9 are different putative transformants and Lane 5 is 1 kb DNA ladder. (B) Lane 1-5 and Lane 7-12 are different putative transformants and Lane 6 is 1 kb DNA ladder. (C) Lane 1-5 and Lane 7-10 are different putative transformants and Lane 6 is 1 kb DNA ladder.

These transformants were checked for targeted integration of the disruption cassette, but we obtained the native gene amplification pattern for all the transformants, indicating that they were not true disruptants (Figure 24A, 24B, 24C) (Table 2).

Table 2 Disruption of *MoALR2* by different approaches

	No. of transformants	**No. of transformants growing on F2DU (5µM)**	**Concentration of $MgSO_4$ used**	**Co (III)Hex. used for secondary selection**	**True Disruptants obtained**
ATMT in wild type B157	202	20	100mM	N.A.	NONE
Protoplast transformation with Disruption cassette in wild type B157	38	N.A.	10mM/100mM	350µM/400µM	NONE
Protoplast transformation with Split Marker (overlap of 1.1Kb) in wild type B157	55	N.A.	10mM/100mM	350µM/400µM	NONE
Protoplast transformation with Split Marker (overlap of 400bp) in wild type B157	44	N.A.	10mM/100mM	350µM/400µM	NONE
Protoplast transformation with KS-MoALR2-HPT (~4Kb) disruption cassette in *Δku80* strain	34	N.A.	100mM	N.A.	NONE

5.9 Protoplast transformation of *M. oryzae Δku80* using *MoALR2* Disruption cassette (pBSKS-*MoALR2*-HPT)

As in other filamentous fungi, the frequency of homologous recombination in *M. oryzae* is low (average 7%). It has been shown that the *MoKU80* gene is essential for non-homologous end joining (NHEJ) of DNA double strand breaks and that *Δku80* mutants show a higher frequency of targeted gene replacement (>80%).

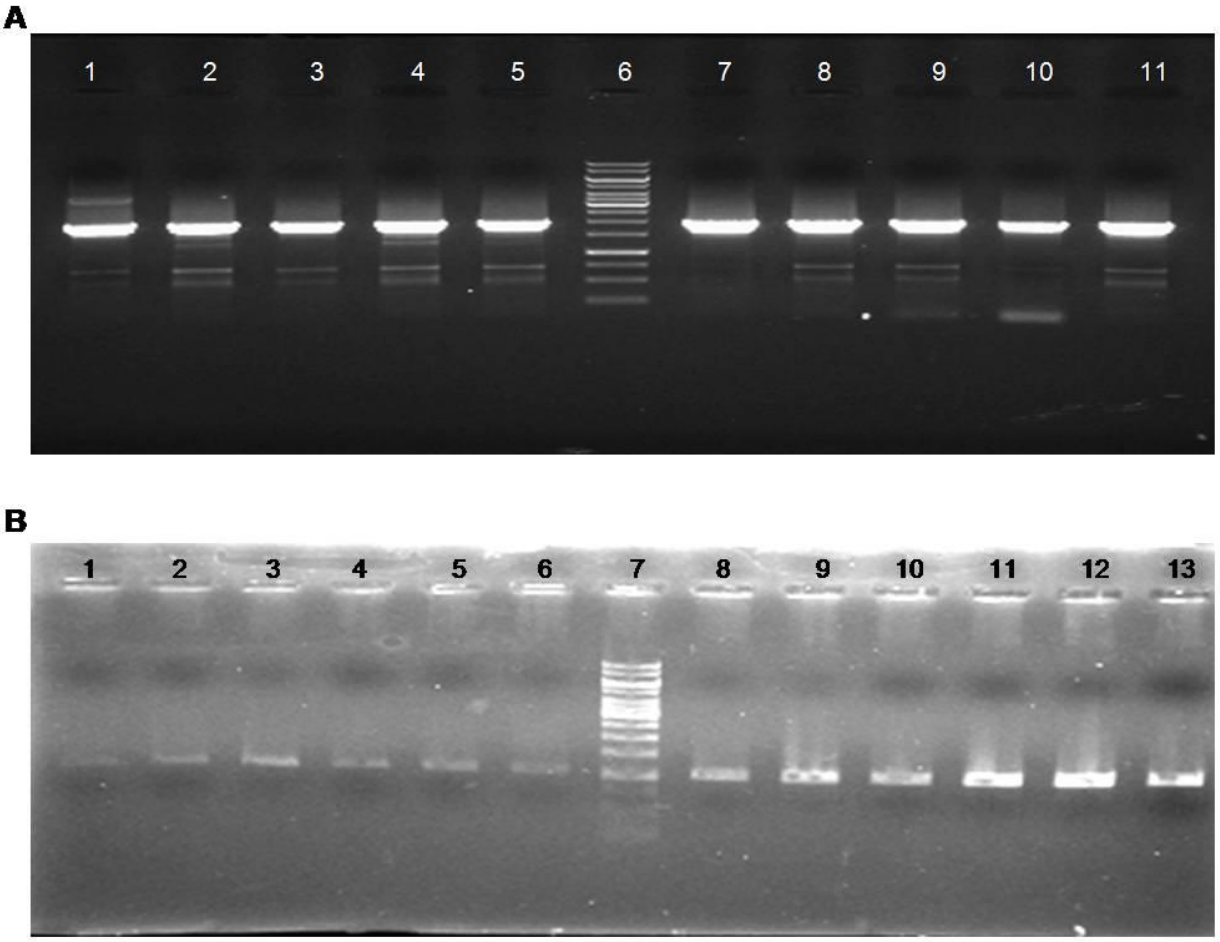

Figure 25: PCR screening of the putative disruption transformants using pBSKS-*MoALR2*-HPT in *Δku80* for *MoALR2*. (A) PCR screening of the transformants with *MoALR2* For and *MoALR2* Rev. Expected size in true disruptants is ~4 kb. Lane 1-5 and Lane 7-11 are different putative transformants and Lane 6 is 1 kb DNA ladder. (B) PCR screening of the transformants with *MoALR2* For and Real *MoALR2* Rev. Expected size in true disruptants is ~3 kb. Lane 1-6 and Lane 8-13 are different putative transformants and Lane 7 is 1 kb DNA ladder.

We attempted targeted disruption of *MoALR2* in the *Δku80* background known to aid homologous integration, where the disruption cassette of *MoALR2* in pBSKS+ (pBSKS-*MoALR2*-HPT) was used for protoplast transformation of the *Δku80* strain (generated in our laboratory in WT B157), and transformants were selected on Hygromycin (200µg ml^{-1}) and 100mM Mg^{2+}. We obtained 34 transformants. But screening of all the transformants yielded only ectopic integrants (Figure 25A, 25B).

5.10 Protoplast transformation of *M. oryzae* B157 using knockdown constructs (pSD2-*siALR2* and pSilent-*MoALR2*$_{1400bp}$)

The knockdown constructs were used for protoplast transformation of WT fungus. Putative knockdown transformants were selected on Hygromycin (200µg ml^{-1}) and Geneticin (1mg ml^{-1}). Further, pSD2-*siALR2* was introduced into *Δmnr2* (for knockdown of *MoALR2* in a *MoMNR2* knockout background). Untransformed *M. oryzae* was kept as a control which did not grow on either Hygromycin or Geneticin medium. Empty vector transformation was also done as a control. 23 transformants were obtained for WT transformation with pSilent-*MoALR2*$_{1400bp}$, 12 for WT transformation with pSD2-*siALR2* and 21 transformants were obtained for *Δmnr2* transformation with pSD2-*siALR2*.

5.11 Relative Expression analysis of CorA Mg^{2+} transporters at transcript level

The knockdowns were validated by analysis of relative expression of *MoALR2* and *MoMNR2* by quantitative Real Time PCR (qRT-PCR) in the transformants. Transformants in the WT background (WT+siALR2) showed transcript levels of *MoALR2* ranging from 48% to 85%, while those in the background of *Δmnr2* (*Δmnr2*+siALR2) showed transcript levels ranging from 66% to 88% compared to WT (Table 3).

Table 3 Relative expression of CorA Mg^{2+} transporters in knockdown transformants

Knockdown transformants	**Relative Expression of *MoALR2* (%)**	**Relative Expression of *MoMNR2* (%)**
RNAi knockdown transformants in WT		
R1	43	64
R2	54	62
R3	60	67
R5	57	81
R10	68	83
R19	55	76
Anti-sense knockdown transformants in WT		
A2	43	52
A3	54	57
A4	65	59
A10	47	60
A13	73	54
A15	30	37
A19	80	90
MoALR2 silencing in WT		
WT_1	85	93
WT_4	81	90
WT_5	48	89
WT_6	56	90
WT_8	75	87
WT_9	78	94
MoALR2 silencing in *Δmnr2*		
*Δmnr2*_3	88	0
*Δmnr2*_4	83	0
*Δmnr2*_7	81	0
*Δmnr2*_9	86	0
*Δmnr2*_10	80	0
*Δmnr2*_18	78	0
*Δmnr2*_20	66	0

No transcripts of *MoMNR2* were detected in *Δmnr2* background transformants, while the levels of *MoMNR2* did not change in the *MoALR2* knockdown transformants in wild type background, thereby confirming the specificity of the cassette (pSD2-*siALR2*) used for *MoALR2* silencing. Since *MoALR2* could not be silenced more strongly in the *Δmnr2* background, to obtain transformants with further reduced transcript levels of *MoALR2*, an alternative knockdown approach for simultaneous silencing of both *MoALR2* and *MoMNR2* was also used. As these two genes show high similarity in the CorA domain, we carried out

simultaneous silencing using an antisense construct targeted to this region. The knockdown was validated by qRT-PCR of *MoALR2* and *MoMNR2* in the transformants. The transformants showed transcript levels ranging from 30% to 80% and 37% to 90% for *MoALR2* and *MoMNR2* respectively, compared to WT (Table 3).

5.12 Growth assay of the knockout and knockdown transformants in presence of Co(III) Hex.

To be sure that reduced transcript levels translated into decline in transporter levels, we used a Co(III) Hexaammine sensitivity test. CorA knockout/knockdown strains are less sensitive to cation hexaammines than the WT, demonstrating that the inhibition is mediated by an interaction between CorA and the hexaammine.

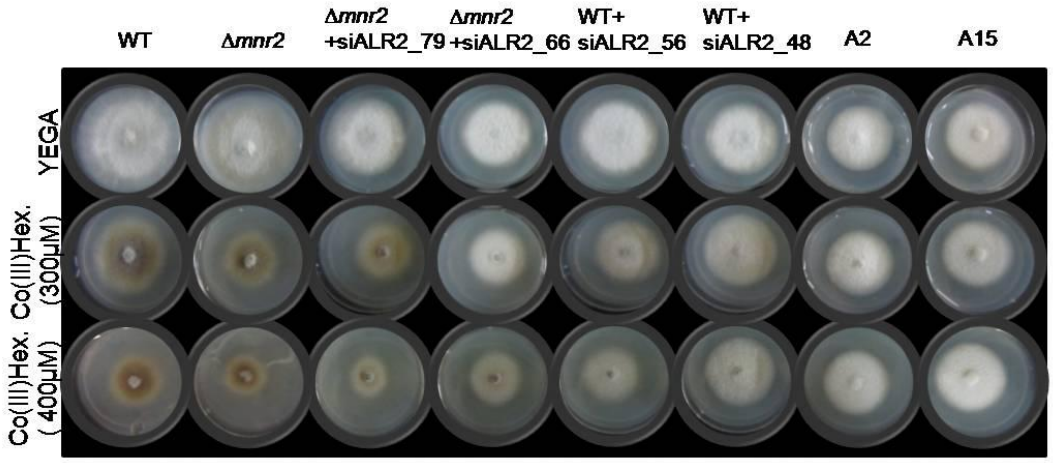

Figure 26: Sensitivity assay in presence of Co(III) Hex. for the knockout and knockdown transformants. CorA specific inhibitor (Cobalt (III) hexaammine (Co (III) Hex.), was added to YEG medium at concentrations of 300μM and 400μM. The sensitivity was assessed relative to Wild type (WT) five days post inoculation and growth was measured for WT, *Δmnr2* and knockdown transformants.

Cation hexammines like Co(III) Hexaammine are selective inhibitors of CorA Mg^{2+} transporters that prevent Mg^{2+} uptake, while they are not themselves transported into the cell. We tested the sensitivity of knockdown transformants as compared to WT. Two independent knockdown transformants from each category, namely Alr2 silencing (WT+siALR2), *Δmnr2*+siALR2 and simultaneously silenced for *MoALR2* and *MoMNR2*, which were least sensitive to Co(III)Hex., were selected for further study (Figure 26). The degree of resistance

to Co(III)Hex. of the selected transformants, *Δmnr2*+siALR2_79, *Δmnr2*+siALR2_66, WT+siALR2_56, WT+siALR2_48, A2 and A15, correlated with the degree of silencing of *MoALR2*.

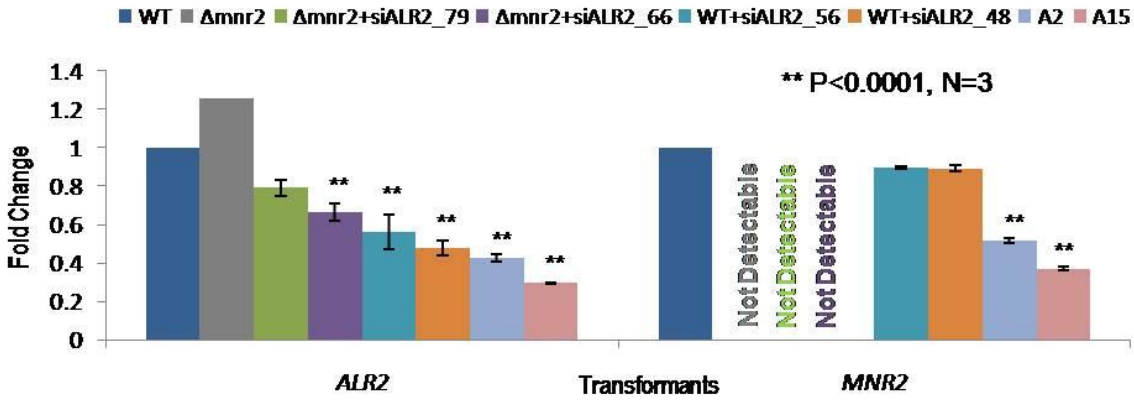

Figure 27: Expression analysis of *MoALR2* and *MoMNR2* in the knockout and knockdown transformants. mRNA levels of *MoALR2* and *MoMNR2* were estimated by qRT-PCR. The transcript levels were expressed as relative values, with 1 corresponding to WT.

The relative expression levels of *MoALR2* and *MoMNR2* in the transformants were 1.26 and 0 for *Δmnr2*, 0.79 and 0 for *Δmnr2*+siALR2_79, 0.66 and 0 for *Δmnr2*+siALR2_66, 0.56 and 0.90 for WT+siALR2_56, 0.48 and 0.89 for WT+siALR2_48, 0.43 and 0.52 for A2 and 0.30 and 0.37 for A15 (Figure 27). Interestingly, the *Δmnr2* knockout was more sensitive to Co(III)Hex. than wild type. This is consistent with the observation that expression of *MoALR2* is higher in *Δmnr2* than in WT.

5.13 Southern blot analysis of the knockdown transformants

Southern blot analysis was done to check the number of integrations in the selected knockdown transformants. Genomic DNA of WT, pSD2 transformants and knockdown transformants both in the background of WT and *Δmnr2* was digested with *Eco*RI and probed with 1.2 kb fragment upstream to *MoALR2* to confirm the integration of silencing cassette.

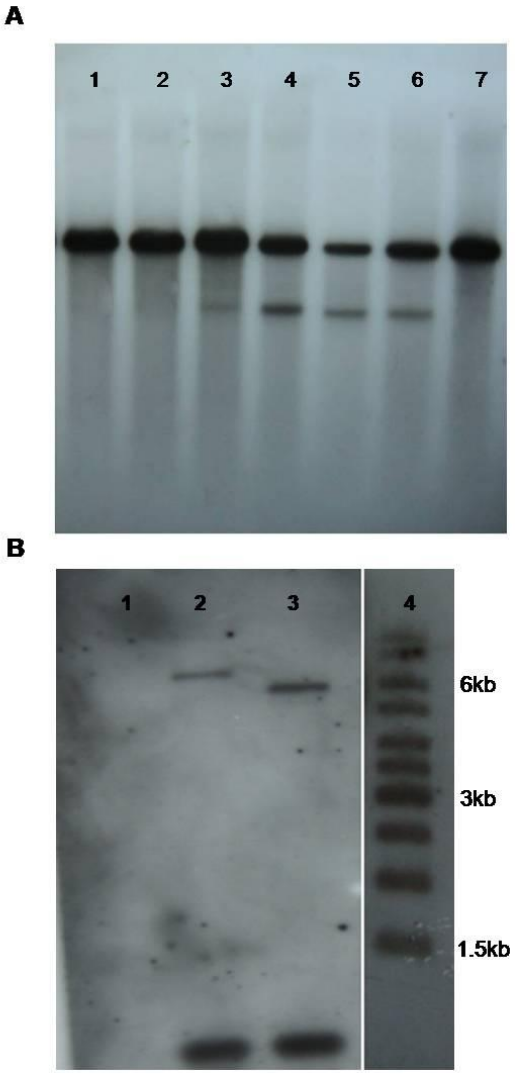

Figure 28: Southern blot analysis of knockdown transformants. (A) WT, pSD2 transformants and knockdown transformants both in the background of WT and *Δmnr2* were digested with *EcoR*I and probed with 1.2 kb fragment upstream to *MoALR2* to confirm the integration of silencing cassette. Lane 1 pSD2_T1, 2 pSD2_T2, 3 *Δmnr2* +siALR2_79, 4 *Δmnr2* +siALR2_66, 5 WT+siALR2_56, 6 WT+siALR2_48, 7 WT. (B) WT and simultaneously silenced transformants, A2 and A15, were digested with *Sal*I and probed with TrpcP to confirm integration of silencing construct. Lane 1 WT, Lane 2 A2, Lane 3 A15, Lane 4 1 kb DNA ladder.

pSD2 transformants (pSD2_T1, pSD2_T2) like WT showed a single band, while the knockdown transformants showed an extra band corresponding to single integration of the knockdown cassette (Figure 28A). Genomic DNA of WT and simultaneously silenced transformants, A2 and A15, was digested with *Sal*I and probed with TrpcP to confirm integration of the silencing construct. No signal was expected in WT, while *Sal*I had a restriction site in the pTrpC promoter, thus giving two signals (400 bp+ >2 kb) (Figure 28B). We obtained two signals in both A2 and A15; the band size in A2 and A15 was different,

suggesting integration of the knockdown cassette at two different loci in the genome. Southern blot analysis confirmed single site integration in these transformants.

5.14 Heterologous expression of CorA domain of *MoMNR2* (*PMNR2*), purification of MoMnr2 CorA domain protein and antibody generation

In order to express the CorA domain of *MoMNR2* (*PMNR2*), it was amplified (1 kb) from genomic DNA as it had no intron. It was first cloned in pBluescript KS (+) vector at *Eco*RV site to give pBSKS-*PMNR2*. Cloning was confirmed by restriction digestion with *Pvu*II (2.513 kb+1.440 kb), and *Kpn*I and *Nde*I (2.922 kb+983 bp+48 bp) (Figure 29A). *PMNR2* excised from pBSKS-*PMNR2* was cloned in the bacterial expression vector pET30a (+) vector at *Nde*I and *Kpn*I site translationally in-frame with $(His)_6$ tag at the C terminus to give pET30-*PMNR2*. This was confirmed by restriction digestion with *Eco*RV (5.917 kb + 374 bp), *Kpn*I and *Xba*I (5.276 kb + 1.015 kb), and *Kpn*I and *Nde*I (5.314 kb + 977 bp) (Figure 29B). *E. coli* BL21 DE3 cells transformed with the protein expression construct, pET30-*PMNR2*, showed an induced band of ~40kDa, which corresponded to the expected size of the CorA domain of MoMnr2 (Figure 29C). The recombinant protein was purified by Ni-NTA affinity chromatography (Figure 29D).

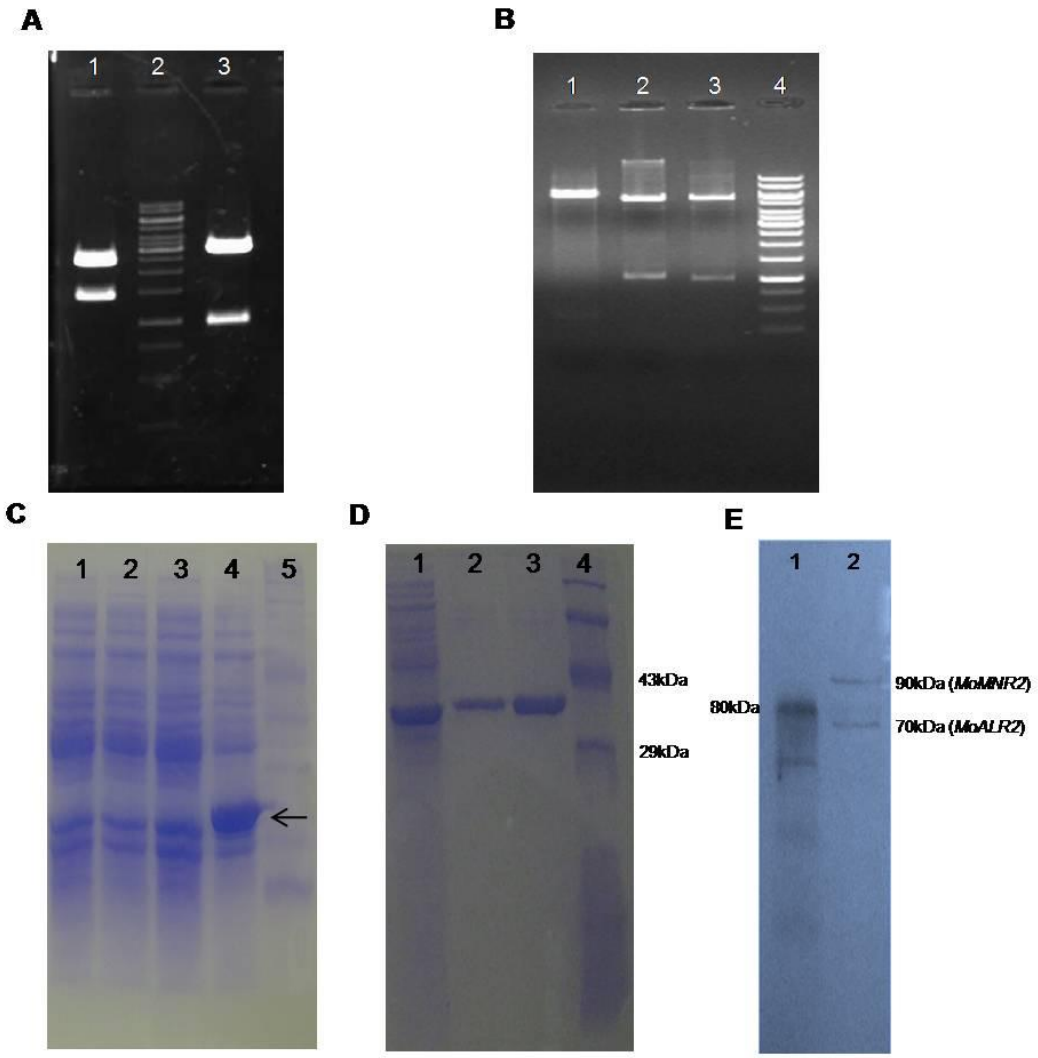

Figure 29: Expression of CorA domain of MoMnr2 in *E. coli* BL21 DE3 and generation of antibodies against CorA domain. (A) Cloning of CorA domain (PMNR2, 1 kb) amplified from genomic DNA of WT B157 in pBSKS+ at *EcoR*V site to give pBSKS-PMNR2. Clone was confirmed by restriction digestion. Lane 1, 3 pBSKS-PMNR2 digested with *Pvu*II, *Kpn*I and *Nde*I respectively. Lane 2 is 1 kb DNA ladder. (B) Cloning of PMNR2 at *Kpn*I and *Nde*I site in pET30a vector to give pET30-PMNR2. Clone was confirmed by restriction digestion. Lane 1, 2, 3 pET30-PMNR2 digested with *EcoR*V, *Kpn*I and *Xba*I, *Kpn*I and *Nde*I respectively. Lane 4 is 1 kb DNA ladder. (C) Induction of protein encoding CorA domain of MoMnr2. 10% SDS-PAGE was run to check the induction. Lane 1 *E. coli* BL21 DE3 transformed with pET30 uninduced, Lane 2 *E. coli* BL21 DE3 transformed with pET30 induced, Lane 3 *E. coli* BL21 DE3 transformed with pET30-PMNR2 uninduced Lane 4 *E. coli* BL21 DE3 transformed with pET30-PMNR2 induced, Lane 5 Protein marker (Bangalore Genei, Bangalore, India). (D) Ni-NTA affinity based purification of induced protein. Lane 1 Flow through, Lane 2 elute with 50mM Imidazole, Lane 3 elute with 200mM Imidazole, Lane 4 Protein marker (Bangalore Genei, Bangalore, India). (E) Western blot analysis to detect both the CorA proteins, MoAlr2 and MoMnr2. Lane 1 Protein marker (New England Biolabs, UK), Lane 2 Total protein from WT B157.

The purified protein was used to raise polyclonal antibodies in New Zealand White Rabbit using 20 µg of purified protein. Antibody titer was estimated by indirect-enzyme linked immunosorbent assay (ELISA) using HRP conjugated anti-rabbit IgG (Bangalore Genie, Bangalore, India) as the secondary antibody.

Further western blot analysis was done to detect both the CorA proteins; since the sequence of the CorA domain from MoMnr2 has 50% identity with that of MoAlr2, the antibodies raised against the CorA domain detected both MoAlr2 (70 kDa) and MoMnr2 (90 kDa). Western blot analysis confirmed that both MoAlr2 and MoMnr2 are expressed simultaneously in *M. oryzae* (Figure 29E).

5.15 Western blot analysis of the knockdown transformants

Western blot analysis of selected transformants was done to determine whether protein levels were also reduced in them.

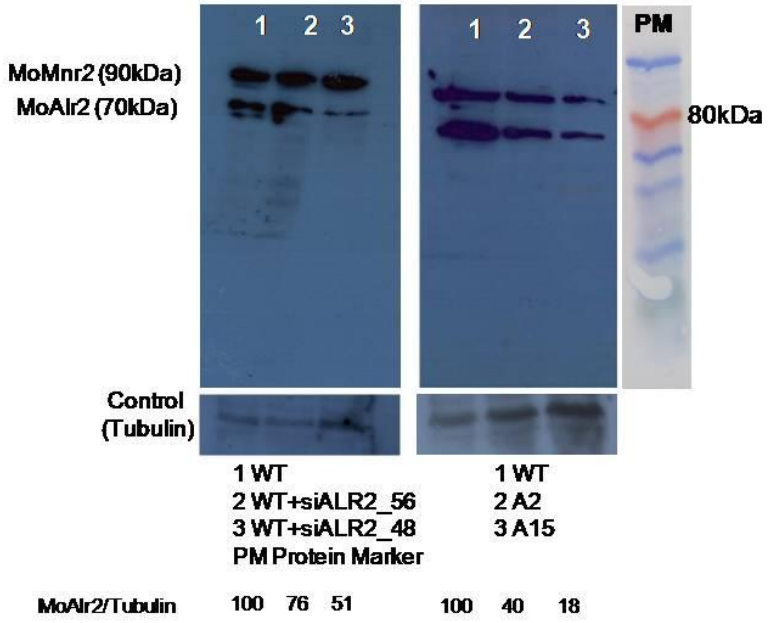

Figure 30: Western blot analysis of MoAlr2 and MoMnr2 in the knockout and knockdown transformants. Western blot analysis of knockdown transformants showing levels of MoAlr2 and MoMnr2 proteins in WT and knockdown transformants using polyclonal antibodies raised against the CorA domain and represented as percentages of MoAlr1 protein in the transformants compared to control.

The transformants studied showed lower protein levels of these CorA Mg^{2+} transporters than wild type B157 (Figure 30).

5.16 Immunolocalisation of MoAlr2 and MoMnr2 in *M. oryzae*

CorA transporters are known to be present on the plasma membrane as well as on organelles to form a system of Mg^{2+} uptake and compartmentalisation that maintains cytoplasmic Mg^{2+} homeostasis. In yeast, ScAlr2 has been shown to be a plasma membrane protein while ScMnr2 is a vacuolar membrane protein. The subcellular localisation of CorA transporters in *M. oryzae* was studied by indirect immunolocalisation using polyclonal antibodies against the MoMnr2 CorA domain. In wild type, the CorA transporters localised to plasma membrane and vacuole (Figure 31).

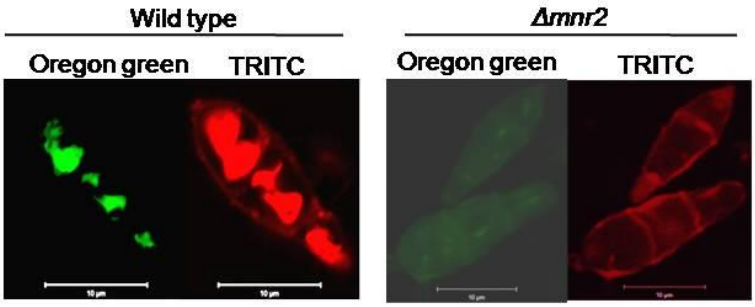

Figure 31: Localisation of CorA proteins by immunostaining. Conidia were harvested and treated with polyclonal antibodies raised against the CorA domain of MoMnr2. TRITC labelled secondary antibodies were used for staining. Oregon green 488 staining was used to visualize the vacuole.

Vacuolar localisation was determined by co-localisation with Oregon Green 488 staining (which stains vacuolar lumen). Immunostaining of *Δmnr2* with CorA antibodies showed staining only of plasma membrane due to MoAlr2, while vacuolar staining was absent (Figure 31). In *Δmnr2*, vacuolar staining by Oregon Green 488 was also very poor, suggesting a defect in pH of the vacuolar lumen (as these dyes fluoresce at acidic pH).

5.17 Mg^{2+} limited and pH dependent growth, extracellular alkalinisation and laccase estimation of WT and *Δmnr2* transformant

Under Mg^{2+} limiting conditions (YEGA+0.5mM EDTA), *Δmnr2* showed more growth inhibition than WT (Figure 32A), suggesting a dependence on MoMnr2 function for Mg^{2+} requirements under Mg^{2+} deficient conditions. A similar requirement has previously been

shown in *S. cerevisiae*, where a *Mnr2* mutant is unable to access Mg^{2+} stores from vacuoles. This suggests that Mnr2 plays an important role in the regulation of intracellular Mg^{2+}.

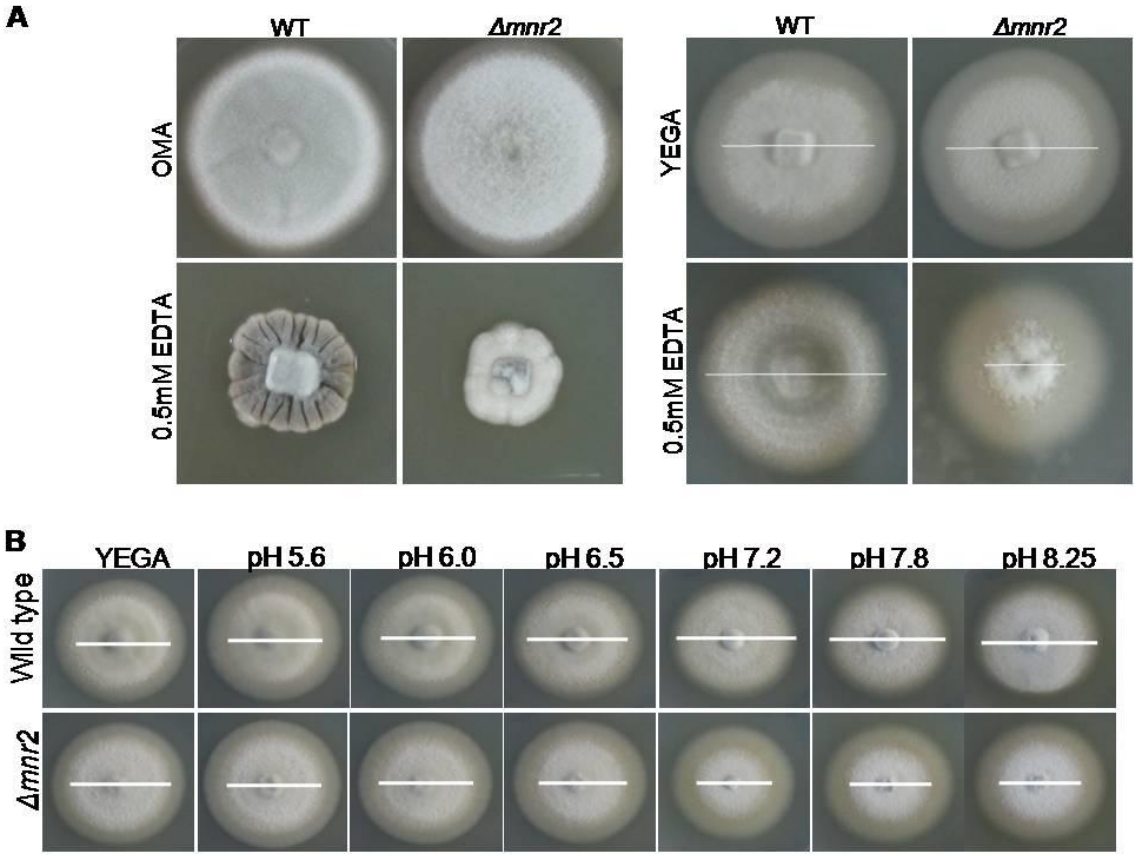

Figure 32: Growth of WT and *Δmnr2* on media with low Mg^{2+} and different pH. (A) Growth of WT and *Δmnr2* on media supplemented with EDTA. WT and *Δmnr2* were grown on OMA and YEGA supplemented with 0.5mM EDTA. Growth was assessed 5dpi. (B) WT and *Δmnr2*, strains were grown on YEGA buffered to pH 5.6-8.25 using 20mM HEPES. Sensitivity to different pH values was studied by growth of the fungus 5 days post inoculation.

It is likely that similar to the *S. cerevisiae* Mnr2, MoMnr2 too mediates efflux of Mg^{2+} from storage organelles. This efflux is also regulated by the Mg^{2+}/H^{+} exchanger in *S. cerevisiae*. Loss of function of MoMnr2 in *Δmnr2* could lead to imbalance of regulation of Mg^{2+} efflux by Mg^{2+}/H^{+} exchanger and hence a pH defect in *Δmnr2* (as seen by the lack of staining of the spores with Oregon Green 488). With this possibility in mind we studied the growth of WT and *Δmnr2* on YEGA buffered at pHs from 5.6-8.25 using 20mM HEPES, and measured growth 5 dpi. There was slower growth of *Δmnr2* at pH 6.5, 7.2, 7.8 and 8.25 compared to WT (Figure 32B). This growth difference at different pH values led us to study the ability of

WT and *Δmnr2* to alkalinise the extracellular media in presence of bromocresol green (which turns blue as the pH of the medium increases towards alkaline).

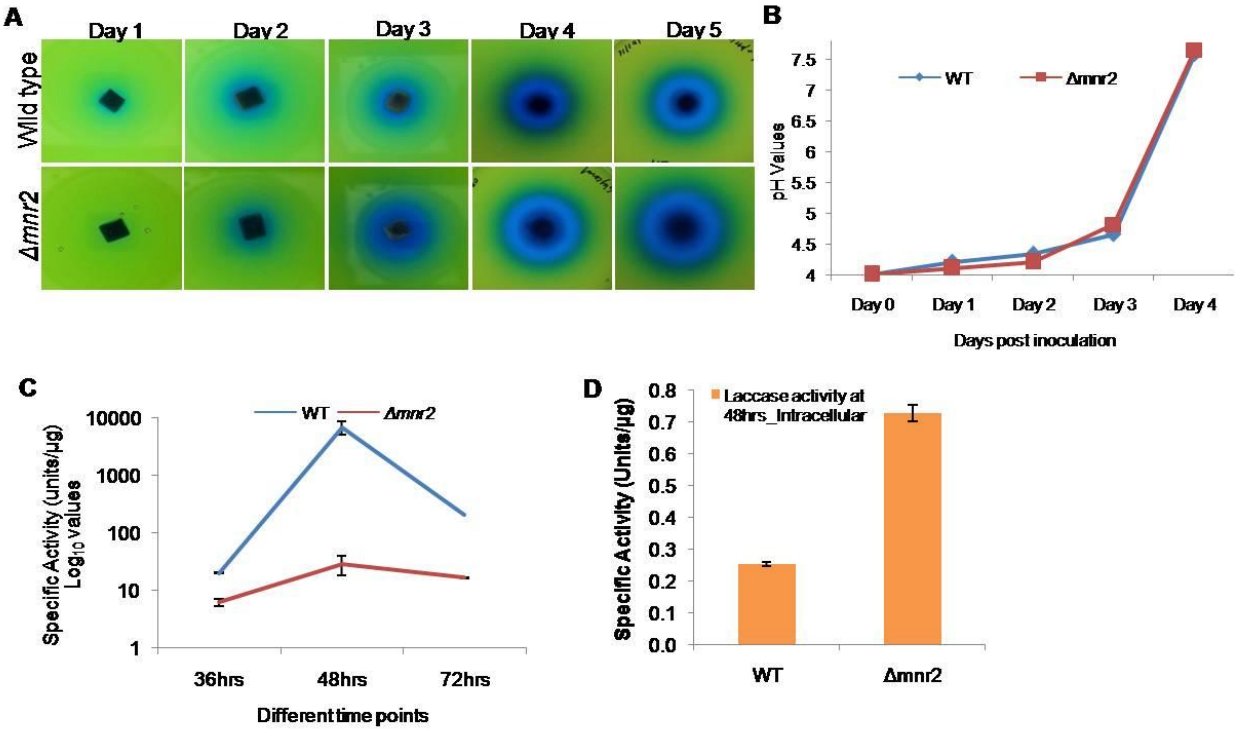

Figure 33: Alteration in pH and extracellular laccase activity. (A) Alteration in extracellular alkalinization in WT and *Δmnr2* was carried out on media containing bromocresol green (pH indicator dye), adjusted to pH 4.0 and 4% agar without glucose. (B) Change in extracellular pH of medium was monitored for WT and *Δmnr2* for 4 days. (C) Extracellular laccase activity was monitored in WT and *Δmnr2* at 36, 48 and 72 hrs. (D) Intracellular laccase activity was monitored in WT and *Δmnr2* at 48 hrs. Specific laccase activity of WT and *Δmnr2* was expressed as Units/µg. The experiment was performed three times.

We found that *Δmnr2* was unable to alkalinise till day 1 post inoculation. By day 2, the alkalinisation was similar to that of WT, but at day 3 and beyond (day 4 and 5) post inoculation, *Δmnr2* showed more alkalinisation than WT (Figure 33A). Also when the pH change of the medium with WT and *Δmnr2* was measured (quantitatively), *Δmnr2* showed a greater increase in pH of the medium from day 2 to day 3 compared to WT (Figure 33B), similar to the observation made in qualitative plate assays, suggesting that *Δmnr2* does have an alteration in pH regulation, and that MoMnr2 is therefore likely to have a role in the maintenance of pH within the cell.

Laccase is a copper containing enzyme which catalyses the oxidation of a phenolic substrate by coupling it to the reduction of oxygen to water. Fungal laccases are known to catalyse the

polymerisation, depolymerisation and methylation of phenolic compounds (Leonowicz *et al.*, 2001) and are also involved in degradation of lignin. The role of laccase has been shown in pigmentation in *Aspergillus nidulans* (Clutterbuck, 1990) and *Aspergillus fumigatus* (Tsai *et al.*, 1999). Earlier reports suggest that vacuolar acidification is important for the post translational modifications of laccase (Panepinto and Williamson, 2006). Consistent with previous result, there was a defect in the pH response seen in *Δmnr2* compared to WT. Hence we assayed laccase activity in *Δmnr2* and WT and found that at 36 hours, *Δmnr2* had 3.2 fold less laccase activity, while at 48 and 72 hours, the activity decreased to 238.7 fold and 12.39 fold in *Δmnr2* respectively compared to WT (Figure 33C). The decreased laccase activity in *Δmnr2* could be due to a secretion defect of functional enzyme and hence less extracellular activity, or there could be a defect in post-translational modification of laccase due to vacuolar dysregulation of acidification in *Δmnr2*. We therefore looked at the activity of laccase at 48 hours (time point which showed maximum activity of laccase in WT) both extracellularly and intracellularly in WT and *Δmnr2*. The intracellular level of laccase in *Δmnr2* was approximately 3 fold higher than that of WT. But 3 fold increase in intracellular levels of laccase activity could not compensate for the 238.7 fold decrease in extracellular laccase activity seen in *Δmnr2*.

5.18 Impaired sexual reproduction in *Δmnr2*

M. oryzae is a heterothallic fungus as it exists in two different mating types, *MAT1-1* and *MAT1-2*. When fertile isolates of opposite mating types are paired together on an appropriate medium, they form sexual fruiting bodies called perithecia. WT B157 is a *MAT1-1* mating type strain. WT and *Δmnr2* were crossed with the opposite mating type strain Guy11 (*MAT1-2*) and perithecia formation was assessed.

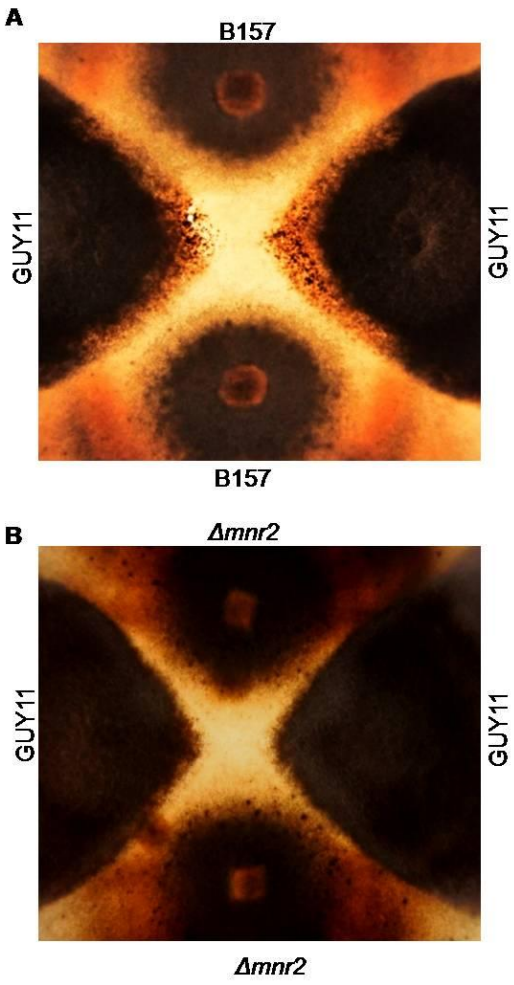

Figure 34: Impaired sexual reproduction in *Δmnr2* transformant. (A) Mating assay between WT B157 and Guy11. (B) Mating assay between *Δmnr2* and Guy11. Photographs were taken 21 dpi.

WT B157 did not form any perithecia (B157 is female sterile), but it induced the opposite mating type, Guy11 (female fertile), to form perithecia; hence B157 is a male fertile strain. In contrast to the numerous perithecia developed in Guy11 by the mating of WT B157 and Guy11, no perithecia were observed in Guy11 when crossed with *Δmnr2* (Figure 34). This suggests that *MoMNR2* is required for male fertility.

5.19 Generation of localisation cassette of *MoALR2* and cloning in pBSKS+ to give KS-Loc*MoALR2*-GFP-Zeo^r

A PCR based technique was used to generate a localisation cassette of *MoALR2* (Yu JH *et al.*, 2004) wherein first Loc*MoALR2* (having the promoter and coding sequence of *MoALR2* of

~3.5 kb) was fused to GFP (~750 bp) to give Loc*MoALR2*-GFP using *ALR2* Promoter Nest (F) and GFP (R) of 4.0 kb in size (Figure 35B).

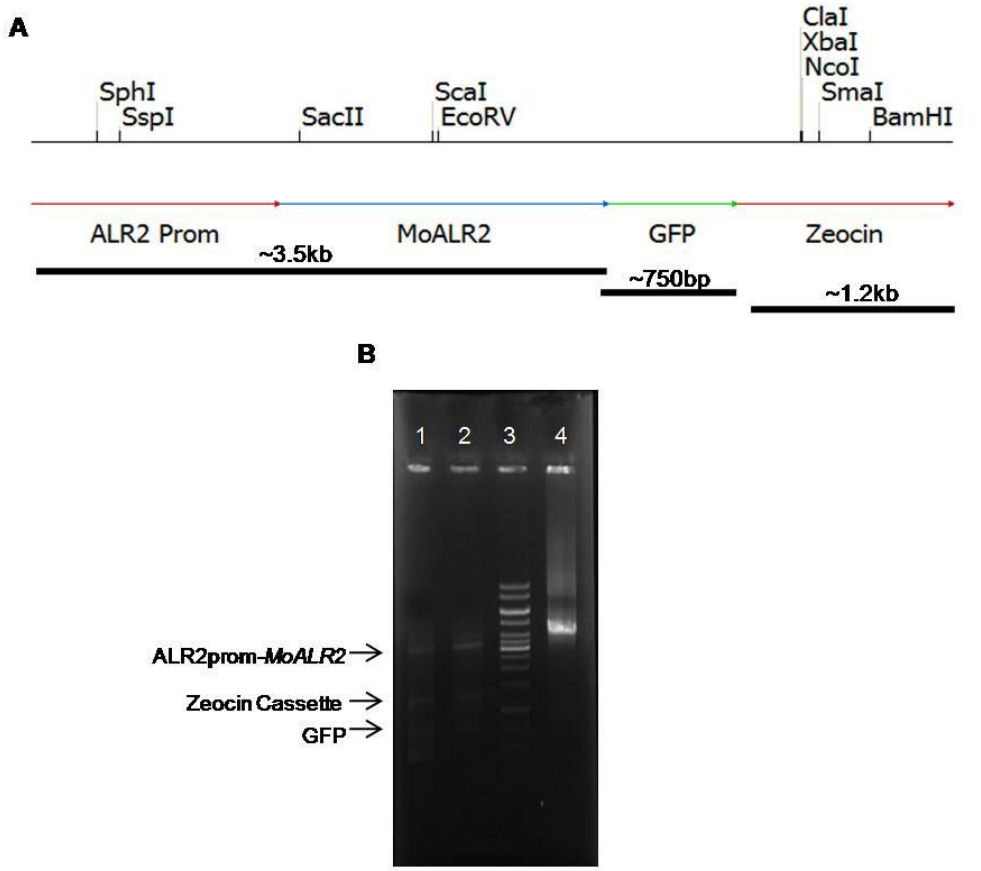

Figure 35: Double joint PCR based generation of localisation cassette for *MoALR2*. (A) Schematic representation of localisation cassette of *MoALR2*. (B) Fusion PCR for amplification of localisation cassette. Lane 1 and 2 is fusion of all three products, *MoALR2* promoter-*MoALR2* (3.5 kb), GFP (750 bp) and Zeocin^r cassette (1.2 kb), simultaneously. Lane 3 is 1 kb DNA ladder. Lane 4 is fusion of *MoALR2* promoter-*MoALR2* (Loc*MoALR2*, 3.5 kb) and GFP (750 bp) to give a product of ~4.0 kb.

The PCR product was gel eluted and cloned in pBSKS+ at *Eco*RV site to give KS-Loc*MoALR2*-GFP, which was confirmed by PCR using *MoALR2* Prom Nest For + GFP Rev (~3.97 kb), *MoALR2* For + GFP Rev (~2.57 kb), GFP For + GFP Rev (750 bp), *MoALR2* Prom Nest For + RT *MoALR2* Rev (~3.23 kb) and restriction digestion with *Spe*I (6.935 kb), *Cla*I and *Spe*I (4.01 kb + 2.92 kb), *Kpn*I and *Spe*I (4.05 kb + 2.89 kb), *Xba*I and *Eco*RV (5.21 kb + 1.72 kb), and *Pst*I (6.935 kb) (Figure 36).

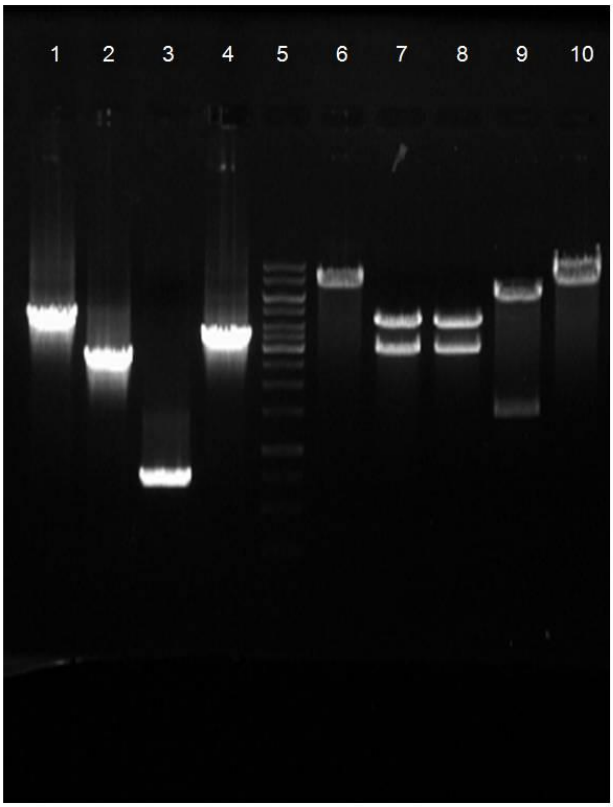

Figure 36: Cloning of Loc*MoALR2*-GFP at *EcoRV* to give KS-Loc*MoALR2*-GFP. KS-Loc*MoALR2*-GFP cloning was confirmed by PCR and restriction digestion and run on 0.8% agarose gel. Lane **1, 2, 3 and 4** PCR with ***MoALR2*** Prom Nest For + GFP Rev, ***MoALR2*** For + GFP Rev, GFP For + GFP Rev, ***MoALR2*** Prom Nest For + RT ***MoALR2*** Rev respectively. Lane **6, 7, 8, 9 and 10** KS-Loc***MoALR2***_GFP digested with ***Spe*I, *Cla*I and *Spe*I, *Kpn*I and *Spe*I, *Xba*I and *EcoRV* and *Pst*I** respectively. Lane **5 is 1 kb** DNA ladder.

Next, Loc*MoALR2*-GFP (~4.0 kb) was amplified from KS-Loc*MoALR2*-GFP and fused with Zeo^r (~1.2 kb) to obtain Loc*MoALR2*-GFP-Zeo^r of ~5.2 kb. The two products were taken in equal molar ratio and PCR was carried out with *MoALR2* Prom Nest For and Zeo Rev using different volumes (1µl, 2µl and 3µl) of the above mixture. The yield of the final product (Loc*MoALR2*-GFP-Zeo^r, 5.2 kb) was very low (Figure 37A). To increase the yield, first a touchdown PCR was performed, taking equal molar ratio of both the products, without primers and then taking different volume of 1:100 dilutions (1 µl and 2 µl). The final product was amplified using *MoALR2* Prom Nest For and Zeo Rev (Figure 37B).

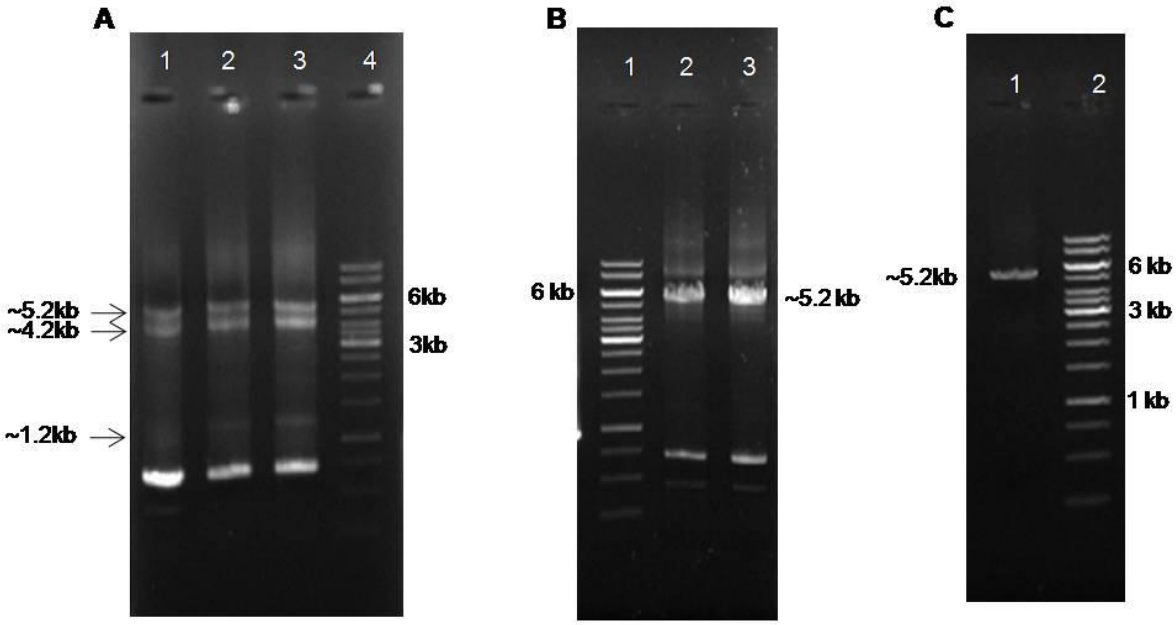

Figure 37: Double joint PCR based generation of localisation cassette for *MoALR2*. (A) PCR with *MoALR2* Prom Nest For and Zeo Rev for amplification of localisation cassette of *MoALR2*. Lane 1, 2, 3 PCR with 1µl, 2µl and 3µl of Loc*MoALR2*_GFP and Zeo^r mix (equal molar ratio) as template. Lane 4 is 1 kb DNA ladder. (B) Touchdown PCR followed by full length PCR with *MoALR2* Prom Nest For and Zeo Rev using different volume of 1:100 dilutions (Lane 2 1 µl and Lane 3 2 µl). Lane 1 is 1 kb DNA ladder. (C) Gel elution of Loc*MoALR2*-GFP-Zeo^r. Lane 1 purified product. Lane 2 is 1 kb DNA ladder.

The PCR product was gel eluted (Figure 37C) and cloned at *Eco*RV site in pBSKS+ to give KS-Loc*MoALR2*-GFP-Zeo^r.

The clone was confirmed by restriction digestion with *Eco*RI (2.95 kb + 2.7 kb + 1.2 kb + 775 bp + 556 bp), *Hind*III (5.35 kb + 1.95 kb + 525 bp + 332 bp), *Nco*I (8.2 kb), *Pvu*II (5.7 kb + 2.5 kb), *Sac*I (6.15 kb + 1.15 kb + 543 bp + 353 bp), and *Xho*I (4.31 kb + 1.7 kb + 2(516) bp + 423 bp + 229 bp + 172 bp) (Figure 38A) and further confirmed by PCR using *MoALR2* Prom Nest For + Zeo Rev (~5.2 kb), *MoALR2* Prom Nest For + GFP Rev (~3.97 kb), GFP For + Zeo Rev (~1.9 kb), RT *MoALR2* For + Zeo Rev (~2.5 kb), and Zeo For + Zeo Rev (1.2 kb) (Figure 38B).

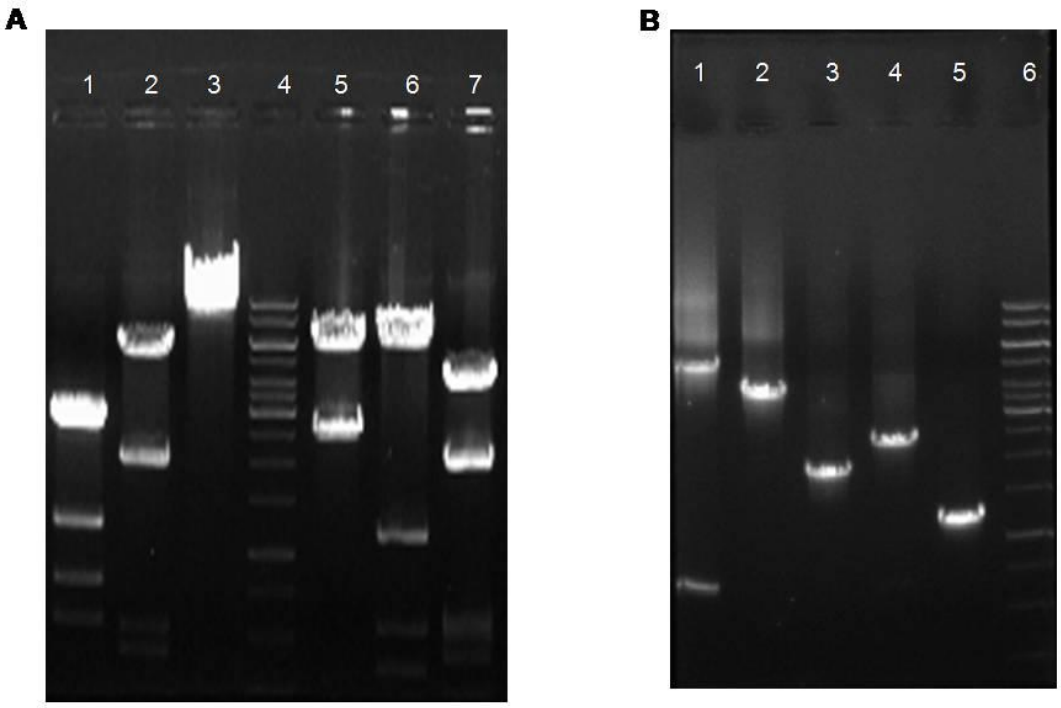

Figure 38: Cloning of Loc*MoALR2*-GFP-Zeo^r at *EcoRV* to give KS-Loc*MoALR2*-GFP-Zeo^r. (A) KS-LocALR2-GFP-Zeo^r cloning was confirmed by restriction digestion and run on 0.8% agarose gel. Lane 1, 2, 3, 5, 6 and 7 KS-Loc*MoALR2*-GFP-Zeo^r digested with *EcoR*1, *Hind*III, *Nco*I, *Pvu*II, *Sac*I and *Xho*I respectively. Lane 4 is 1 kb DNA ladder. (B) KS-LocALR2-GFP-Zeo^r cloning was confirmed by PCR and run on 0.8% agarose gel. Lane 1, 2, 3 and 4 PCR with *MoALR2* Prom Nest For + Zeo Rev, *MoALR2* Prom Nest For + GFP Rev, GFP For + Zeo Rev, RT *MoALR2* For + Zeo (R) and Zeo For + Zeo (R) respectively.

5.20 Transformation of *M. oryzae* B157 with localisation cassette of *MoALR2* (KS-Loc*MoALR2*-GFP-Zeo^r)

The localisation cassette of *MoALR2* in (pBSKS-Loc*MoALR2*-GFP-Zeo^r) was used for protoplast transformation of WT B157 and transformants were selected on Zeocin (300µg ml^{-1}). We obtained 25 transformants growing on media containing Zeocin (300µg ml^{-1}). All the transformants were screened by looking at GFP fluorescence, but none showed any fluorescence. We looked at the integration of the localisation cassette in the genome. Genomic DNA of all the transformants was isolated and initial screening was done with GFP For + Zeo Rev (1.9 kb) to look for the integration of the localisation cassette in the genome. The transformants showed an amplification product of the expected size (1.9 kb), but WT

(negative control) also showed weak amplification of the same product size, suggesting non-specific binding of the primers (Figure 39A).

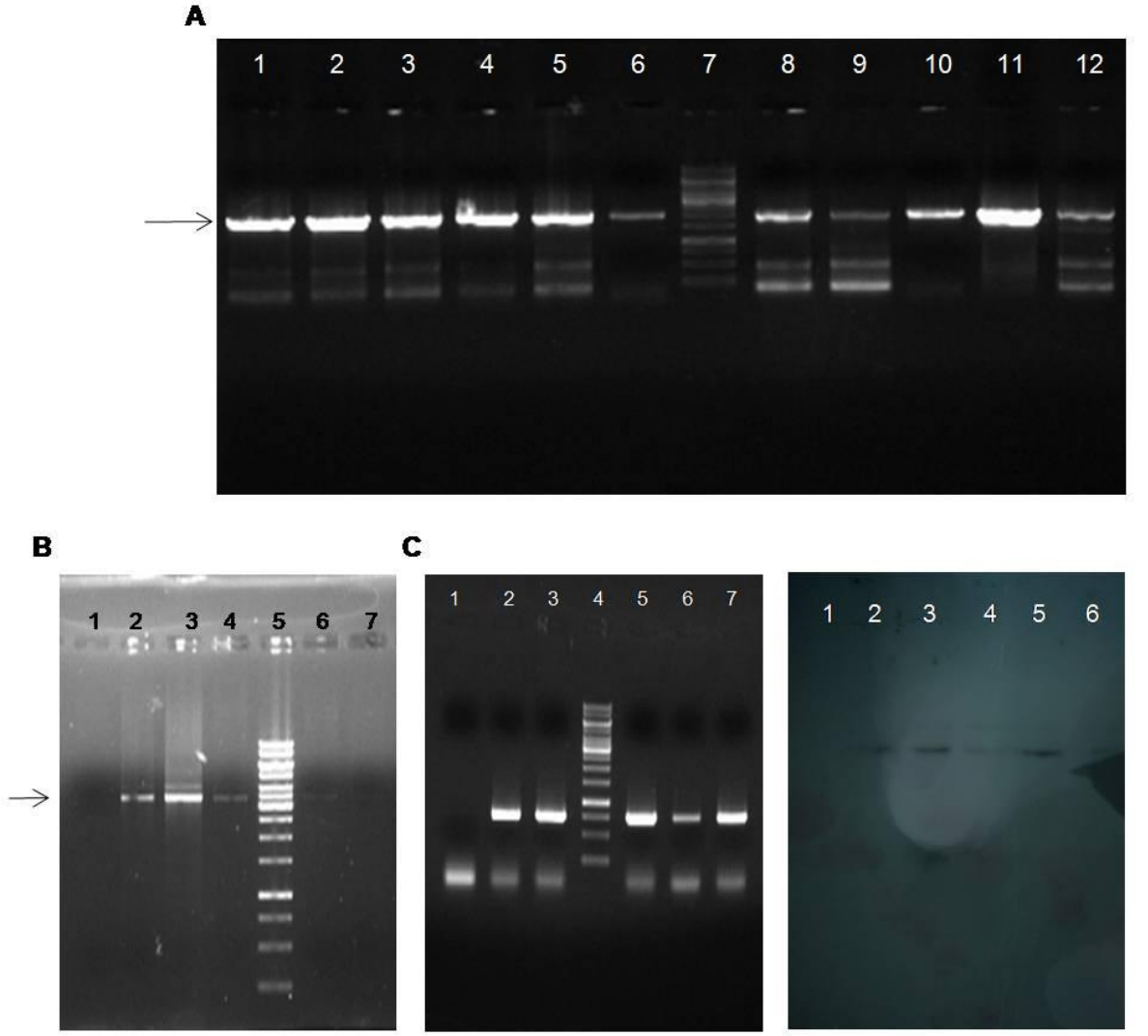

Figure 39: Screening of putative transformants transformed with localisation cassette of *MoALR2* (Loc*MoALR2*-GFP-Zeo^r). (A) Screening of transformants with GFP For + Zeo Rev (1.9 kb). Lane 1-6, 8-10 are transformants, Lane 11 is positive control (KS-Loc*MoALR2*-GFP-Zeo^r), Lane 12 is WT and Lane 7 is 1 kb DNA ladder. (B) Screening of transformants with *MoALR2* For + Zeo Internal Rev (3.5 kb) using genomic DNA. Lane 2-4, 6-7 are transformants, Lane 1 is WT and Lane 5 is 1 kb DNA ladder. (C) Screening of transformants with GFP For + GFP Rev (750 bp) using cDNA. Lane 2-3, 5-7 are transformants, Lane 1 is WT and Lane 4 is 1 kb DNA ladder. (D) Western blot analysis of the selected transformants with Anti-GFP as 1^{0}Ab. Lane 1 is WT, Lane 2-6 are transformants.

Various primer combinations were tried and with *MoALR2* For + Zeo internal Rev (3.5 kb), 5 of the transformants showed amplification of the expected product size (3.5 kb), while WT did not show any amplification (Figure 39B). In these five transformants, GFP transcripts were also checked using GFP For + GFP Rev. WT, as expected, did not show any GFP

amplification from cDNA while all the 5 transformants did (Figure 39C). GFP signal was also checked in these transformants at protein level using anti-GFP as primary Antibody. All the 5 transformants showed a signal, while WT did not (Figure 39D). This probably suggests that the chimeric protein may be failing to fold properly.

5.21 Element analysis in the knockdown transformants

Since the protein levels of MoAlr2 decreased in the knockdown transformants, we next investigated whether a decrease in Mg^{2+} transporter levels affects the intracellular levels of metal ions (mainly Mg^{2+} and Ca^{2+}), using X- ray Fluorescence Analysis (XRF) of hyphae grown under standard conditions (medium containing 4mM Mg^{2+}). We found a decrease in the intracellular levels of Mg^{2+} in the knockdown transformants (Figure 40A), while Ca^{2+} levels increased. This led to a rise in the Ca^{2+}/Mg^{2+} ratio (Figure 40B). Significant decrease in Mg^{2+} levels was seen when the silencing of *MoALR2* was >50%. For instance, XRF analysis of A2 and A15 showed that Mg^{2+} levels were reduced to 25% and 21% of WT levels respectively. Thus we show that CorA Mg^{2+} transporters play a significant role in maintenance of intracellular metal ion composition.

Next, to look at the effect of extracellular Mg^{2+} availability we determined the intracellular Mg^{2+} levels in presence of extracellular EDTA (a Mg^{2+} chelator). The intracellular levels of Mg^{2+} in WT decreased in presence of EDTA (Figure 40C), indicating a need for extracellular Mg^{2+} and its uptake for maintenance of the intracellular ionic milieu.

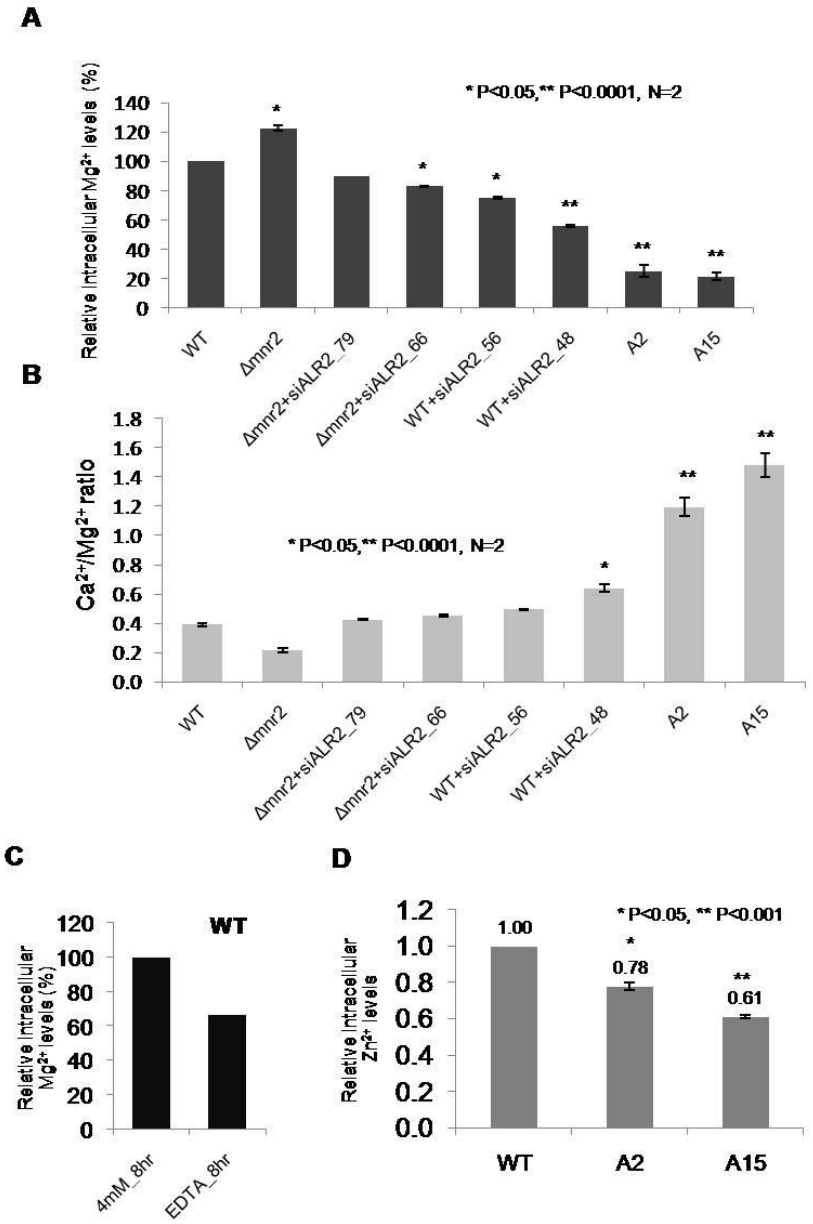

Figure 40. CorA Mg^{2+} transporters alters metal ion composition in *M. oryzae*. (A) Intracellular levels of Mg^{2+} in the knockout and knockdown transformants were estimated by XRF. The values are expressed as percentage values, with 100 corresponding to WT at 4mM Mg^{2+}. (B) Ratio of Ca^{2+} to Mg^{2+} for *Δmnr2* and knockdown transformants was estimated at 4mM Mg^{2+}. (C) Intracellular levels of Mg^{2+} in presence of 4mM and EDTA were estimated at 8hrs. The values are expressed as percentage values, with 100 corresponding to WT at 4mM Mg^{2+}. (D) Intracellular levels of Zn^{2+} in WT, A2 and A15 were estimated by XRF. The values are expressed as relative values, with 1 corresponding to the Wild type (WT) at 4mM Mg^{2+}.

To investigate whether extracellular Mg^{2+} supplementation could restore intracellular Mg^{2+} levels in the knockdown transformants, the two knockdowns which showed maximum silencing of *MoALR2*, A2 and A15, were grown in presence of high concentrations of extracellular Mg^{2+} (50mM and 250mM). When supplemented with 50mM Mg^{2+}, the

intracellular Mg^{2+} levels in A2 and A15 increased to 62% and 42% of the WT level (from 25% and 21%) respectively (Figure 41A) and increased further at 250mM Mg^{2+} (Figure 41B).

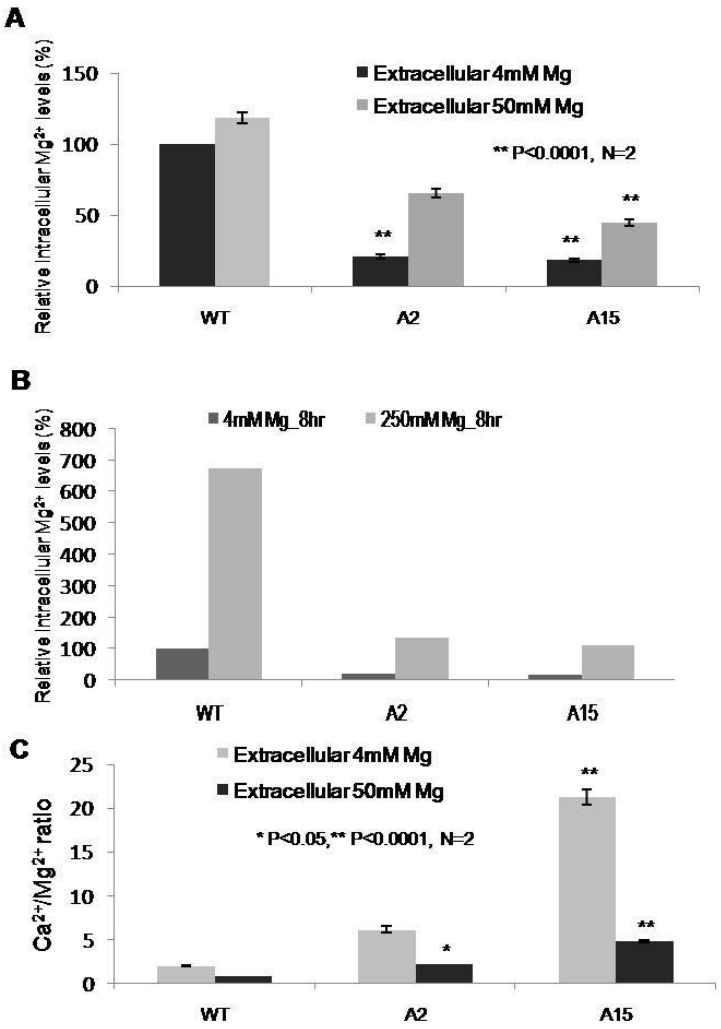

Figure 41. XRF analysis of knockdown transformants. (A), (B) Intracellular levels of Mg^{2+} at 4mM, 50mM and 250mM extracellular Mg^{2+} in the double knockdown transformants, A2 and A15 and WT was estimated. The values are expressed as percentage values, with100 corresponding to the Wild type (WT) at 4mM Mg^{2+}. (C) Ratios of Ca^{2+} to Mg^{2+} at two different concentrations of Mg^{2+} in WT, A2 and A15 was quantified. Values are the mean of two independent replicates. Error bar denote SD.

This increase could be either due to enhanced uptake by the CorA transporters in the knockdown transformants, or due to non-specific transport at higher levels of Mg^{2+} by other metal ion transporters. The increased Ca^{2+}/Mg^{2+} ratio observed in A2 and A15 at 4mM Mg^{2+}, also returned to lower levels in presence of 50mM Mg^{2+} (Figure 41C).

5.22 Mg^{2+} dependent expression of *MoALR2* and *MoMNR2*

The expression profile of *MoALR2* and *MoMNR2* was studied in WT grown in presence of EDTA, 50mM and 250mM extracellular Mg^{2+} for different lengths of time (2 and 6 hours).

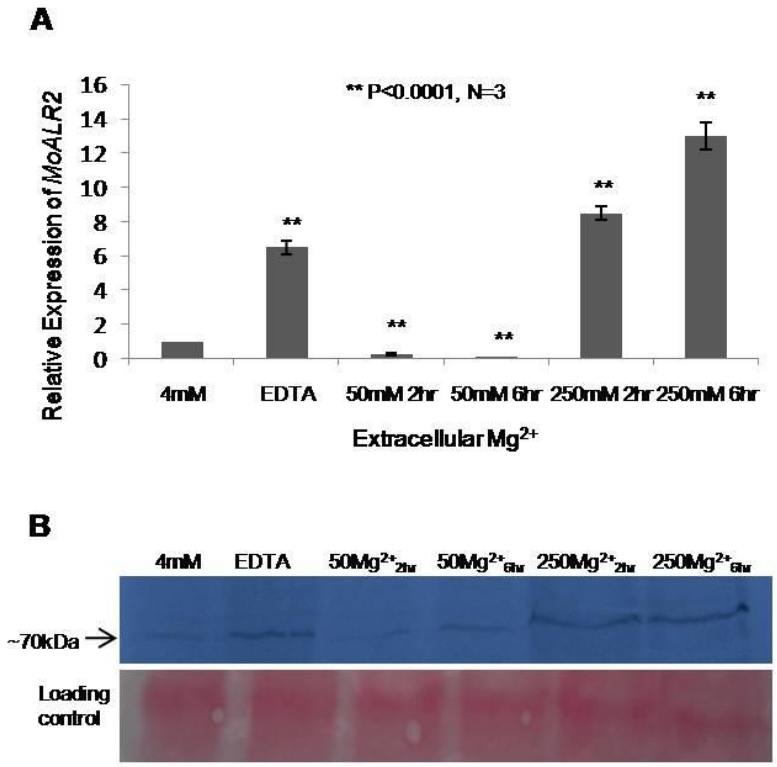

Figure 42. Regulation of *MoALR2* at mRNA and protein level with respect to extracellular Mg^{2+}. (A) mRNA levels of *MoALR2* were estimated by qRT-PCR at different concentrations of extracellular Mg^{2+}. The transcript levels were expressed as relative values, with 1 corresponding to levels at 4mM. (B) Western blot analysis for MoAlr2 at different concentrations of extracellular Mg^{2+}.

The addition of EDTA resulted in up-regulation of both *MoALR2* and *MoMNR2*. Transcript levels of *MoALR2* decreased at 50mM Mg^{2+} both at 2 and 6 hours, while at 250mM Mg^{2+}, the transcript level increased both at 2 and 6 hours (Figure 42A). The transcript levels of *MoMNR2* decreased with increasing concentrations of Mg^{2+} (Figure 43A).

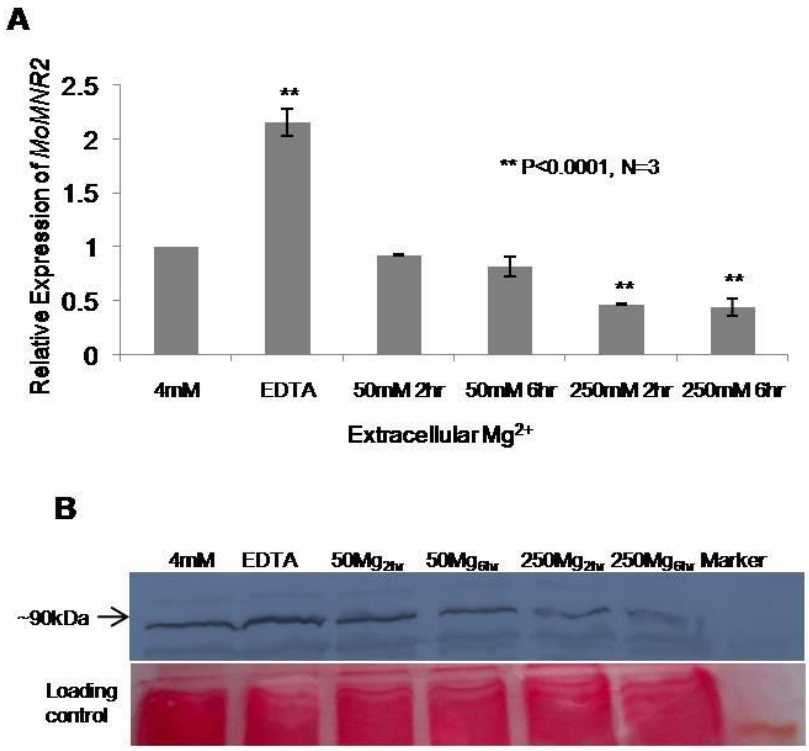

Figure 43. Regulation of *MoMNR2* at mRNA and protein level with respect to extracellular Mg^{2+}. (A) mRNA levels of *MoMNR2* were estimated by qRT-PCR at different concentrations of extracellular Mg^{2+}. The transcript levels were expressed as relative values, with 1 corresponding to levels at 4mM. (C) Western blot analysis for MoMnr2 at different concentrations of extracellular Mg^{2+}.

To examine how the levels of MoAlr2 and MoMnr2 proteins change with extracellular Mg^{2+} levels, Western blot analysis was also done. The levels of both MoAlr2 and MoMnr2 proteins increased in presence of EDTA. In the presence of 50mM Mg^{2+} the level of MoAlr2 was comparable to that seen with 4mM Mg^{2+} alone (i.e. no EDTA), both at 2 and 6 hours, but increased at 250mM Mg^{2+} both at 2 and 6 hours compared to that at 4mm Mg^{2+} (Figure 42B). However, the increase in protein at 250mM Mg^{2+} after 6 hours was small compared to the increase at the transcript level. The level of MoMnr2 protein showed the same trend as seen at transcript level, decreasing with increasing concentration of Mg^{2+} and with increasing time (Figure 43B). Under Mg^{2+} limiting conditions (in presence of EDTA), both MoAlr2 and MoMnr2 are up-regulated, which ensures that a basal level of Mg^{2+} within the cell is maintained either through uptake from extracellular milieu through MoAlr2 or through export of Mg^{2+} from MoMnr2 present on organellar membrane. At 250mM extracellular Mg^{2+}

expression of MoAlr2 increases, which probably brings in more Mg^{2+} into the cytoplasm and at the same condition, MoMnr2 show decreased expression which decreases any export of Mg^{2+} from the storage organelle into the cytosol.

5.23 Ca^{2+} dependent expression of *MoALR2* and *MoMNR2*

Calcium (Ca^{2+}) is a natural antagonist of Mg^{2+}. To evaluate how expression of the plasma membrane Mg^{2+} transporter *MoALR2* changes with increasing concentration of Ca^{2+}, transcript and protein levels were studied in WT. The transcript level of *MoALR2* increased at 50mM and 250mM extracellular Ca^{2+} compared to control (where extracellular Ca^{2+} was chelated with EGTA) (Figure 44A). MoAlr2 protein too was increased compared to EGTA-treated control, but MoMnr2 protein level remained constant even at high concentrations of Ca^{2+} (Figure 44B). We hypothesise that high intracellular concentrations of Ca^{2+} induce increased expression of *MoALR2* as part of a feedback mechanism to maintain a favorable Ca^{2+}/Mg^{2+} ratio.

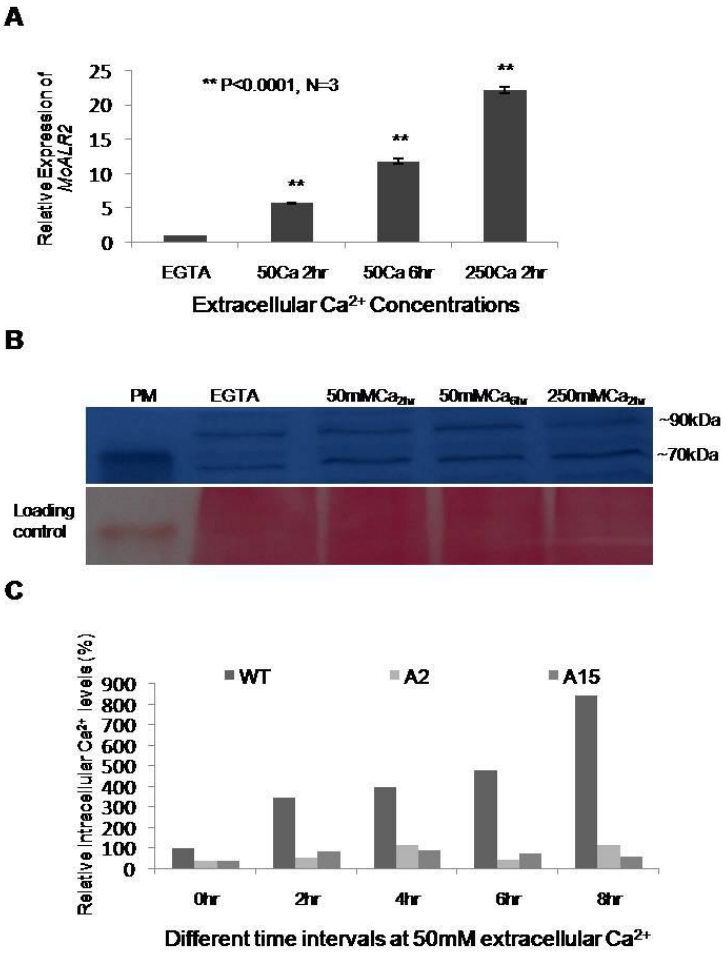

Figure 44. Regulation of *MoALR2* at mRNA and protein level with respect to extracellular Ca^{2+}. (A) mRNA levels of *MoALR2* were estimated by qRT-PCR at different concentrations of extracellular Ca^{2+}. The transcript levels were expressed as relative values, with 1 corresponding to levels at 4mM. Error bar denote SD. (B) Western blot analysis for MoAlr2 at different concentrations of extracellular Ca^{2+}. (C) XRF analysis of intracellular levels of Ca^{2+} at 50mM extracellular Ca^{2+} at increasing time intervals in the WT, A2 and A15. The values are expressed as percentage values, with 100 corresponding to the WT at 0hr.

Element analysis revealed that with longer incubation at 50mM extracellular Ca^{2+}, the intracellular levels of Ca^{2+} increased in WT (Figure 44C). Interestingly, A2 and A15 did not show any significant increase in intracellular levels of Ca^{2+} in spite of functional Ca^{2+} transporters, suggesting cross-talk between different cation systems to maintain a favorable Ca^{2+}/Mg^{2+} ratio within the cell for basic metabolic activity.

5.24 Altered Cation sensitivity in knockdown transformants

Mg^{2+} is the most abundant divalent cation within the cell. A change in Mg^{2+} levels within the cell affects metal ion homeostasis and may alter sensitivity to heavy metal ions. We have

shown that Mg^{2+} levels in the knockdown transformants are decreased. Further, we wanted to assay the sensitivity of *Δmnr2* and the knockdown transformants to various cations in comparison to WT. The Minimal Inhibitory Concentration (MIC) of WT for different cations was determined. A2 and A15 showed enhanced sensitivity to Aluminium (Al^{3+}) (Figure 45). This is consistent with the observation in *S. cerevisiae* that over-expression of the Mg^{2+} transporter provides resistance to Al^{3+}, justifying the **ALR** (**Al**uminium **R**esistance) nomenclature. The knockdown transformants were also more sensitive to Copper (Cu^{2+}) and Iron (Fe^{3+}) (Figure 45). Al^{3+} has been shown to disrupt plasma membrane, inhibit cell division, alter cell shape and vacuolisation (Illes *et al.*, 2006). Al^{3+} is known to inhibit several enzymes utilising ATP as it has higher affinity than Mg^{2+} for ATP. Excess Cu^{2+} has been shown to inhibit growth and photosynthetic electron transport in plants. Fe^{3+} via the Fenton reaction generates hydroxyl radicals which can damage lipids, proteins and DNA (Connolly and Guerinot, 2002). Mg^{2+} is known to provide resistance towards oxidative stress, and is required for regulation of cell proliferation and maintenance of DNA structure. The increased sensitivity of the knockdown transformants towards Al^{3+}, Fe^{3+} and Cu^{2+}, suggests that Mg^{2+} is required to provide resistance against these cations.

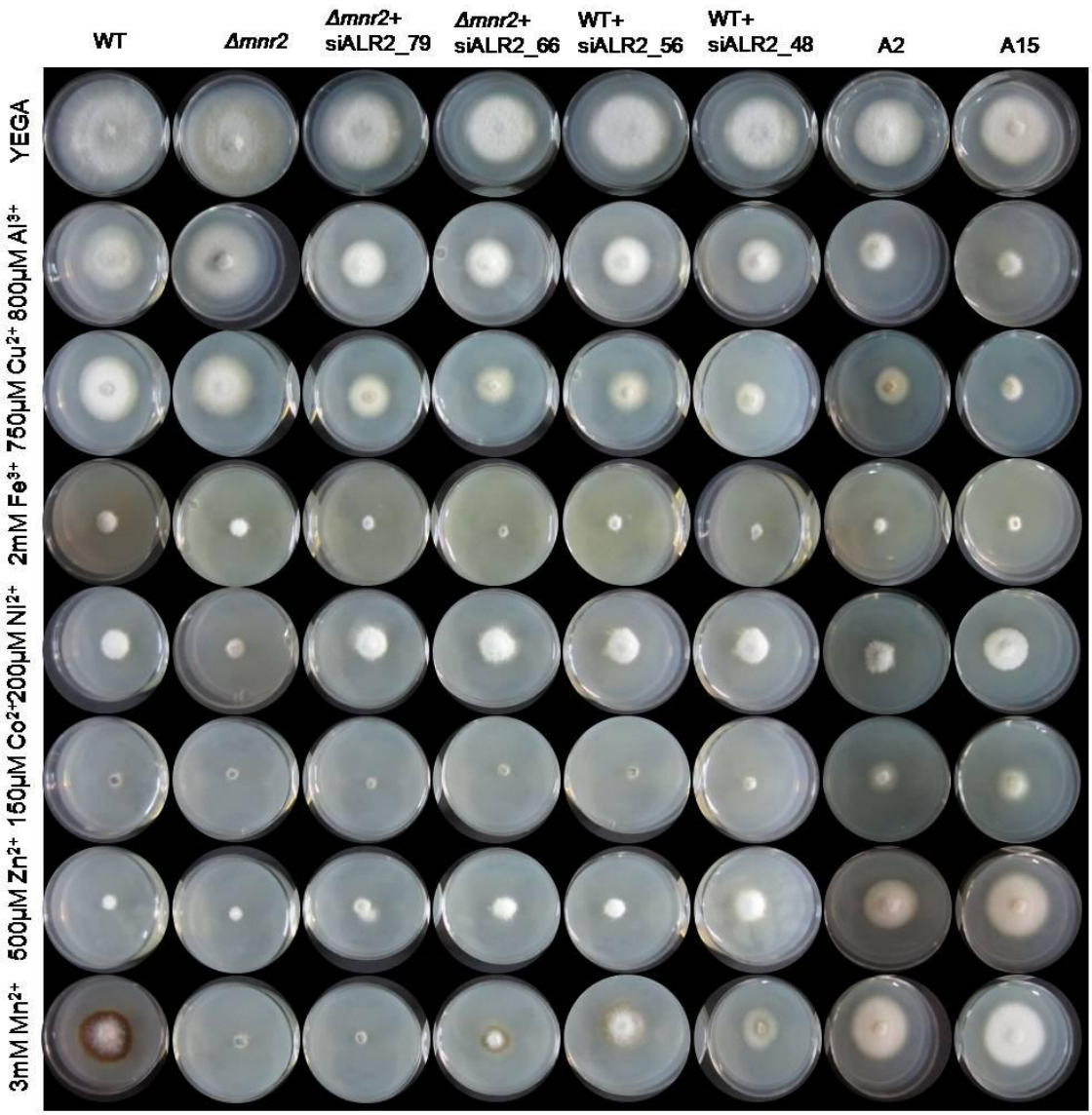

Figure 45. Altered Cation sensitivity in the knockdown transformants. WT, *Δmnr2* and knockdown transformants were inoculated on YEG and YEG supplemented with different cations. The sensitivity to cation was assessed relative to growth of WT and photographs were taken 5 days post inoculation.

Conversely, A2 and A15 were more resistant to Nickel (Ni^{2+}), Cobalt (Co^{2+}), Zinc (Zn^{2+}) and Manganese (Mn^{2+}) (Figure 45). The *Δmnr2* knockout too showed greater sensitivity to Ni^{2+}, Co^{2+}, Zn^{2+} and Mn^{2+}. These cations have been reported to be transported by CorA transporters, so the higher resistance of the knockdown transformants to them is likely to be due to reduced uptake by the lower number of Mg^{2+} transporters. This is also supported by the intracellular levels of Zn^{2+} in A2 and A15 in which Zn^{2+} levels were reduced to 78% and 61% of WT levels (Figure 40D).

5.25 CorA transporters are required for mycelial growth and survival in *M. oryzae*

We next set out to evaluate the effect of reduced *MoALR2* and *MoMNR2* levels on development in *M. oryzae*.

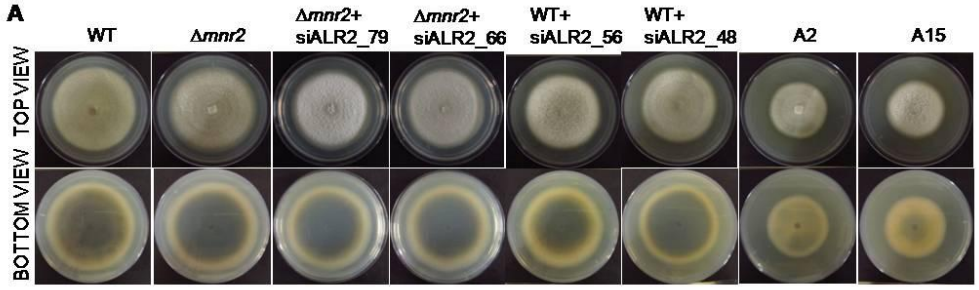

B

Transformants	Growth 5dpi (centimeters)
WT	6.00±0.06
Δmnr2	5.70±0.11
Δmnr2+siALR2_79	5.67±0.04
Δmnr2+siALR2_66	5.43±0.07
WT+siALR2_56	5.40±0.06
WT+siALR2_48	5.27±0.04
A2	4.70±0.06
A15	4.53±0.04

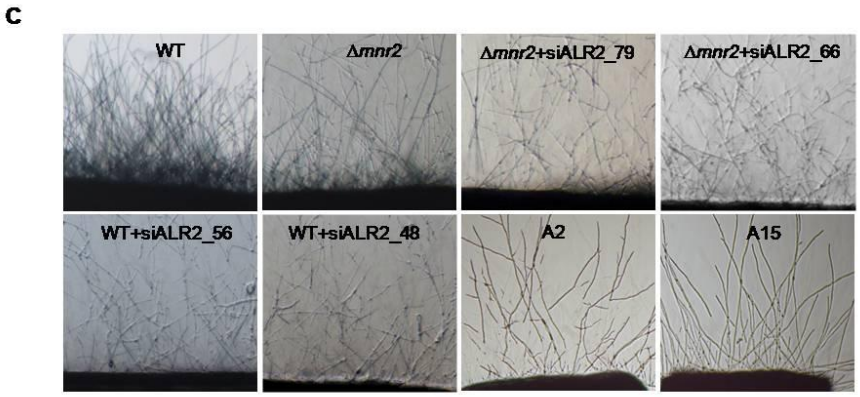

Figure 46. CorA transporters are required for mycelial growth. (A) Colony growth and melanization of WT, *Δmnr2* and knockdown transformants were checked on OMA. Photographs were taken 9 days post inoculation. (B) Growth was measured on OMA 5 days post inoculation. Data are presented as mean±SD from three independent experiments. (C) Aerial hyphal growth of WT, *Δmnr2* and knockdown transformants were checked on 0.8% agarose 2 days post inoculation.

The *MoMNR2* knockout (*Δmnr2*) showed ~5% reduction in growth of hyphae compared to WT, and failed to produce melanin in the aerial hyphae. The *MoALR2* knockdown transformants showed ~6% to 25% reduction in growth on Oat Meal Agar (OMA) medium (Figure 46B) and this reduction was correlated with the degree of silencing of *MoALR2*.

To investigate whether similar growth defects are also observed in situations of low Mg^{2+} availability, growth of WT was assayed in Mg^{2+} limiting conditions, using EDTA to lower Mg^{2+} availability.

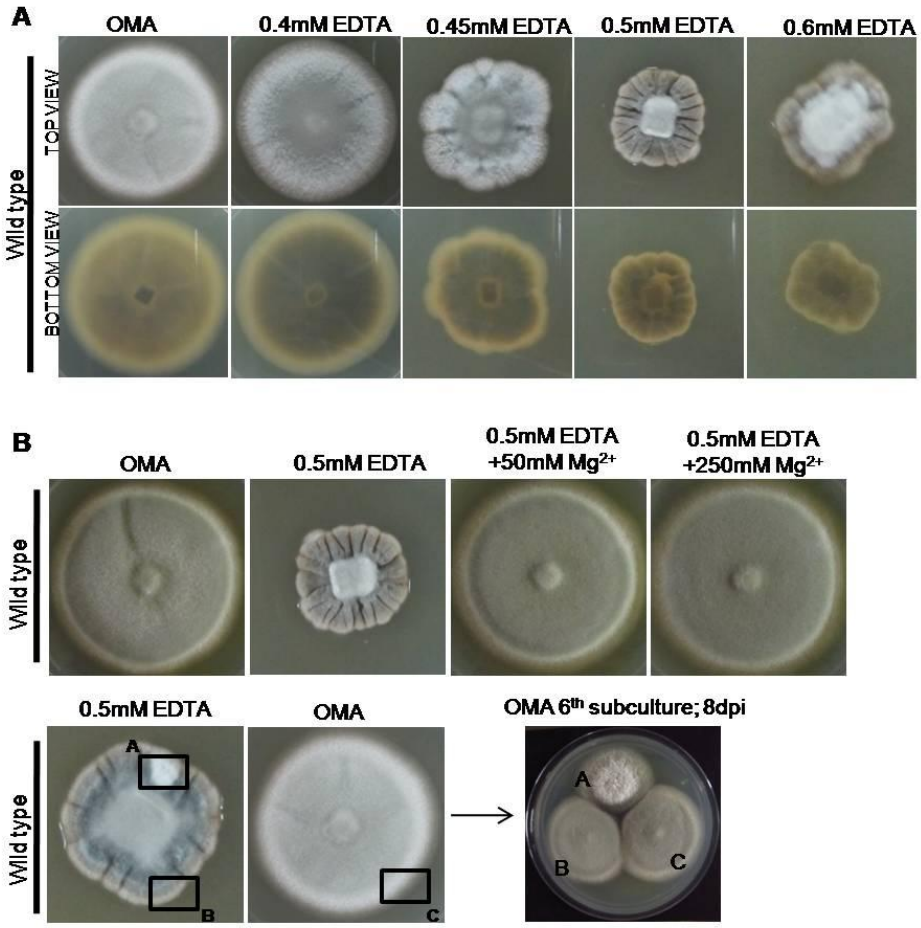

Figure 47. Growth of WT under Mg^{2+} limiting conditions (EDTA). (A) Growth in presence of different concentrations of EDTA was tested for WT. 3x3 mm mycelial plugs were inoculated on OMA with and without EDTA and growth was assessed 5 days post inoculation. (B) Restoration of growth on Mg^{2+} supplements in presence of EDTA. Growth of sectored colonies obtained under stress conditions (EDTA). Growth of different sectors was assessed on OMA.

Growth on OMA was severely reduced with increasing concentrations of EDTA, being retarded significantly at 0.5mM EDTA (Figure 47A). On supplementing this medium with 50mM extracellular Mg^{2+}, growth was restored to normal (Figure 47B). At a concentration of 0.6mM EDTA, there was complete growth inhibition. Under 0.5mM EDTA stress, WT frequently formed sectored colonies with certain sectors showing phenotypic differences (less melanised whitish sectors and melanised grayish sectors). Given the frequency with which such sectors appeared, it is likely that their altered phenotypes were due to epigenetic

changes. When the sectors and WT (grown on OMA without EDTA) were grown again in the absence of 0.5mM EDTA stress, the phenotypically different sector maintained the phenotype (less melanised and whitish) as observed over six rounds of sub-culturing (Figure 47B).

Hyphal growth on OMA was observed at regular intervals. As early as 12 dpi, *Δmnr2* and *MoALR2* knockdown transformants displayed autolysis at the centre of the colony (Figure 48A). WT did not show any such phenotype even up to three weeks. The autolysis was more severe in transformants with *MoALR2* expression below 50%, namely, WT+siALR2_48, A2 and A15 (Figure 48A). We followed *Δmnr2* for a longer time under different extracellular Mg^{2+} concentrations. Though at 12dpi *Δmnr2* showed autolysis only at the centre, by 16 dpi, autolysis had spread to include a large proportion of the *Δmnr2* colony. 50mM and 250mM extracellular Mg^{2+} supplement delayed the onset of autolysis and as a result the autolysis area observed at 16 dpi was reduced (Figure 48B). EDTA, on the other hand, hastened the process with *Δmnr2* displaying the phenotype even at 11dpi with increasing severity on subsequent days (Figure 48B). Thus *MoMNR2* is essential for long term survival of *M. oryzae*, as it shows early senescence (12dpi) compared to WT.

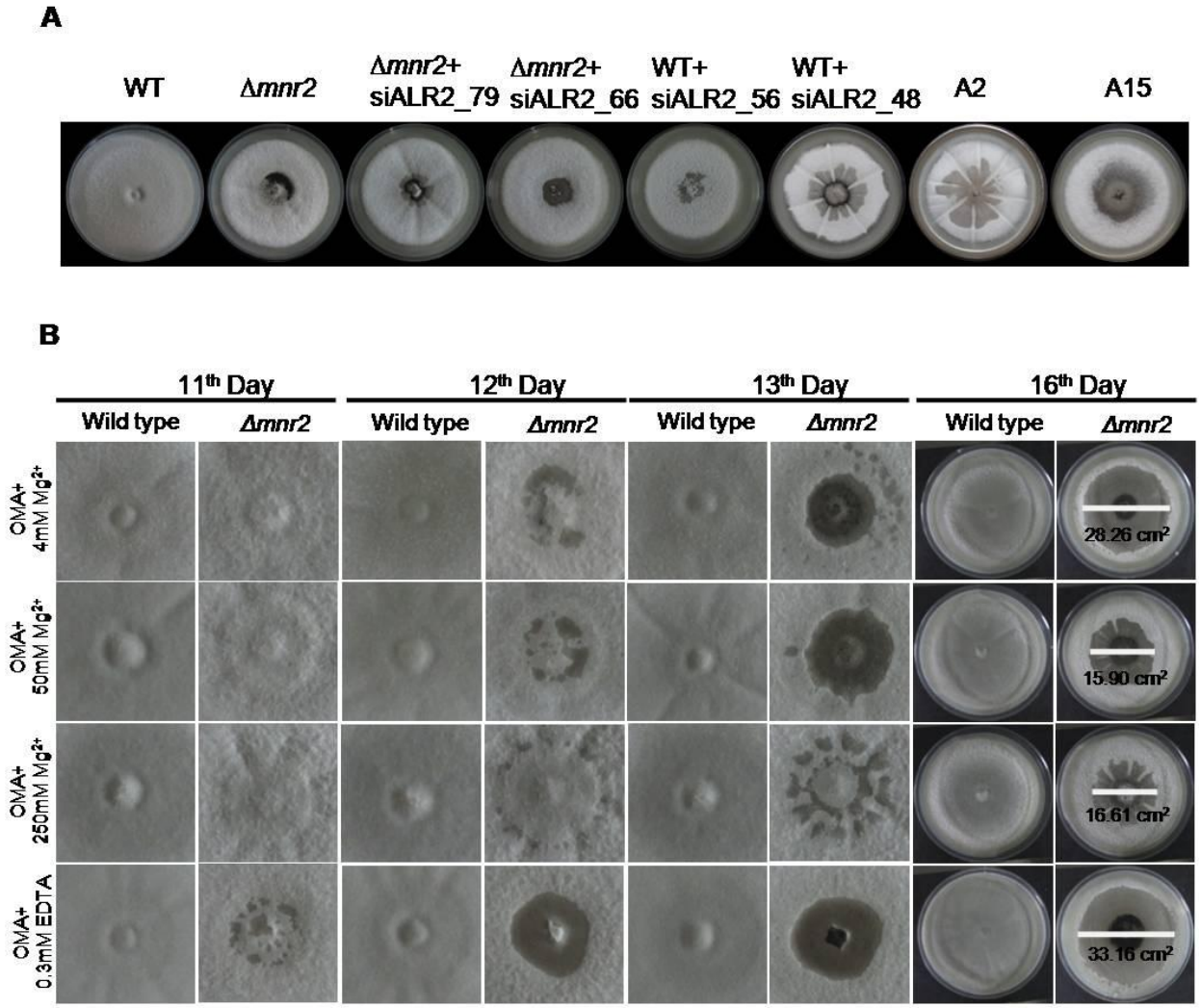

Figure 48. CorA transporters are required for preventing autolysis. (A) WT, *Δmnr2* and knockdown transformants were grown on OMA for 12 days. Early autolysis was monitored compared to WT and photographed. (B) WT and *Δmnr2* was grown on OMA supplemented with 4mM, 50mM, 250mM extracellular Mg^{2+} and 0.3mM EDTA. Autolysis was monitored from 10dpi to 16dpi and area under autolysis was measured at 16dpi.

These observations suggest that Mg^{2+} uptake by *MoALR2* is important for survival of *M. oryzae* as high extracellular Mg^{2+} in *Δmnr2* delayed the onset of autolysis.

5.26 CorA transporters are required for surface hydrophobicity in *M. oryzae*

Hydrophobins are surface proteins produced by filamentous fungi that are important for aerial growth of hyphae and attachment to solid supports. Reduced surface hydrophobicity leads to a "wettable" phenotype where water droplets do not form beads on the surface of aerial hyphae as they do in the wild type. Such a wettable phenotype has been observed previously

in *M. oryzae* in hydrophobin (*MoMHP1*, *MoMPG1*) and phosphodiesterase (*MoPDEH*) mutants (Stringer *et al.*, 1991; Bell-Pedersen *et al.*, 1992; Lauter *et al.*, 1992; Talbot *et al.*, 1993; Van Wetter *et al.*, 1996; Spanu, 1998; Kim *et al.*, 2005).

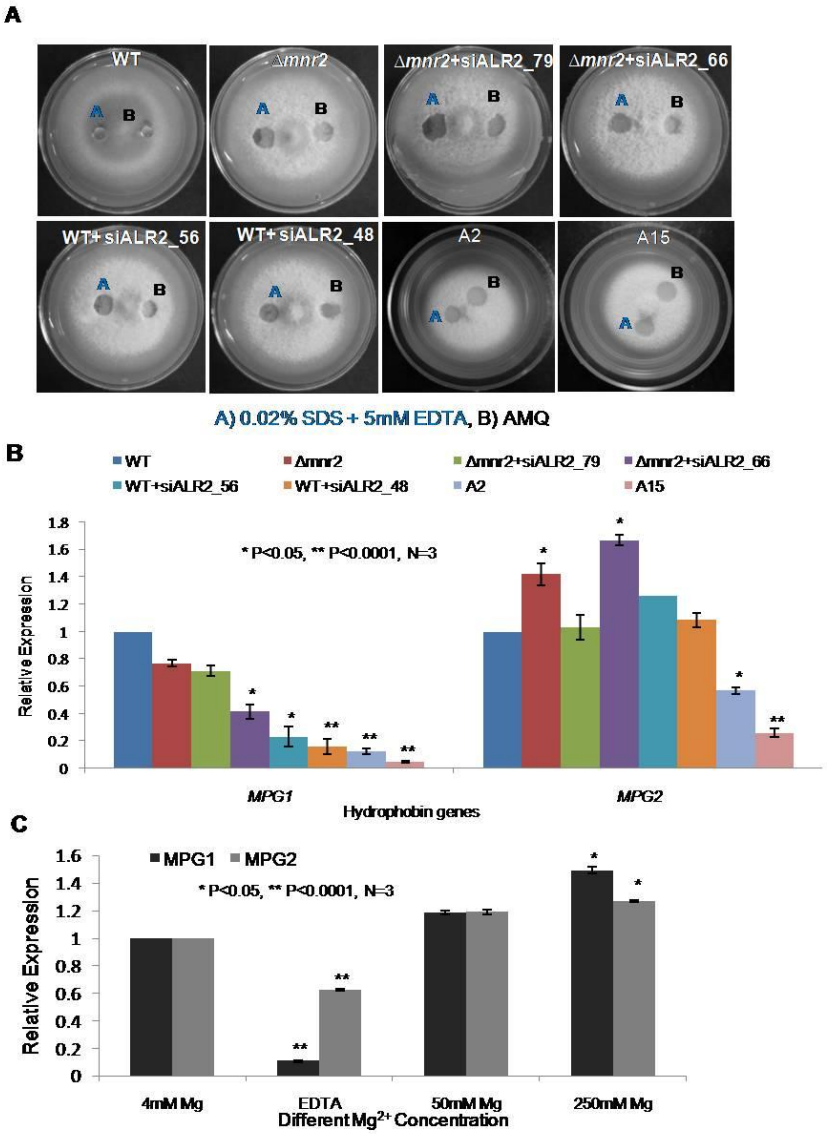

Figure 46. CorA transporters are required for surface hydrophobicity in *M. oryzae*. (A) 10 µl of water or detergent solution containing 0.02% SDS+5mM EDTA were placed on the surfaces of the WT, *Δmnr2* and knockdown transformants and photographed after 1 min. (B) mRNA levels of *MoMPG1* and *MoMPG2* were estimated by qRT-PCR in *Δmnr2* and knockdown transformants. All transcript levels were expressed as relative values, with 1 corresponding to levels in WT. (C) mRNA levels of *MoMPG1* and *MoMPG2* were estimated by qRT-PCR at two different concentrations of extracellular Mg^{2+} in WT. All transcript levels were expressed as relative values, with 1 corresponding to levels at 4mM. Error bar denote SD.

Δmnr2 and *MoALR2* knockdown transformants were tested for their ability to retain drops of water and detergent solution to assess effects of *MoALR2* and *MoMNR2* on surface hydrophobicity. Compared to WT, the knockdown transformants showed an easily wettable phenotype (Figure 46A). *Δmnr2* showed a wettable phenotype both with water and detergent

solution, but could hold water longer than *MoALR2* knockdown transformants, suggesting that *MoMNR2* plays a partial role in cell surface hydrophobicity while *MoALR2* is the major determinant. To investigate whether this wettable phenotype was mediated through hydrophobins, we measured the expression levels of the hydrophobin genes, *MoMPG1* (Mgg_10315) and *MoMPG2* (Mgg_01173) in the *Δmnr2* and knockdown transformants. There was substantial decrease in the expression of *MoMPG1* in the knockdown transformants and in A15 the levels decreased by ~95%. The levels of *MoMPG1* decreased to 33% in *Δmnr2*. The levels of *MoMPG2* did not change significantly (at $P<0.0001$) in all the knockdown transformants (Figure 46B).

To check whether extracellular Mg^{2+} availability regulates expression of *MoMPG1* and *MoMPG2*, their transcript levels in WT were studied at different concentrations of Mg^{2+} and in presence of EDTA. In presence of EDTA, the expression of *MoMPG1* decreased to as little as 10% while *MoMPG2* still showed 60% expression (significant at $P<0.0001$) (Figure 46C). At 50mM and 250mM Mg^{2+} the expression of *MoMPG1* and *MoMPG2* was similar to that of control at 4mM. Thus, we show that in *M. oryzae*, decrease in Mg^{2+} levels, either by silencing of transporter function (in the knockdown transformants), or by using EDTA (in WT), has a direct effect on the expression of both hydrophobins, especially *MoMPG1*.

5.27 Magnesium uptake by CorA transporters is essential for progression of the infection cycle in *M. oryzae*

In the life cycle of pathogenic fungi including *M. oryzae*, the capability to sporulate is critical to the spread of infection. The ability of knockdown transformants to sporulate was analysed on OMA medium from 6 dpi to 10 dpi.

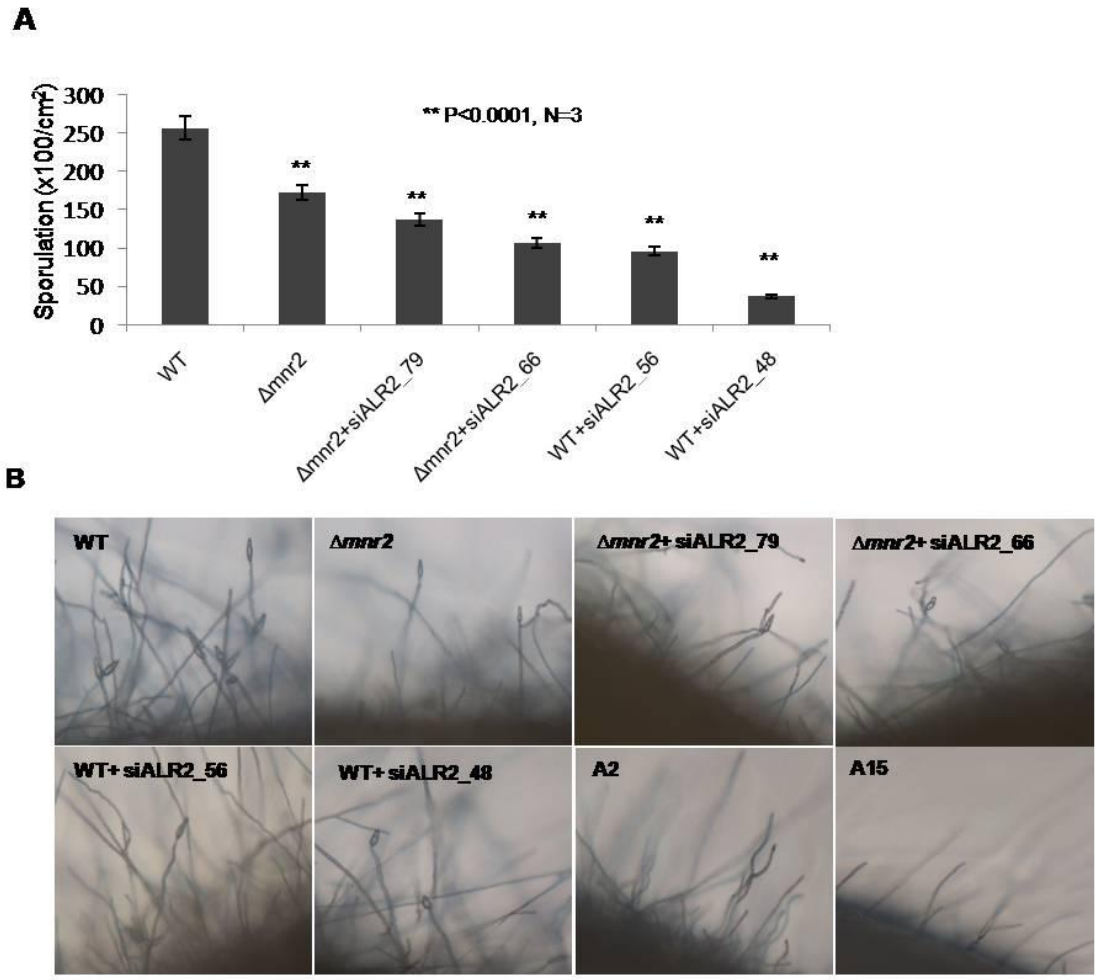

Figure 50. CorA transporters are required for Sporulation. (A) Ability of *Δmnr2* and knockdown transformants to sporulate was checked on OMA 8 days post inoculation and quantified. (B) The aerial hyphal and conidial development was also assessed for *Δmnr2* and knockdown transformants at 48 hpi.

The *Δmnr2* knockout showed a 23% reduction in spore count. In the *MoALR2* knockdowns, the sporulation efficiency decreased with a reduction in the expression of *MoALR2*, reaching as low as 20% of WT in WT+siALR2_48 (Figure 50A, 50B). Notably, A2 and A15 completely failed to sporulate, suggesting that maintenance of *MoALR2* levels is critical for conidiogenesis.

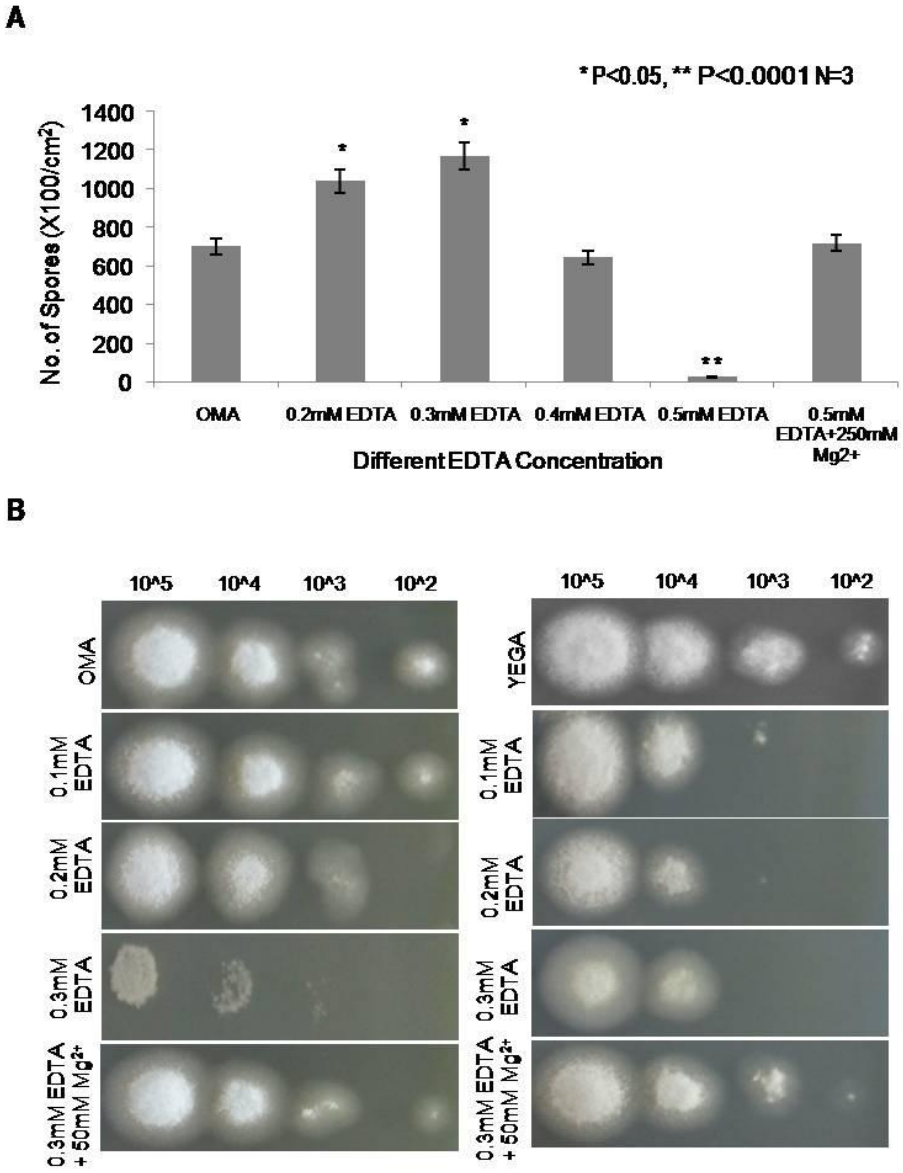

Figure 51. Effect of low Mg^{2+} availability on sporulation and mycelial growth. (A) The ability of WT to sporulate was checked on OMA with different concentrations of EDTA 8 days post inoculation and quantified. (B) Ability of WT spores to form vegetative hyphal growth following germination was assessed on YEGA and OMA with different concentrations of EDTA. 10µl of spores with increasing dilution was spotted onto the plates. The ability of Mg^{2+} to restore the germination capability of spores was also checked on Mg^{2+} supplemented medium in presence of EDTA.

We further studied the ability of WT to sporulate in presence of EDTA. Sporulation increased up to 0.3mM EDTA as compared to control (OMA with no EDTA), and then decreased at higher concentrations (Figure 51A). At 0.5mM EDTA, sporulation was completely abolished. There was no significant improvement in the sporulation at 0.5mM EDTA by using 50mM Mg^{2+} supplementation. However, Mg^{2+} supplementation of 250mM was able to rescue this

decrease in sporulation at 0.5mM EDTA, suggesting that adequate Mg^{2+} levels are required for sporulation.

Vegetative hyphal growth from WT spores following germination on nutrient rich media was checked on OMA and YEGA with different concentrations of EDTA. At 0.3mM EDTA growth from spores was severely restricted, while 50mM Mg^{2+} could rescue the growth defect (Figure 51B).

M. oryzae infection is initiated by attachment of the conidium to the rice leaf cuticle. Upon recognition of the hydrophobic surface and hydration, a single, polarized germ tube emerges from the spore. The germ tube grows along the leaf surface and differentiates into the appressorium. To evaluate the role of *MoALR2* and *MoMNR2* in the ability of spores to germinate and form appressoria, spores were inoculated on hydrophobic Gelbond film and incubated under moist conditions for 6 and 12 hours. The percentage of spores that germinated and appressoria formed at 6 and 12 hours was determined (Figure 52A). While in WT 90% of spores had germinated by 12 hours, in knockdown transformants the percentage of ungerminated spores ranged from 33% in *Δmnr2*+siALR2_79 to 41% in WT+siALR2_48. In WT, the percentage of appressoria formed increased from 41% at 6 hours to 85% at 12 hours. In *Δmnr2* the percentage of appressoria formed at 12 hours was 83% which is comparable to WT (Figure 52B). In the *MoALR2* knockdown transformant, WT+siALR2_48,the percentage of appressoria formed at 12 hours was only 33% (Figure52B).

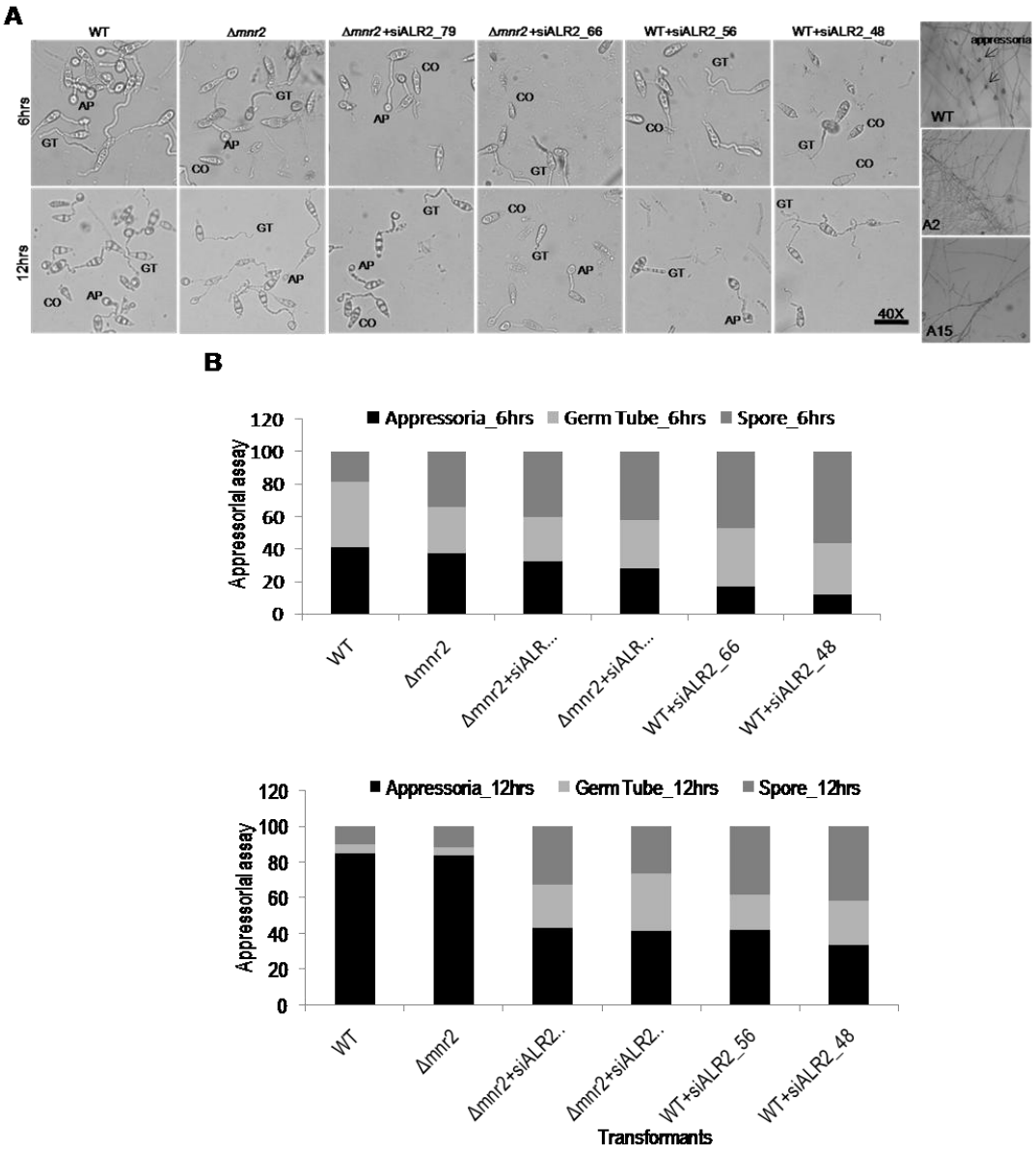

Figure 52. CorA transporters are required for Appressorium formation. (A) Appressorial assay for *Δmnr2* and knockdown transformants was performed on hydrophobic gelbond film and the ability to form infection structure was assessed and quantified at 6 and 12 hours (CO-Conidium, GT-Germ tube, AP-Appressorium). Mycelial blocks were placed on hydrophobic surface and incubated upto 72 hours at 28^{0}C for non-sporulating transformants. (B) The values are represented as percentage of spore (ungerminated), germ tube and appressoria formed at the given time interval.

The percentage of spores that failed to germinate and form appressoria increased with the increase in level of silencing in the knockdown transformants. Since A2 and A15 failed to sporulate, mycelial plugs from actively growing transformants were inoculated on hydrophobic surface and incubated under moist conditions for 48 hours (as mycelial tips are also capable of forming appressoria-like structures). The mycelial tip of A2 and A15 failed to develop any appressorium-like structure of the kind seen in the WT (Figure 52A). Thus it is

evident that a minimal level of *MoALR2* expression is critical for appressorium formation from germinated spores as well as from hyphae.

To test the ability of the conidia to germinate and form appressoria in presence of EDTA and EDTA with 50mM Mg^{2+} supplementation, appressorium formation was studied at different time points of 2, 8, 12 and 24 hours in WT (Figure 53, 54A).

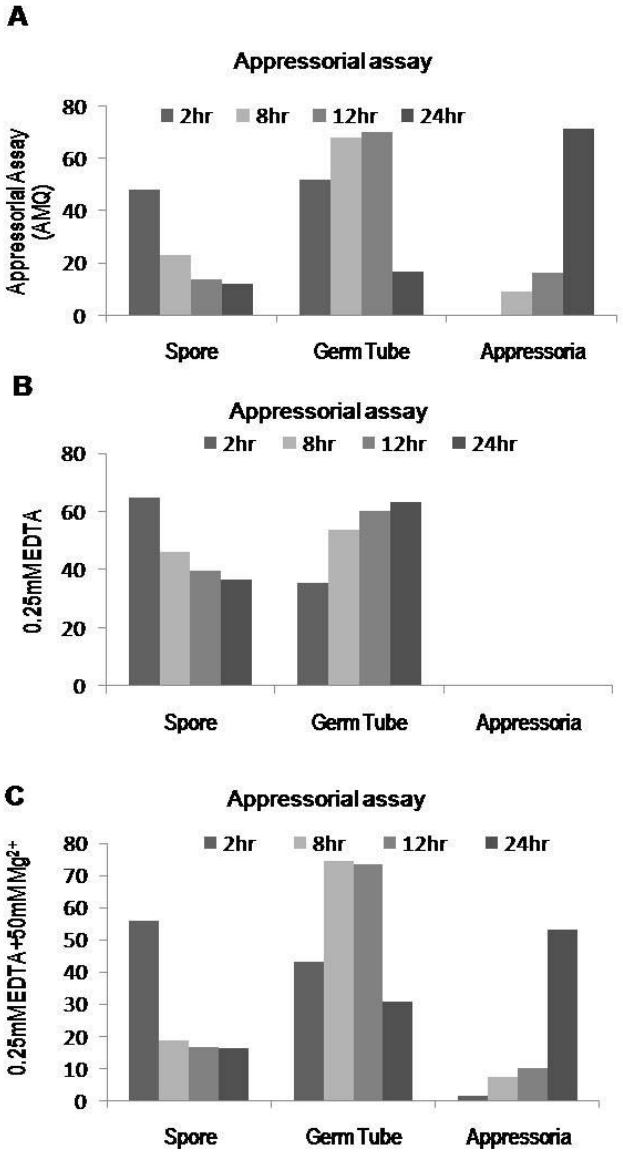

Figure 53. Appressorium formation in WT under Mg^{2+} limiting conditions (EDTA). The ability to form appressoria, the infection structures, in water (A) , 0.25mM EDTA (B) and 0.25mM EDTA+50mM Mg^{2+} (C) was observed at different time intervals in WT and percentages of spores (ungerminated), germ tubes and appressoria formed were calculated for each time interval and for each condition.

In the presence of 0.25mM EDTA, the spores failed to form appressoria even at 24 hours (for every time point n>100). Most of the spores (63%) were stalled in the germ tube stage

(Figure 53B). Extracellular Mg^{2+} (50mM) was able to rescue the defect in appressorium formation in presence of EDTA in WT. At 24 hours, approximately 53% of the spores had formed appressoria in presence of 50mM Mg^{2+} and 0.25mM EDTA (Figure 53C).

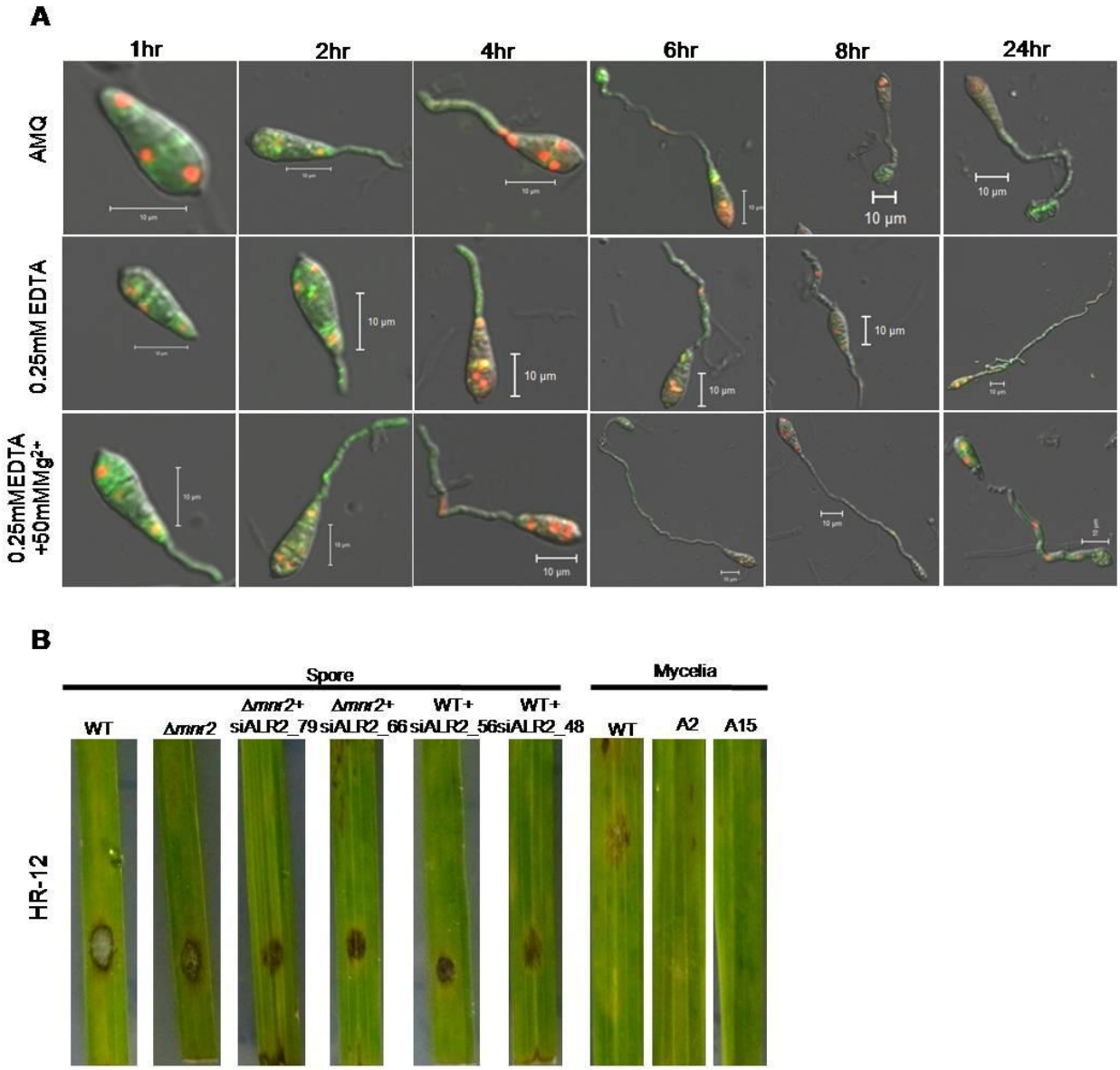

Figure 54. Mg^{2+} uptake by CorA transporters is essential for progression of the infection cycle. (A) The ability to form appressoria, the infection structures, in water, 0.25mM EDTA and 0.25mM EDTA+50mM Mg^{2+} was observed at different time intervals in WT tagged with H1:RFP and Tub:GFP. (B) Detached rice leaves of cultivar HR12 were inoculated with spores (1x10⁴/ml) and mycelial plugs. Disease symptoms (lesions) were assessed 4 days post inoculation.

The differentiated germ tube leading to formation of mature appressoria generate enormous turgor pressure (up to 8MPa) which ruptures the leaf cuticle, allowing invasive growth. Subsequently, colonisation leads to formation of lesions. Detached leaf infection tests showed

that the severity of infection decreased in the knockdown transformants (Figure 54B), consistent with a decrease in the levels of *MoALR2*, indicating the importance of *MoALR2* for pathogenicity in *M. oryzae*. Thus, extracellular Mg^{2+} availability and transport are critical at all stages of the infection cycle including hyphal growth, conidiation, spore germination, appressorium formation and disease progression in *M. oryzae*.

5.28 *MoALR2* affects intracellular cAMP levels in *M. oryzae*

In *M. oryzae,* cAMP mediated signalling through MAPK (*MoPMK1*, Mgg_09565) has been shown to be crucial for conidiation and appressorium initiation (Lee and Dean, 1993; Choi and Dean, 1997). cAMP synthesis is controlled by Mg^{2+}-dependent adenylate cyclase (Pasternak *et al.*, 2010; Zimmermann *et al.*, 1998). In view of the low Mg^{2+} levels in the knockdown transformants, we looked for changes in intracellular cAMP levels. The levels of cAMP in *Δmnr2* and the knockdown transformants varied from 97 to 20 fmol mg^{-1} as compared to 105 fmol mg^{-1} seen in WT (Figure 55A). The cAMP levels correlated with the transcript levels of *MoALR2* and intracellular Mg^{2+} levels in the transformants.

The cAMP levels increased in A2 in the presence of EDTA and 50mM Mg^{2+} as compared to the levels at 4mM Mg^{2+}. In A15, levels of cAMP did not change at 50mM Mg^{2+} but showed an increase in the levels of cAMP in presence of EDTA. In WT, cAMP levels decreased in presence of EDTA and were restored at 50mM Mg^{2+} at 8 hours (Figure 55B).

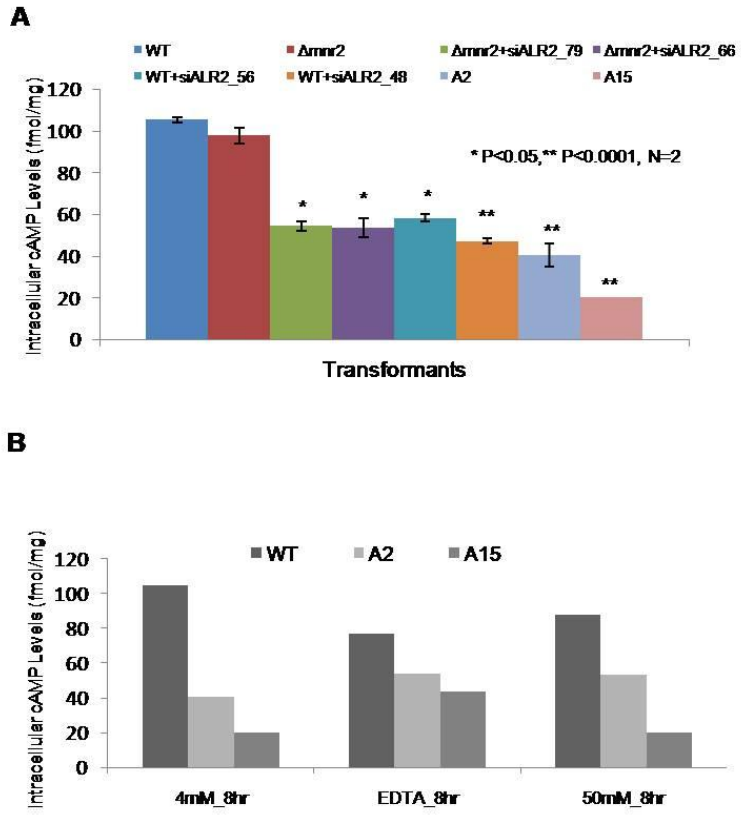

Figure 55. *MoALR2* affects intracellular cAMP levels. (A) Intracellular cAMP levels were estimated in WT, *Δmnr2* and knockdown transformants. The bar graph represents cAMP levels in fmol mg^{-1}. (B) Estimation of intracellular levels of cAMP at 50mM extracellular Mg^{2} in the double knockdown transformants, A2 and A15 in presence of 4mM, no Mg^{2+} (EDTA) and at 50mM Mg^{2+}. The values are expressed in fmol mg^{-1}.

We studied the expression of the adenylate cyclase gene, *MoMAC1* (Mgg_09898) and of *MoPMK1* (encoding MAPK) in the knockdown transformants and found significant decrease in their expression, with transcript levels decreasing to 43% and 20% of wild type respectively in A15 (Figure 56A, 57A). To study whether extracellular Mg^{2+} affects expression of *MoMAC1* and *MoPMK1*, we looked at their levels in A2 and A15 with 50mM Mg^{2+} supplementation, and found that expression was restored to WT levels (Figure 56B, 57B).

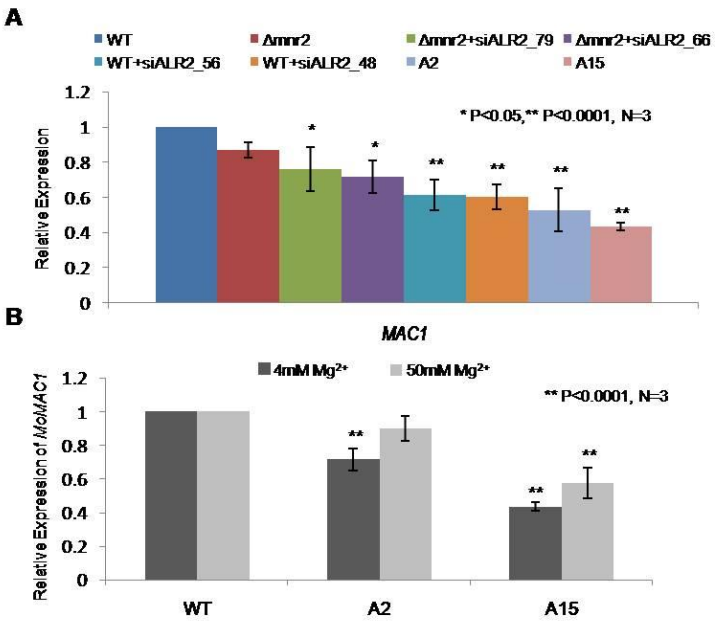

Figure 56. Expression analysis of *MoMAC1* in the knockout and knockdown transformants. (A) mRNA levels of *MoMAC1* was estimated by qRT-PCR in WT, *Δmnr2* and knockdown transformants. (B) mRNA levels of *MoMAC1* was estimated by qRT-PCR at two different concentrations of extracellular Mg^{2+} in WT, A2 and A15. The transcript levels were expressed as relative values, with 1 corresponding to WT. Error bar denote SD.

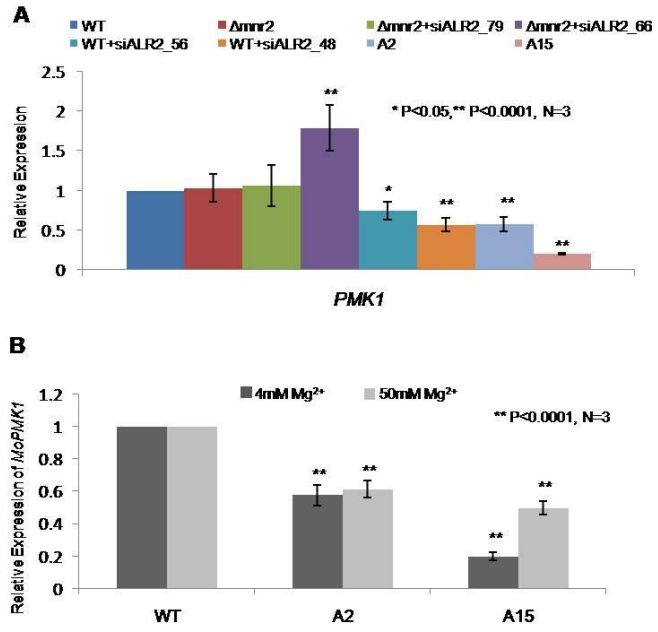

Figure 57. Expression analysis of *MoPMK1* in the knockout and knockdown transformants. (A) mRNA levels of *MoPMK1* was estimated by qRT-PCR in WT, *Δmnr2* and knockdown transformants. (B) mRNA levels of *MoPMK1* was estimated by qRT-PCR at two different concentrations of extracellular Mg^{2+} in WT, A2 and A15. The transcript levels were expressed as relative values, with 1 corresponding to WT. Error bar denote SD.

We conclude that low levels of intracellular cAMP and reduced flux through the cAMP mediated MoPmk1 signalling pathway could be one of the factors responsible for the

decreased ability to conidiate and form appressoria of the knockdown transformants of *MoALR2*.

5.29 *MoALR2* knockdown transformants show altered cell wall structure

Mg^{2+} is vital for the integrity of the cell wall and cell membrane (Wiesenberger *et al.*, 2007; Asbell *et al.*, 1996; Zimelis and Jackson, 1973; Prescott *et al.*, 1988; Trofimova *et al.*, 2010). We asked whether decreased Mg^{2+} levels lead to changes in cell wall integrity (CWI).

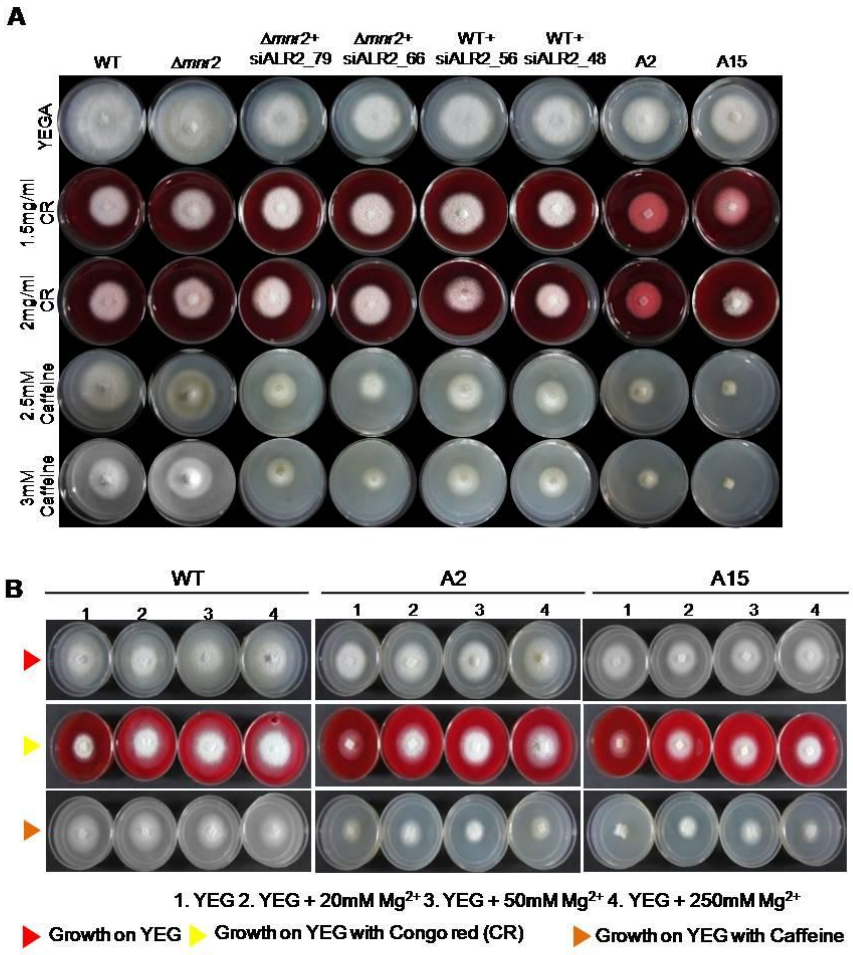

Figure 58. Cell Wall Integrity assay of the knockdown transformants. (A) 2X2 mm mycelial plugs of WT, *Δmnr2* and knockdown transformants were inoculated on YEG and YEG supplemented with Congo Red and Caffeine. Growth was assessed 5 dpi. (B) Recovery of growth on Mg^{2+} supplements in double knockdown transformants. YEG and YEG with Congo Red (1.5mg/ml) and Caffeine (2.5mM) were supplemented with different concentrations of Magnesium. 2X2 mm mycelial plugs of WT and knockdown transformants A2 and A15 were inoculated. Recovery in growth was assessed 5 dpi.

Growth was measured on media containing the cell wall stressors Congo Red (CR) and Caffeine. CR is an anionic dye that interacts with β linked glucans and nascent chitin chains,

thereby inhibiting the assembly enzymes that connect chitin to β-1, 3 glucan and β-1, 6 glucan (Ram and Klis, 2006). *Δmnr2* transformants showed a similar level of resistance to CR (at 1.5 and 2 mg ml^{-1}), as WT. However the knockdown transformants, both in WT and *Δmnr2* backgrounds, were more sensitive to CR, with A2 and A15 showing the greatest sensitivity (Figure 58A). Caffeine, an inhibitor of cAMP phosphodiesterase, stimulates the MAP Kinase component of cell wall integrity signalling and mutants with cell wall defects are sensitive to caffeine (Martin *et al.*, 2000; Calvo *et al.*, 2009; Munro *et al.*, 2007). A2 and A15 were the most sensitive to caffeine (Figure 58A), while *Δmnr2* transformants behaved similar to WT. The degree of sensitivity towards cell wall stressors increased in proportion to silencing of *MoALR2*. Mg^{2+} supplementation could rescue the growth defects in A2 and A15 (Figure 58B). These results indicate that regulation of Mg^{2+} levels by *MoALR2* is critical for the integrity of the cell wall.

To understand the cell wall defects in the knockdown transformants better, we looked at expression of cell wall maintenance related genes. Chitin, an important component of the fungal cell wall, is synthesised by Chitin Synthases, which catalyse the transfer of N-acetylglucosamine from uridine diphosphate N- acetylglucosamine (UDPGlcNAc) to a growing chain of β 1, 4 linked N-acetylglucosamine residues. We found decreased expression of two chitin synthase genes *MoCHS1* (Mgg_01802) and *MoCHS4* (Mgg_09962) in the knockdown transformants (Figure 59A).

In *S. cerevisiae*, Mg^{2+} deprivation results in up-regulation of genes involved in cytoskeletal organisation, namely actin-binding protein 1 (*ABP1*) and *MTI1* (Wiesenberger *et al.*, 2007). We analysed the expression of the genes *MoABP1* (Mgg_06358) and *MoMTI1* (Mgg_04116), in *Δmnr2* and the knockdown transformants by qRT-PCR.

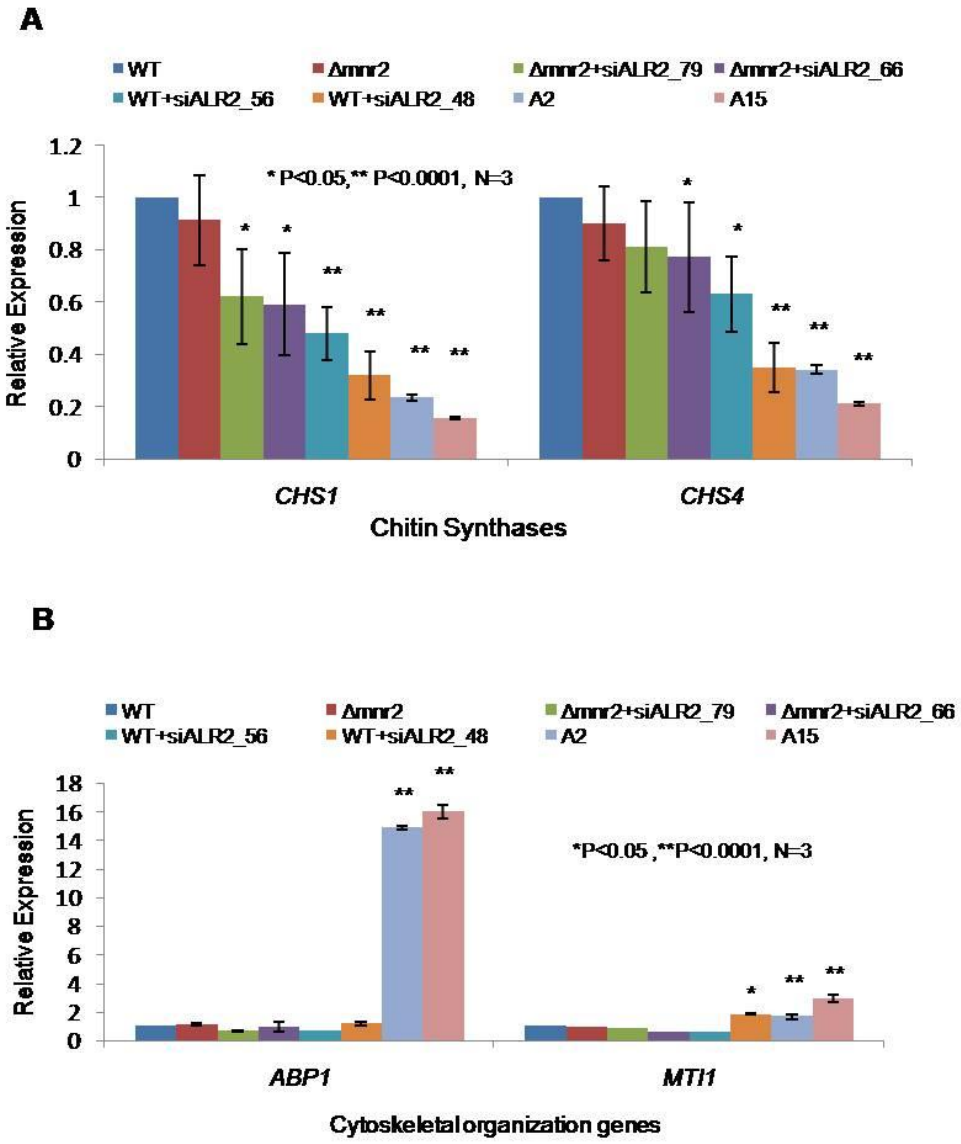

Figure 59. Expression analysis of Chitin synthases and genes involved in cytoskeletal organisation in the knockdown transformants. (A) mRNA levels of *MoCHS1* and *MoCHS4* were estimated by qRT-PCR. The transcript levels were expressed as relative values, with 1 corresponding to WT. (B) mRNA levels of *MoABP1* and *MoMTI1* were estimated by qRT-PCR. All transcript levels were expressed as relative values, with 1 corresponding to WT. Error bar denote SD.

There was significant up-regulation of both *MoABP1* and *MoMTI1* in A2 and A15 (at $P<0.05$) (Figure 59B). The expression of *MoABP1* was 15 fold higher, implying that MoAbp1 might play a role in stabilising the cytoskeleton and membranes to compensate for the lack of Mg^{2+}, which is known to be crucial in stabilising the cell shape and membrane integrity.

We further studied the expression of genes involved in the CWI pathway in *Δmnr2* and knockdown transformants.

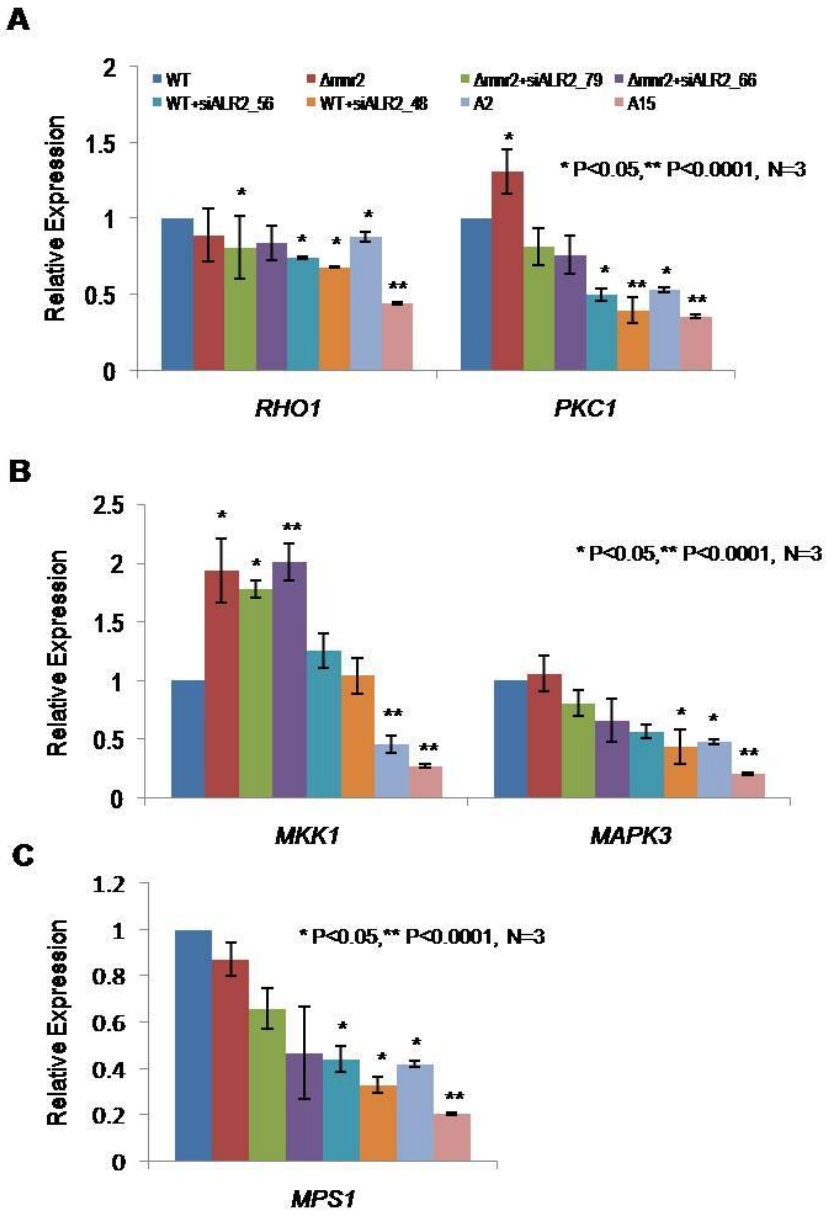

Figure 60. Expression analysis of genes involved in the CWI Pathway in knockout and knockdown transformants. (A) mRNA levels of *MoGTBP1* and *MoPKC1*,(B) *MoMAPK3* and *MoMKK1* and (C) *MoMPS1* were estimated by qRT-PCR. All transcript levels were expressed as relative values, with 1 corresponding to WT. Error bar denote SD.

In simultaneously silenced transformants (for *MoALR2* and *MoMNR2*), A2 and A15, there was significantly decreased expression of all the genes involved in the Pkc1 activated mitogen activated protein (MAP) kinase cascade including *MoPKC1*, *MoMKK1*, *MoMAPK3* and *MoMPS1* (at P<0.05) (Figure 60), with the exception of *MoGTBP* (Mgg_07176) (*Rho1*) (at P<0.0001). In *Δmnr2*, expression of *MoPKC1* increased, while that of *MoMKK1* increased in the *MoALR2* knockdown transformants both in the background of *Δmnr2*

(*Δmnr2*+siALR2) and WT (WT+siALR2). Overall, we infer that loss of *MoMNR2* function leads to a response involving up-regulation of *MoPKC1* and *MoMKK1*, consistent with the cell wall stress resistance seen against CR and caffeine in *Δmnr2*, while a decrease in MoAlr2 function makes the knockdown transformants more sensitive towards cell wall stress molecules through a reduced flux through the cell wall integrity signaling genes.

We further looked at the expression of downstream effectors *MoFKS1* (Mgg_00865) and *MoCRZ1* (Mgg_05133) regulated by *MoMPS1* (Mgg_04943) and involved in CWI signaling. These two genes also showed significantly decreased expression in the knockdown transformants (Figure 61A). The expression of *MoMPS1* in A2 and A15 was restored to WT levels when supplemented with 50mM Mg^{2+} (Figure 61B), indicating that Mg^{2+} levels affect the expression of *MoMPS1*. The decreased expression of CWI signalling genes in the knock-down transformants explains the sensitivity towards cell wall stress and demonstrates the role of *MoALR2* in maintenance of Mg^{2+} levels critical for cell wall integrity.

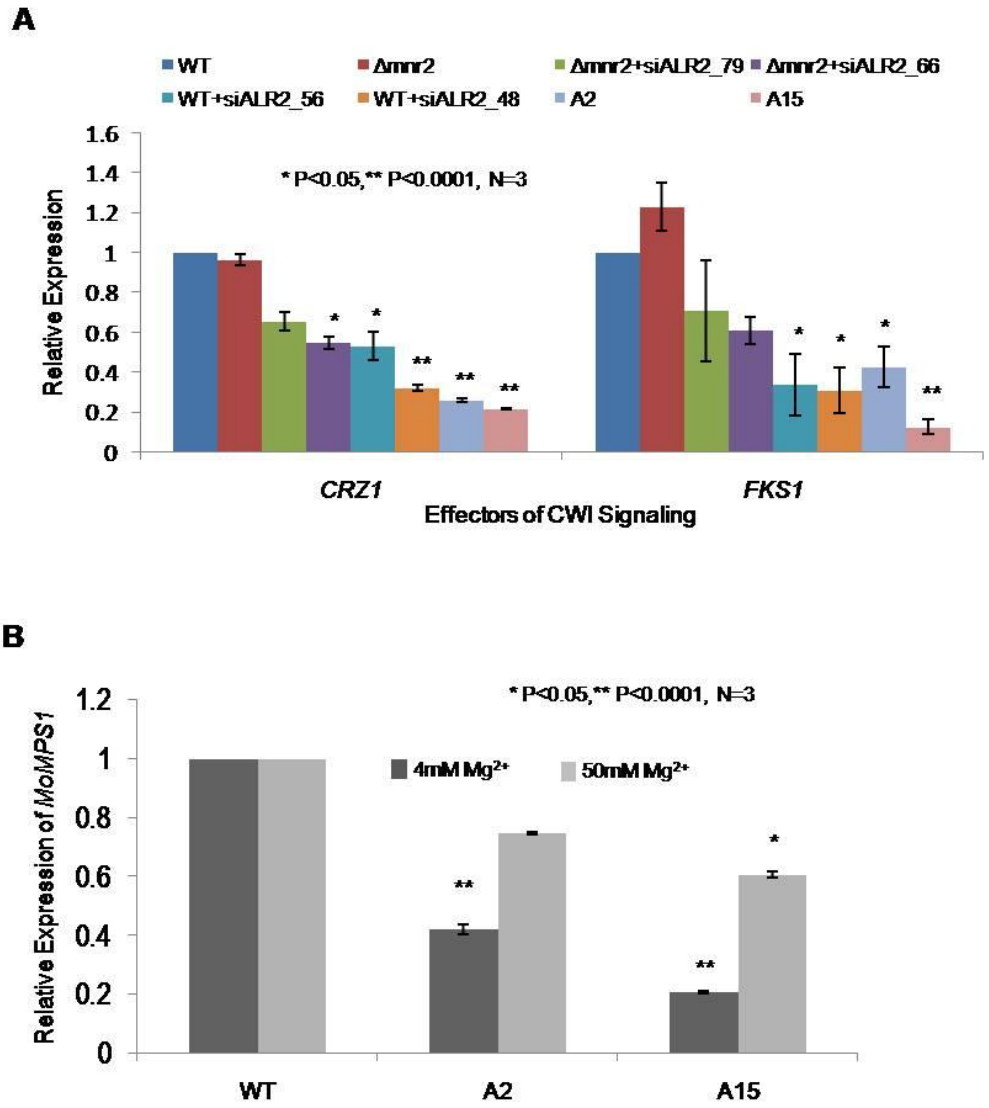

Figure 61. Expression analysis of effector genes involved in the CWI Pathway in knockout and knockdown transformants. (A) mRNA levels of *MoCRZ1* and *MoFKS1* were estimated by qRT-PCR. (B) mRNA levels of *MoMPS1* were estimated by qRT-PCR at two different concentrations of extracellular Mg^{2+} in WT, A2 and A15. All transcript levels were expressed as relative values, with 1 corresponding to WT. Error bar denote SD.